AFWAL-TR-82-3087
Volume I

AUTOMATED DESIGN OF DAMAGE RESISTANT STRUCTURES

Volume I - Theory and Application

R. F. Taylor

University of Dayton Research Institute
Dayton, Ohio 45469

October 1982

Final Report for Period 1 June 1979 - 30 April 1982

FLIGHT DYNAMICS LABORATORY
AIR FORCE WRIGHT AERONAUTICAL LABORATORIES
AIR FORCE SYSTEMS COMMAND
WRIGHT-PATTERSON AIR FORCE BASE, OHIO 45433

NOTICE

When Government drawings, specifications, or other data are used for any purpose other than in connection with a definitely related Government procurement operation, the United States Government thereby incurs no responsibility nor any obligation whatsoever; and the fact that the government may have formulated, furnished, or in any way supplied the said drawings, specifications, or other data, is not to be regarded by implication or otherwise as in any manner licensing the holder or any other person or corporation, or conveying any rights or permission to manufacture, use, or sell any patented invention that may in any way be related thereto.

This technical report has been reviewed and is approved for publication.

VIPPERLA B. VENKAYYA
Project Engineer
Design & Analysis Methods Group

FREDERICK A. PICCHIONI, Lt Col, USAF
Chf, Analysis & Optimization Branch

FOR THE COMMANDER:

RALPH L. KUSTER, JR., Col, USAF
Chief, Structures & Dynamics Div.

"If your address has changed, if you wish to be removed from our mailing list, or if the addressee is no longer employed by your organization please notify AFWAL/FIBRA, W-P AFB, OH 45433 to help us maintain a current mailing list."

Copies of this report should not be returned unless return is required by security considerations, contractual obligations, or notice on a specific document.

UNCLASSIFIED

SECURITY CLASSIFICATION OF THIS PAGE *(When Data Entered)*

REPORT DOCUMENTATION PAGE		READ INSTRUCTIONS BEFORE COMPLETING FORM
1. REPORT NUMBER AFWAL-TR-82-3087, Volume I	2. GOVT ACCESSION NO.	3. RECIPIENT'S CATALOG NUMBER
4. TITLE *(and Subtitle)* AUTOMATED DESIGN OF DAMAGE RESISTANT STRUCTURES Volume I - Theory and Application		5. TYPE OF REPORT & PERIOD COVERED Final Report Covering Period From 6/1/79 - 4/30/82 6. PERFORMING ORG. REPORT NUMBER
7. AUTHOR(s) R. F. Taylor		8. CONTRACT OR GRANT NUMBER(s) F33615-79-C-3209
9. PERFORMING ORGANIZATION NAME AND ADDRESS University of Dayton Research Institute 300 College Park Avenue Dayton, Ohio 45469		10. PROGRAM ELEMENT, PROJECT, TASK AREA & WORK UNIT NUMBERS 24010233
11. CONTROLLING OFFICE NAME AND ADDRESS Flight Dynamics Laboratory (AFWAL/FIBRA) Air Force Wright Aeronautical Laboratories(AFSC) Wright-Patterson Air Force Base, Ohio 45433		12. REPORT DATE October 1982 13. NUMBER OF PAGES 137
14. MONITORING AGENCY NAME & ADDRESS*(if different from Controlling Office)*		15. SECURITY CLASS. *(of this report)* Unclassified 15a. DECLASSIFICATION/DOWNGRADING SCHEDULE

16. DISTRIBUTION STATEMENT *(of this Report)*

Approved for public release; distribution unlimited.

17. DISTRIBUTION STATEMENT *(of the abstract entered in Block 20, if different from Report)*

18. SUPPLEMENTARY NOTES

This report consists of two volumes. Volume II is titled, "Program User's Manual."

19. KEY WORDS *(Continue on reverse side if necessary and identify by block number)*

structural analysis	stress analysis
vulnerability analysis	deflection analysis
structural optimization	finite element analysis
damage	automated design

20. ABSTRACT *(Continue on reverse side if necessary and identify by block number)*

This report documents an effort to develop an optimality criterion approach to the design of damage tolerant structures subject to stress, deflection, and frequency requirements. Damage conditions are treated in an integral manner in the resizing algorithm. An iterative reanalysis procedure is used to improve the efficiency of the static analyses that are needed as the optimization proceeds. In this volume of the report,

DD FORM 1 JAN 73 1473 EDITION OF 1 NOV 65 IS OBSOLETE

UNCLASSIFIED

SECURITY CLASSIFICATION OF THIS PAGE *(When Data Entered)*

(Block 20 Continued)

the theoretical development is given together with applications to representative structures. Detailed applications include the development of designs for a metal and a composite A7D outer wing panel. Volume II of the report gives user information on the computer program used in these applications.

FOREWORD

This final report documents work performed by the Aerospace Mechanics Division of the University of Dayton Research Institute (UDRI) for the Structures and Dynamics Division of the Flight Dynamics Laboratory, Air Force Wright Aeronautical Laboratories (AFWAL), Wright-Patterson Air Force Base, Ohio. The work was performed under contract F33615-79-C-3209. Dr. V. B. Venkayya was the AFWAL Project Engineer.

This report consists of two volumes. Volume I, entitled, "Theory and Application," describes the theory behind the design optimization method and gives design results. In Volume II, "Program User's Manual," detailed instructions are given for use of the ADDRESS (Automated Design of Damage Resistant Structures) computer code on the Wright-Patterson Air Force Base CDC computing system. The report covers work conducted between 1 June 1979 and 30 April 1982.

The author acknowledges the important technical assistance of Mrs. Elizabeth Stanley McCoy, Messrs. Carl King, J. Gebara, and A. Faloughi formerly of the UDRI. Acknowledgement is also made of the valuable student programming assistance of Miss Terri McMahon for her work on design scaling and the finite element modeling of the A7D outer wing panel. Dr. Fred Bogner was the Project Manager.

Messrs. Jim Maris, Nick Zikos, and Brian Cazzell of the Vought Corporation, Dallas, Texas, were subcontractors on the A7D design. Acknowledgement is made of their continuing support and essential input to the program. Vought drawings, design work, and test plan information are documented as a separate contract item.

TABLE OF CONTENTS

TABLE OF CONTENTS (Concluded)

LIST OF ILLUSTRATIONS

LIST OF ILLUSTRATIONS (Concluded)

LIST OF TABLES

SECTION 1
INTRODUCTION

The University of Dayton Research Institute (UDRI) has completed an exploratory development contract with the Flight Dynamics Laboratory (AFWAL/FIBR) to develop a computer program for the design and analysis of damage resistant structures. In addition, the Vought Corporation utilized UDRI computer output to redesign an A7D aircraft outer wing panel. This report documents the theoretical development behind the computer code referred to as ADDRESS (Automated Design of Damage Resistant Structures) and presents applications to typical aircraft structures. Volume II of the report gives details of the computer code. Detailed design information and a test plan for the A7D panel are submitted under separate cover as required by the contract.

This introductory section gives the background of the technological requirement, and a statement of the overall objective. It concludes with a summary of the major accomplishments.

1.1 BACKGROUND

By the very nature of their reason for existence, military aircraft are susceptible to damage. The performance of a damaged aircraft can be affected in a variety of ways depending on which of the aircraft systems are affected and to what degree the damage is inflicted. Structural damage to aircraft has been responsible for a significant number of aircraft losses. Consequently, it is extremely important that military aircraft maintain an adequate degree of structural integrity under damaged conditions. The best way to insure the structural adequacy of damaged aircraft is to make the proper provisions during the design phase.

One obvious way to provide adequate residual strength for damaged structures is to increase the size of the various members and components which make up the structures. This simplistic approach, however, is at odds with the constant quest to reduce

aircraft weight and cost. Consequently, aerospace engineers strive to design aircraft which are structurally adequate but which have lower weight and/or cost than alternative designs. Conventional methods (largely intuitive) permit engineers to reduce the weight of initial designs by resizing. However, these procedures do not, in general, yield designs which are "best" in any sense; they are just better than previous trials. In addition, vulnerability is usually considered only as an afterthought. Consequently, there is a real need for the development of logical procedures, based on sound mathematical principles, which will produce damage tolerant structural designs that satisfy a criterion of merit such as minimum weight.

Although there has been considerable progress in structural optimization, these developments have been largely academic. However, there is now sufficient evidence to indicate that optimization can be a valuable practical tool in reducing weight and cost, and in improving performance. Therefore, in view of the above mentioned need to provide damage tolerant military structures, the aims of this current program have been to put optimization into the damage tolerant design cycle. The objective of the program is stated in the following paragraph.

1.2 OBJECTIVE

The primary objective of this research program was to transition some of the theoretical developments into structural optimization of the last 20 years into practical design tools so that significant cost reductions can be achieved in the design of future aerospace vehicles. Particular emphasis was focused on damage-susceptible structures.

1.3 SUMMARY

An optimality criterion approach is presented which will aid in the design of damage tolerant structures subject to stress, deflection, and frequency requirements. Damage conditions are

treated in an integral manner in the resizing algorithm. An iterative reanalysis procedure is used to improve the efficiency of the static analyses that are needed as the optimization proceeds. Several representative structural components have been resized with the procedure and a test plan is outlined which will help to verify the damage tolerant characteristics. For wing structures, size and location of damage are the driving features of the process. Criteria are presented to aid the analyst in determining the critical stress allowables.

The major accomplishments of this contract are: (1) an extensive revision and consolidation of several important Air Force structural analysis and optimization codes; (2) an in-depth investigation of structural reanalysis techniques; and (3) the transfer of technology from a research environment to one of design, fabrication, and testing. Additionally, the study of representative structures aided in the establishment of ballistic damage criteria.

In the computer code development area, it is now possible to analyze, resize, and assess the effect of ballistic damage on wing structures. Stresses, deflections, and vibration characteristics can be computed and damage sensitivities established for both metal and composite structures within the framework of a single computer code. The program has detailed documentation and can be extended to consider additional design requirements.

Reanalysis techniques were studied and mathematical criteria established for the convergence of the static iterations. A new design scaling technique was developed to meet a fixed frequency requirement and an energy criterion simultaneously. The efficiency of the reanalysis was found to be highly dependent on the programming techniques used.

The redesign of the A7D outer wing panel presented herein required that structural optimization technology be transferred to an aircraft design environment. As a result of the computer

optimization studies, aircraft designers were able to develop a lighter weight and more damage tolerant wing structure than could be done by conventional means. Full-scale detailed design drawings were made and a test plan developed to verify the results of the structural optimization code.

SECTION 2
REVIEW OF THE LITERATURE

Structural optimization algorithms have been continuously improved over the last 20 years. There are a number of practical approaches now available to large scale structural optimization of airframe structures.[1] However, there has been little attempt to verify the validity of the optimized designs under actual service conditions. Of particular concern for military aircraft is the sensitivity of the optimized structure to loss or reduction of stiffness in members due to damage. In this section optimization for damage tolerance is reviewed, followed by a discussion of the literature on structural reanalysis.

2.1 OPTIMIZATION FOR DAMAGE TOLERANCE

The body of the literature on structural optimization is now quite large, but there have been relatively few investigations dealing specifically with the optimal design of damage tolerant structures. Arora, et al.[2] have included strength, stiffness, and damage requirements in an optimal design strategy. A design sensitivity analysis is coupled with a steepest descent algorithm to design damage tolerant structures. An application is made to an open truss helicopter tail-boom. Venkayya, et al.[3] present an iterative technique which demonstrates the feasibility of including damage considerations in a design procedure based on an optimality criterion approach. Applications are made to truss and wing structures.

Reference 2 enumerates an important list of basic definitions regarding damage tolerant design. These definitions are reproduced here because they apply to the current work also. They are as follows:

(1) Damage-tolerant structure. A structure is called damage tolerant or fail-safe if it continues to perform its basic function even after it sustains a specified level of damage.

(2) Damage condition. A damage condition for the structure is defined to consist of complete or partial removal of a selected member or groups of members of the structure. Some nodes of the structure may be removed as a result of the damage.

(3) Optimal damage-tolerant structure. A damage-tolerant structure is called optimal if it is designed to minimize a merit function, subject to constraints that must hold for the undamaged structure and under projected damage conditions.

The open truss helicopter tail boom problem studied in Reference 2 contains 108 axial bar elements and 38 nodes. The members are grouped so that only 42 are considered free design variables. It is important to note that use was not made in this study of efficient reanalysis techniques to compute the response for the damage cases.

Reference 3 makes extensive use of reanalysis procedures to compute response to structural damage. Elastic strength, yielding, and frequency and mode shape changes are estimated. Applications are to optimized truss and wing structures; no attempt was made to include the reanalysis procedures within the framework of an optimization scheme. It was concluded that the reanalysis procedures were simple, accurate, and a natural extension of the finite-element based structural optimization procedures.

2.2 REANALYSIS METHODOLOGY

In order to perform an optimization of a structural design which is subject to multiple damage conditions, it is essential to perform efficiently the reanalysis of the damage conditions. This subsection contains a review of the literature which has application to reanalysis problems. First, the methodologies for static reanalysis are considered, followed by techniques for predicting mode shape and frequency trends as structural modifications are made.

2.2.1 Reanalysis of Static Cases

Several categories of methods are available for the reanalysis of structures with local modifications. The methods all involve the solution of the modified linear equations and may be classified as follows: (1) direct[4-7], (2) iterative[3,8-11], (3) implicit differentiation[12-15], (4) reduced basis[14-16], or (5) mixed[17-18]. In the current study, methods one and two were investigated in detail due to their relative simplicity and ease of programming.

By direct reanalysis methods the solution to the modified static equations are obtained in one step. References 4, 5, and 7 solve the modified equations

$$([K] - [K_1])\{\bar{x}\} = \{F\} \tag{2.1}$$

based on the stiffness matrix of the unmodified system

$$[K]\{x\} = \{F\} \tag{2.2}$$

where $[K]$ is the system stiffness matrix, $[K_1]$ is the modification, $\{F\}$ is the applied load, and $\{x\}$ and $\{\bar{x}\}$ are the response vectors for the unmodified and modified structures, respectively. Use of the Sherman-Morrison identity[5], a technique which gives an explicit solution to equation (2.1) when $[K_1]$ is a vector outer product, yields

$$\{\bar{x}\} = \left([K]^{-1} - \sum_{j=1}^{R} \tau_j \, [K]^{-1}\{u_j\}\{u_j\}^T \, [K]^{-1} \right) \{F\} \tag{2.3}$$

where

$$\tau_j = (\{u_j\}^T [K]^{-1} \{u_j\} - \sigma_j^{-1})^{-1} \quad \text{and}$$

σ_j and u_j are the eigenvalues and eigenvectors of the modification matrix $[K_1]$, and R is the rank of $[K_1]$.

Kavlie and Powell[7] point out the fact that the Sherman-Morrison identify seems to require the explicit inverse

of the [K] matrix. However, when equation (2.2) is used in (2.3), it can be shown that simplifications occur which negate the requirement of an explicit inverse of the stiffness matrix. A main drawback of the method is more obviously the requirement of the outer product representation of the modification matrix in terms of all of its eigenvectors. The eigenanalysis plus the matrix multiplications of equation (2.3) could easily exceed the cost of resolution of equation (2.1) by the Choleski method, for example.

Reanalysis methods which use iteration may be slow to converge, if at all, when large changes in the design are made. Kirsch and Rubinstein[8] develop a method to improve convergence based on an expression of the matrix of changes in stiffness as a linear combination of two matrices. Phansalker[9] makes similar conclusions, as does Switzky[10]. Reference 10 improves the convergence of the iterations by selecting good initial guesses for the modified responses. Venkayya[11] develops an iterative procedure based on a Taylor series expansion of the response. Details of this procedure are given in Section 3.3 herein.

References 12 and 13 propose using implicit differentiation of the governing equations to obtain response gradient information. In Reference 14, a combined Taylor series-iterative technique using first-order sensitivities is developed and applied with good results to space truss structures. Reference 15 documents a similar study, and shows how sensitivity information can be incorporated into an optimality criterion or a mathematical programming method for structural optimization.

The work of Noor and Lowder[17-18] develops a "mixed method" for reanalysis; i.e., the fundamental unknowns include both force and displacement parameters. The merits of the Taylor series approach are assessed as applied with the mixed approach and compared with the displacement method. It is also shown that the displacement approach can be greatly improved by choosing the design variables to be reciprocals of the sizing variables.

The statement by Kirsch and Rubinstein[8] that no single method of reanalysis is superior in all cases for static problems seems to summarize the reanalysis state of the art. A method should be evaluated and selected on the basis of its ease of use, computational efficiency, and convergence characteristics. In the work reported herein, simple iterations in conjunction with an acceleration technique fit the above criteria.

2.2.2 Reanalysis of Eigenvalue Problems

Reanalysis techniques for eigenvalue problems are classified herein as either (1) derivative-based[19-21] or (2) iterative-based[22-24]. In the former case, implicit differentiation of the eigenvalue problem is performed to obtain first order gradient information. The iterative techniques may in some cases also lead to gradients. However, iterations can also be used to estimate discrete changes in the eigenvalues and eigenvectors.

Fox and Kapoor[19] developed expressions for the rate of change of eigenvalues and eigenvectors of a discrete model of a vibrating system. For a given increment in the structural variables, the modified eigenvalues and eigenvectors were computed using a one term Taylor series expansion. The rates of change of the i^{th} eigenvalues were expressed by Fox and Kapoor in terms of the rates of change of the mass and stiffness matrices and the i^{th} eigenvector.

Reference 19 presents two formulations for the rates of change of the eigenvectors. In the first formulation, the expression for the i^{th} generalized mass is differentiated with respect to the variables and the resulting system is solved for the rate of change of the eigenvector. The system of equations involves only the i^{th} vector. The second formulation uses an eigenvector expansion theorem to represent the eigenvector derivative as a linear combination of all the vectors of the given problem. The coefficients are then determined using the orthogonality properties of the vectors. The disadvantage of the second method is that it requires that all the vectors be computed. Fox and Kapoor briefly comment that it may be possible to use a

partial sum to represent the eigenvector derivative. Hence, for small structural changes, not all the vectors may be needed to approximate the eigenvector derivatives.

Rogers[20] explored the work of Fox and Kapoor further and concluded that it could also be extended to eigenvalue problems where the matrices are nonsymmetric and complex. The expressions for the eigenvalues and eigenvectors included products of both the left and right eigenvectors. Thus, it is necessary to solve an additional system of equations to obtain the required derivatives. The Rogers expressions are useful in studying design trends in nonconservative systems.

Nelson[21] developed a simplified procedure for determining eigenvector derivatives which is more efficient than previous methods when large systems are considered. The matrix technique for determining the eigenvector derivative is similar to the first formulation of Fox and Kapoor discussed above. However, the original eigensystem of rank (n-1) is modified to convert it to rank n and then solved for a vector which is used to compute the eigenvector derivative. The system of equations was solved without extensive matrix manipulations as indicated by Fox and Kapoor.

Another class of methods[22-24] involves matrix iterations. Rudisill and Chu[22] proposed an iteration based on a rearrangement of terms in the Rayleigh quotient. Both self-adjoint and nonself-adjoint systems can be handled in this manner. Andrew[23] proved the convergence of the Rudisill-Chu iteration and examined its rate of convergence. It was concluded by Andrew that the iterative procedures should be used rather than the "direct method" (i.e., the approach in References 19-21) when the number of iterations is less than n/3, where n is the order of the system.

Hemming, Venkayya, and Eastep[24] studied the problem of flutter speed degradation of damaged optimized lifting surfaces. Since a modal flutter analysis approach was used, it was necessary

to determine the effect of design perturbations (i.e., damage) on the natural frequencies and mode shapes. The perturbed frequencies were obtained by the use of the Rayleigh quotient. Mass and stiffnesses in this quotient were for the damage structure. As a first approximation, the modes for the undamaged case were used to compute the approximate triple products. The modal vectors were improved by solving a system of equations iteratively, which required the decomposition of a different coefficient matrix for each damage case.

In summary, it appears that iterative techniques are more efficient than the Fox and Kapoor type of approach. However, in the case when changes in the structure are large, the convergence of these techniques is sometimes questionable. The work reported herein uses an iterative procedure somewhat along the same lines as Reference 24 with the improvement that a new coefficient matrix need not be decomposed for each damage case. In the cases of large damage, it is possible that stress and deflection requirements are more important than frequency and mode shape considerations. So the convergence of the iterations, although an interesting mathematical problem, may be a moot consideration when strength requirements are present.

SECTION 3
THEORETICAL DEVELOPMENT

In this section the theoretical development of the analysis and optimization procedures for damage resistant structures are given. The finite element technique is discussed, followed by the vibration analysis algorithm used in this work. The reanalysis procedures are next presented, and the section concludes with the presentation of various aspects of the design optimization strategy such as design scaling.

3.1 STATIC ANALYSIS

The structural model for the static analysis calculations is based on the finite element displacement method.
The current library includes the following element types:

1. Bar (axial force member)
2. Membrane triangle
3. Membrane quadrilateral
4. Shear panel
5. Beam

The local coordinate system for the element types shown in Figure 3.1 is the same as in Reference 25. The bar element is a constant strain line element and is equivalent to a NASTRAN rod element. Four constant strain membrane triangles are used to form the quadrilateral element by a merging process, followed by static reduction to eliminate the interior node. The shear panel is formed in a manner similar to the membrane quadrilateral; however, only shear energy is considered in forming the stiffness matrix. The details of the beam element are included in the next subsection. Further details of the elements other than the beam are given in Reference 25.

The efficiency of the static analysis is highly dependent upon the programming of the solution technique to the equilibrium equations

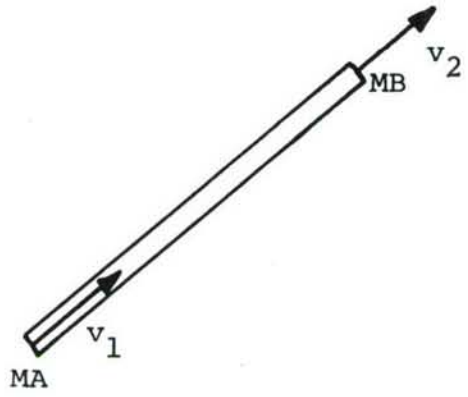

(a) Bar Element

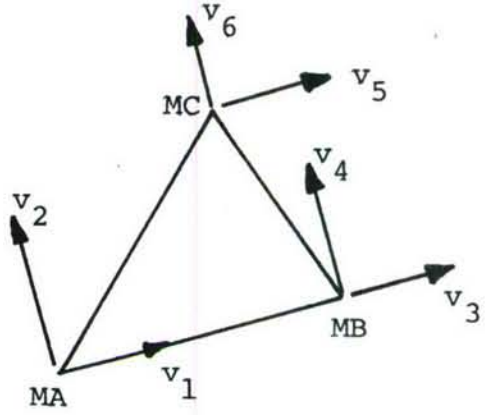

(b) Triangular Membrane Element

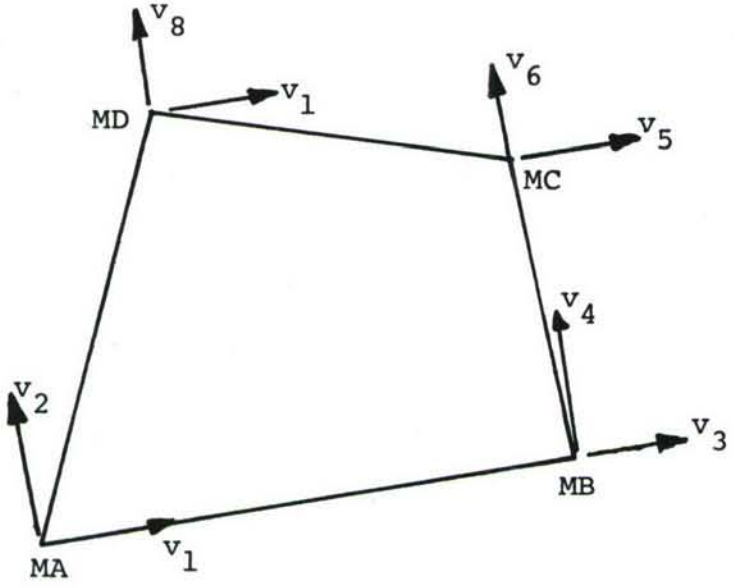

(c) Quadrilateral or Shear Panel

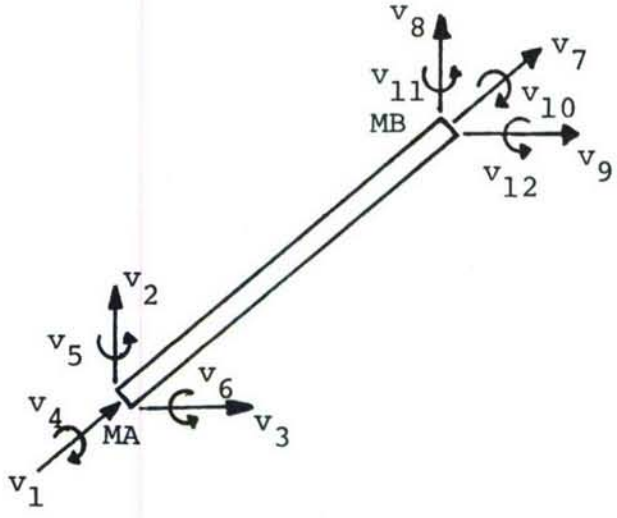

(d) Beam Element

Figure 3.1. Elements and Local Coordinate System

$$[K]\{x\} = \{F\} \tag{3.1}$$

where [K] is the global stiffness matrix, {F} is the vector (or vectors) of applied forces, and {x} is the solution vector (or vectors) of displacements and rotations. The Choleski decomposition technique was used for these studies.

The stiffness matrix is thus decomposed into the form

$$[K] = [L]\ [L]^T \tag{3.2}$$

where the components of the lower triangular matrix [L] are

$$\ell_{ii} = \left(a_{ii} - \sum_{k=1}^{i-1} \ell_{ik}^2 \right)^{1/2} \tag{3.3a}$$

$$\ell_{ji} = \left(a_{ii} - \sum_{k=1}^{i-1} \ell_{ik}\, \ell_{jk} \right) \Big/ \ell_{ii} \ , \quad j>i \tag{3.3b}$$

After decomposition, forward

$$[L]\ \{y\} = \{F\} \tag{3.4}$$

and backward substitutions

$$[L]^T\ \{x\} = \{y\} \tag{3.5}$$

are performed to obtain the solution. The efficiency of the Choleski method is nearly double that of the Gaussian elimination procedure in ØPTSTAT[25]. In both ADDRESS and ØPTSTAT advantage is taken of the special "skyline" form of the stiffness matrix so that storage is minimized.

3.2 BEAM BENDING ELEMENT

Figure 3.2 shows the coordinate system and cross-sectional properties of the beam bending element. The beam element is a straight bar with linearly varing properties, and is capable of resisting axial forces, bending moments about two principal axes, and twisting moments. Node 3 is used to determine the cross-section orientation of the beam.

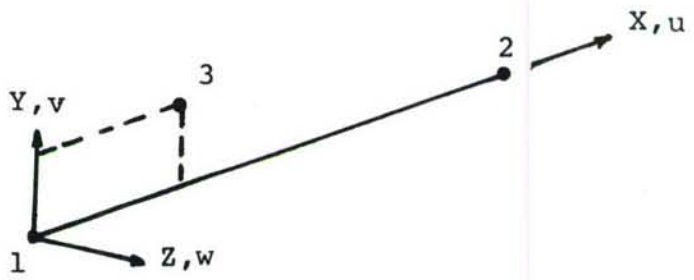

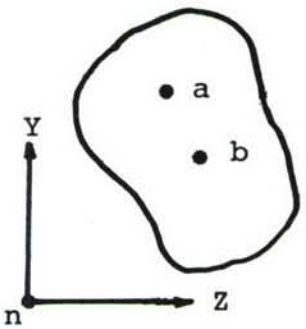

n = Node Point (Shear Center)
a = Mass Centroid Location
b = Geometric Centroid Location

Nodal Degrees of Freedom: u, v, w, θ_X, θ_Y, θ_Z

Figure 3.2. Beam Element Geometry.

The shear center, mass centroid, and geometric centroid are allowed to be distinct points. Any transverse force applied through the shear center causes no torsion of the beam.[26] When the element is twisted, the twist takes place around the shear center (center of twist). When the cross-section has one axis of symmetry, the shear center will be located on that axis. For cases when there are two axes of symmetry, the shear center will coincide with the geometric centroid. The unbalance provided by the mass centroid offset is useful in modeling high aspect ratio lifting surfaces for vibration problems.

The nodal degrees of freedom (three displacements and three rotations) lead to element matrices of order 12. Terms in these matrices are functions of the following properties:

1. Mass centroid location - y_a, z_a
2. Geometric centroid location - y_b, z_b
3. Cross-sectional area - $A(x)$
4. Moments of inertia - $I_y(x)$, $I_z(x)$, $J(x)$
5. Geometric unbalance - $G_y(x)$, $G_z(x)$, $G_{yz}(x)$
6. Mass moments of inertia - $K_y(x)$, $K_z(x)$
7. Mass unbalance - $S_y(x)$, $S_z(x)$
8. Elastic moduli - E, G
9. Material density - $\rho(x)$ (mass/length) or $\rho^*(x,y,z)$ (mass/volume)

The above geometrical and inertia properties are interrelated and are defined by the following integrals:

$$\int_A dA = A(x) \tag{3.6a}$$

$$\int_A y^2 \, dA = I_z(x) + y_b^2 \, A(x) \equiv \bar{I}_z(x) \tag{3.6b}$$

$$\int_A z^2 \, dA = I_y(x) + z_b^2 \, A(x) \equiv \bar{I}_y(x) \tag{3.6c}$$

$$\int_A y \, dA = G_y(x) = y_b \, A(x) \tag{3.6d}$$

$$\int_A z \, dA = G_z(x) = z_b \, A(x) \tag{3.6e}$$

$$\int_A yz \, dA = G_{yz}(x) = y_b \, z_b \, A(x) \tag{3.6f}$$

$$\int_A \rho^* \, y^2 \, dA = \rho \, K_z(x) + y_a^2 \, \rho \, A(x) \equiv \rho \, \bar{K}_z(x) \tag{3.6g}$$

$$\int_A \rho^* \, z^2 \, dA = \rho \, K_y(x) + z_a^2 \, \rho \, A(x) \equiv \rho \, \bar{K}_y(x) \tag{3.6h}$$

$$\int_A \rho^* \, y \, dA = S_y(x) = \rho \, y_a \, A(x) \tag{3.6i}$$

$$\int_A \rho^* \, z \, dA = S_z(x) = \rho \, z_a \, A(x) \tag{3.6j}$$

$$\int_A \rho^* \, yz \, dA = S_{yz}(x) = \rho \, y_a \, A(x) \tag{3.6k}$$

The x, y, z displacements based on the Bernoulli assumptions are, respectively,

$$\bar{U} = u - yv_{,x} - zw_{,x} \tag{3.7a}$$

$$\bar{V} = v - z\theta_x \tag{3.7b}$$

$$\bar{W} = w + y\theta_x \tag{3.7c}$$

The strain-displacement equations are

$$\varepsilon_x = u_{,x} - yv_{,xx} - zw_{,xx} \tag{3.8a}$$

$$\gamma_{xy} = -z\theta_{x,x} \tag{3.8b}$$

$$\gamma_{xz} = y\theta_{x,x} \tag{3.8c}$$

Use of these equations, together with the assumptions $\sigma_y = \sigma_z = \tau_{yz} = 0$ and the stress-strain relations

$$\sigma_x = E\,\varepsilon_x \tag{3.9a}$$

$$\tau_{xy} = G\,\gamma_{xy} \tag{3.9b}$$

$$\tau_{yz} = G\,\gamma_{xz} \tag{3.9c}$$

leads to the strain energy expression

$$U = \frac{1}{2}\int_0^L [EA(x)\,u_{,x}^2 + E\bar{I}_z(x)\,v_{,xx}^2 + E\bar{I}_y(x)\,w_{,xx}^2 + 2E\bar{I}_{yz}(x)v_{,xx}\,w_{,xx} + GJ(x)\,\theta_{x,x}^2 - 2EA(x)\,u_{,x}(y_b v_{,xx} + z_b w_{,xx})]\,dx \tag{3.10}$$

where GJ(x) is the torsional stiffness.

Likewise, the equations (3.7) can be used in the kinetic energy expression

$$T = \frac{1}{2}\int_V \rho^* [\dot{\bar{U}}^2 + \dot{\bar{V}}^2 + \dot{\bar{W}}^2]\,dV \tag{3.11}$$

to obtain for constant beam density,

$$T = \frac{\rho}{2}\int_0^L [A(x)\,(\dot{u}^2+\dot{v}^2+\dot{w}^2) + \bar{K}_z(w)\dot{v}_{,x}^2 + \bar{K}_y(x)\dot{w}_{,x}^2 + 2\bar{K}_{yz}(x)\dot{v}_{,x}\dot{w}_{,x} + (\bar{K}_z(x)+\bar{K}_y(x))\dot{\theta}_x^2 - 2A(x)\dot{u}(y_a\dot{v}_{,x} + z_a\dot{w}_{,x}) + 2A(x)\dot{\theta}_x(y_a\dot{w} - z_a\dot{v})]\,dx \tag{3.12}$$

The displacement patterns are the following polynomials in the variable $\xi = x/L$

$$u = (1-\xi)u_1 + \xi u_2 \tag{3.13a}$$

$$v = (1-3\xi^2+2\xi^3)v_1 + L(\xi-2\xi^2+\xi^3)v_{x1} + (3\xi^2-2\xi^3)v_2 + L(-\xi^2+\xi^3)v_{x2} \tag{3.13b}$$

$$w = (1-3\xi^2+2\xi^3)w_1 + L(\xi-2\xi^2+\xi^3)w_{x1} + (3\xi^2-2\xi^3)w_2 + L(-\xi^2+\xi^3)w_{x2} \tag{3.13c}$$

$$\theta_x = (1-\xi)\theta_{x1} + \xi\theta_{x2} \tag{3.13d}$$

where the subscripts 1 and 2 denote the values at the ends of the beam. It should also be noted that

$$v_{xi} = \theta_{zi} \tag{3.14a}$$

$$w_{xi} = -\theta_{yi} \tag{3.14b}$$

since small rotations are assumed. Using these expressions in Equations (3.10) and (3.12) leads to the quadratic forms for the strain and kinetic energies,

$$U = \frac{1}{2} \{q\}^T [k] \{q\} \tag{3.14}$$

$$T = \frac{1}{2} \{q\}^T [m] \{\dot{q}\} \tag{3.15}$$

respectively, where the generalized coordinates are ordered

$$\{q\} = \{u_1, v_1, w_1, \theta_{x1}, \theta_{y1}, \theta_{z1}, u_2, v_2, w_2, \theta_{x2}, \theta_{y2}, \theta_{z2}\}$$

The [k] and [m] stiffness and mass matrices are of order 12 and include the effect of a linear variation material and geometric properties.

3.3 STATIC REANALYSIS

The static, elastic deflection analysis for an unmodified structure involves computing the solution of equations (3.1) as discussed in Section 3.1. Efficient reanalysis methods should make maximum use of the Choleski decomposition of the unmodified stiffness matrix.

When a set of structural elements are removed or partially removed due to damage, the reanalysis problem becomes

$$[\bar{K}]\ \{\bar{x}\} = \{\bar{F}\} \tag{3.16}$$

where the modified stiffness and loading matrices can be written as the original quantities minus known perturbations as follows:

$$[\bar{K}] = [K] - [K_1] \tag{3.17}$$

$$\{\bar{F}\} = \{F\} - \{F_1\} \tag{3.18}$$

The modified stiffness matrix can be positive definite for small damage; however, $[K_1]$ will be just positive since it contains at least n-m rows and columns of zeros where m is the total number of degrees of freedom affected by the damaged elements.

The work by Venkayya, et al.[3] shows how the perturbed response vector, $\{\bar{x}\}$, can be iteratively determined without directly solving equation (3.16). The reanalysis formula which was developed is

$$\{\bar{x}^{(\nu+1)}\} = [A]\ \{\bar{x}^{(\nu)}\} + \{x\} \tag{3.19}$$

where $[A] = [K]^{-1}\ [K_1]$. This iteration starts with $\{x^{(0)}\} = \{x\}$.

To derive an iteration scheme including $\{F_1\}$, introduce the perturbation parameter, ε, which scales the damage terms of the stiffness matrix and load vector as follows:

$$[K_1] = \varepsilon[K_o] \tag{3.20a}$$

$$\{F_1\} = \varepsilon\{F_o\} \tag{3.20b}$$

As in classical perturbation theory, expand the modified response in a power series

$$\{x\} = \{x_o\} + \varepsilon\{x_1\} + \varepsilon^2\{x_2\} + \varepsilon^3\{x_3\} + \ldots \tag{3.21}$$

where $\{x_o\} = \{x\}$ and $\{x_1\}$, $\{x_2\}$, ... are undetermined vectors.

Next, substitute equations (3.20) and (3.21) into equation (3.16) and group terms into coefficients of ε. This gives a homogeneous system which implies that all coefficients are zero. The following system is thus obtained:

$$\{y_o\} = \{x\} \tag{3.22a}$$

$$\{y_1\} = [A]\{y_o\} - [K]^{-1}\{F_1\} \tag{3.22b}$$

$$\{y_i\} = [A]\{y_{i-1}\} \qquad i = 2,3,\ldots \tag{3.22c}$$

where $\{y_i\} = \varepsilon^i\{x_i\}$ and $[A] = [K]^{-1}[K_1]$. A $(\nu+1)^{th}$-order accurate estimate of $\{\bar{x}\}$ is obtained by adding the first ν equations of (3.22) to get

$$\{\bar{x}^{\nu+1}\} = [A]\{x^{(\nu)}\} + \{x\} - [K]^{-1}\{F_1\} \tag{3.23}$$

It is important to note that $[K]^{-1}$ is never formed when equation (3.23) is applied. The next response iterate is determined by forward and back substitution based on the decomposition of the unmodified stiffness matrix.

In the case that $\{F_1\} = \{0\}$, equation (3.23) has the form

$$\{\bar{x}^{(\nu+1)}\} = \left([A]^{\nu+1} + [A]^{\nu} + \ldots + [A]+[I]\right)\{x\} \tag{3.24}$$

It is easy to show that equation (3.24) is the first $\nu+1$ terms in a Taylor series in ε as follows. Note that the Taylor series

$$\{\bar{x}(\varepsilon)\} = \{x\} + \varepsilon\{\bar{x}_1(0)\} + \frac{\varepsilon^2}{2!}\{\bar{x}_2(0)\}+\ldots+\frac{\varepsilon^{\nu+1}}{(\nu+1)!}\{\bar{x}_{\nu+1}(0)\}$$

$$+\ldots \qquad (3.25)$$

where $\{\bar{x}_j(0)\}$ denotes the $j^{\underline{th}}$ derivative of $\{\bar{x}\}$ at $\varepsilon=0$. By direct differentiation of equation (3.16) it can be shown that

$$\{\bar{x}_j(0)\} = n[K]^{-1}\{\bar{x}_{j-1}(0)\} = \frac{j!}{\varepsilon^j}\,[A]^n\{x\} \qquad (3.26)$$

Use of equation (3.26) in (3.25) yields equation (3.24). Thus each cycle of simple iteration is equivalent to adding an additional higher order term to the Taylor series.

An approach to a convergence study of equation (3.23) is most easily demonstrated by considering the $\{F_1\} = \{0\}$ case. The equation (3.24) is reminiscent of an iterative method for solving a linear eigenvalue problem. Therefore, we can study the convergence of equation (3.24) by considering the following eigenvalue problem

$$\mu_i\,\{\phi_i\} = [A]\,\{\phi_i\} \qquad (3.25)$$

where μ_i and $\{\phi_i\}$ are the $i^{\underline{th}}$-eigenvalue and eigenvector, respectively, or equivalently,

$$\mu_i[K]\{\phi_i\} = [K_1]\{\phi_i\} \qquad (3.26)$$

Since [K] and $[K_1]$ are at least positive semi-definite, with [K] positive definite, then {x} has a unique expansion in terms of the [K]-orthonormalized eigenvector of [A],

$$\{x\} = \alpha \sum_{i=1}^{n} c_i\,\{\phi_i\} \qquad (3.27)$$

where $c_i = \{\phi_i\}^T\,[K]\,\{x\}/\alpha$ and $\alpha = \max(\{\phi_i\}^T\,[K]\,\{x\})$. Substitution of equation (3.27) into (3.24) gives a geometric series in μ_i,

$$\{\bar{x}^{(\nu+1)}\} = \sum_{i=1}^{n} \sum_{j=0}^{\nu+1} c_i \mu_i^j \{\phi_i\} \tag{3.28}$$

Now, if

$$\mu_1 < 1 \tag{3.29}$$

the series converges to

$$\{x\} = \alpha \sum_{i=1}^{n} (c_i/(1-\mu_i))\{\phi_i\} \tag{3.30}$$

where the eigenvalues have been ordered as $\mu_1 \geq \mu_2 \geq \ldots \geq \mu_n$. Thus equation (3.30) is the theoretical limit of the iteration formula (3.24) subject to the convergence criteria of equation (3.29).

A useful quantity in damage assessment can be the ratio of the strain energy in the damaged structure to that of the undamaged one, i.e.,

$$\bar{U}/U = \{\bar{x}\}^T[\bar{K}]\{\bar{x}\}/\{x\}^T[K]\{x\} \tag{3.31}$$

By using equation (3.27) and (3.3), this is computed to be

$$U/U = \sum_{i=1}^{n} (c_i^2/(1-\mu_i))/\sum_{i=1}^{n} c_i^2 \tag{3.32}$$

which by the extremal properties of Rayleigh's quotient is bounded by

$$1/(1-\mu_n) \leq \bar{U}/U \leq 1/(1-\mu_1) \ . \tag{3.33}$$

Thus, if we define a sequence of stiffness damage perturbation matrices, $[K_j]$, j=1,...,N, where N is the number of damage cases, and we define $\mu_1^{(j)}$ to be the maximum eigenvalue associated with the j^{th} eigenproblem (see equation (3.26)), then the potentially most dangerous damage case has

$$\mu_1^* = \max_j \left(\mu_i^{(j)}\right)$$

as its largest eigenvalue. It is easily verified that a first order estimate of μ_1^* is

$$\mu_1^* = \max_i (1+\{\xi\}^T([I]-[K_i])\{\xi\})/\beta \qquad (3.34)$$

where $(\beta,\{\xi\})$ are the dominant eigenpair of the undamaged stiffness matrix; i.e., $(\beta,\{\xi\})$ satisfy

$$[K]\{\xi\} = \beta\{\xi\} \qquad (3.35)$$

This system is easily solved by matrix iteration, and, hence, a trial estimate of the most critical damage case can be quickly identified by Equation (3.34).

3.3.1 Collapse Analysis Based on Direct Stiffness Variation

If the $[K_1]$ modification matrix is of the special form

$$[K_1] = [I] \tag{3.36}$$

the effect of direct stiffness variations (changes in the diagonal terms of the stiffness matrix) can be quickly assessed by the techniques of this section. For changes of the form above, the equivalent iterative expression for the response of the modified system is

$$\left\{\bar{x}^{(\nu+1)}\right\} = \sum_{i=1}^{n} \sum_{j=0}^{\nu+1} c_i \left(\frac{\varepsilon}{\lambda_i}\right)^j \{\phi_i\} \tag{3.37}$$

where $(\lambda_i, \{\phi_i\})$ are the eigenpairs of

$$\lambda_i\{\phi_i\} = [K]\{\phi_i\} \tag{3.38}$$

In order for the above iterations to converge,

$$|\varepsilon| < \lambda_i \qquad i = 1,\ldots,n \tag{3.39}$$

To see how this iteration and convergence criterion can be applied, consider the following simple example. Let

$$[K] = \begin{bmatrix} 5 & 4 & 3 \\ 4 & 7 & 4 \\ 3 & 4 & 4 \end{bmatrix}, \quad \{F\} = \begin{bmatrix} 1 \\ 1 \\ 1 \end{bmatrix}$$

and $\varepsilon = 2$. The first four iterates are

$$\begin{bmatrix} .793 \\ 1.069 \\ .586 \end{bmatrix}, \quad \begin{bmatrix} .840 \\ .731 \\ 1.095 \end{bmatrix}, \quad \begin{bmatrix} .884 \\ 1.281 \\ .258 \end{bmatrix}, \quad \begin{bmatrix} .711 \\ .414 \\ 1.673 \end{bmatrix}$$

The iterates continue to increase in vector norm and essentially become unbounded.

An eigenanalysis using the power method on this matrix shows after five iterations starting with a vector with unit entries, gives $\lambda_1 = 12.9$, the largest eigenvalue. Using the eigenshift technique on the system

$$([K] - \lambda_1[I])\{\phi\} = \mu\{\phi\} \tag{3.40}$$

where

$$\mu = \lambda_n - \lambda_1$$

gives $\lambda_1 = 1.2$ as the smallest eigenvalue. Again the power method is easily applied. Thus, by equation (3.39) we see that direct stiffness modifications must be less than 1.2 in magnitude. When they are larger than this, it causes the stiffness matrix to no longer be positive definite and hence a kinematic instability or collapse mode is possible.

In the above example, if ε is reduced to 1.1, simple iteration will converge to three place accuracy in 67 iterations. Clearly, the need exists to accelerate the convergence of the iterations if possible.

3.3.2 Acceleration of Convergence

Iterations of the form given in equation (3.23) are an n-dimensional generalization of the simple fixed point iteration problem[27-28]:

$$x_{n+1} = g(x_n) \tag{3.41}$$

This generates a sequence $x_1, x_2, \ldots$ which we want

$$\lim_{n\to\infty} x_n = \xi$$

Figure 3.3 shows a convergent fixed point iteration and acceleration by Aitkin's-Δ^2 process. From the figure, note that

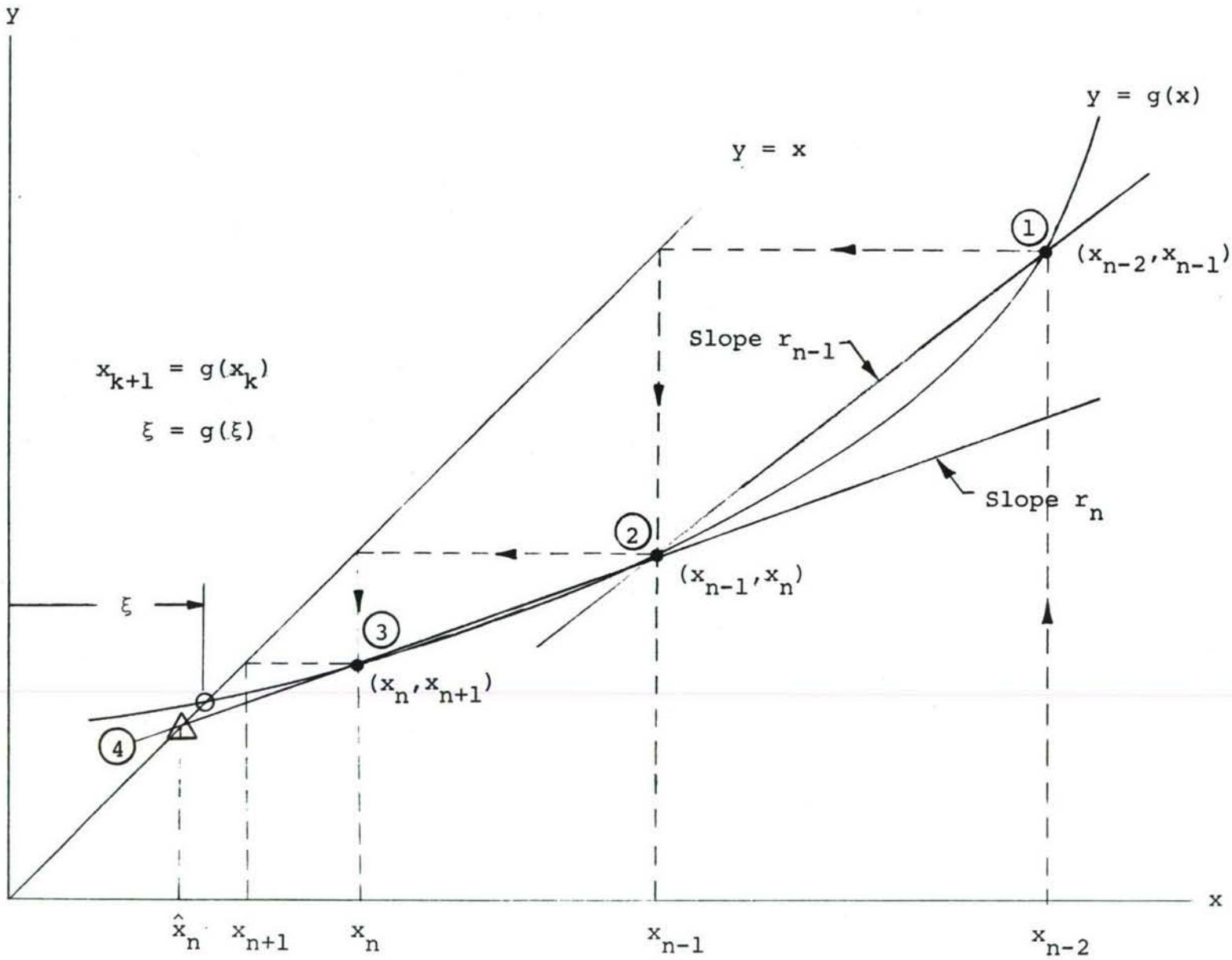

Figure 3.3. Acceleration of Fixed-Point Iteration by Aitken's-Δ^2 Process.

$$r_{n-1} = (x_n - x_{n-1})/(x_{n-1} - x_{n-2}) \tag{3.42}$$

$$r_n = (x_{n+1} - x_n)/(x_n - x_{n-1}) \tag{3.43}$$

When $r_n < 1$ and

$$\frac{r_n - r_{n-1}}{r_n} < \varepsilon \tag{3.44}$$

for some small $\varepsilon > 0$, then Aitken's-Δ^2 process consists of extrapolating the straight line segment joining points 2 and 3 to the intersection with the line y=x (point 4). The rationale is that if $r_n < 1$ and equation (3.44) holds, then the g(x) curve slope is not rapidly changing and then a straight line extrapolation will intersect the line y=x near ξ. The coordinate for the extrapolated point is

$$\hat{x}_n = x_{n+1} - \frac{(\Delta x_n)^2}{\Delta^2 x_{n-1}} \tag{3.45}$$

where

$$\Delta x_k = x_{k+1} - x_k$$

and

$$\Delta^2 x_k = \Delta x_{k+1} - \Delta x_k$$

In the ADDRESS code, the vector of modified responses for each damage case are computed by equation (3.23). For two consecutive iterates, the error is defined as

$$e^{(\nu+1)} = \max_{j=1,..,L} \left[\sum_{i=1}^{N} (\bar{x}_{ij}^{(\nu+1)} - \bar{x}_{ij}^{(\nu)})^2 \right]^{1/2} \tag{3.46}$$

where L is the number of load cases and N is the number of unconstrained degrees of freedom. The ratio of consecutive errors

$$r^{(\nu+1)} \equiv e^{(\nu+1)}/e^{(\nu)} \tag{3.47}$$

is tested to make sure it is less than 1.0 and

$$(r^{(\nu+1)} - r^{(\nu)})/r^{(\nu+1)} < .1 \tag{3.48}$$

is required before the extrapolation

$$\hat{x}_{ij} = x_{ij}^{(\nu+1)} - \frac{(x_{ij}^{(\nu+1)} - x_{ij}^{(\nu)})^2}{x_{ij}^{(\nu+1)} - 2x_{ij}^{(\nu)} + x_{ij}^{(\nu-1)}} \tag{3.49}$$

is performed. Equation (3.49) is the vector analog of equation (3.45). Equations (3.44) and (3.48) are analogous where ε is selected to be 0.1.

3.4 VIBRATION ANALYSIS

This subsection describes the analytical technique that was used to solve the eigenvalue problem

$$\lambda[M]\{x\} = [K]\{x\} \tag{3.50}$$

where [M] is the global mass matrix (including non-structural mass items), and [K] is the global stiffness matrix. The solution to equation (3.50) is given by $(\lambda_i, \{x_i\})$, i=1,...,n where λ_i is the i^{th} eigenvalue (natural frequency squared), and $\{x_i\}$ is the i^{th} eigenvector (mode shape). The order of the system is n, and the lowest m (m < n) frequencies and corresponding mode shapes, and the generalized masses are desired. The generalized masses are defined as

$$m_i = \{x_i\}^T [M]\{x_i\} \qquad i = 1,...,m<n \tag{3.51}$$

The ADDRESS system uses a simultaneous iteration algorithm (SIMIT)[29] to compute the modes and frequencies. This method was selected because of its excellent convergence characteristics and its relative simplicity. The procedure takes a minimum of storage and is easily adapted for the calculation of unrestrained modes. The basic steps of SIMIT are as follows:

1. Set random trial vectors [U] and orthogonalize
2. Solve for [Y]: $[L]^T[Y] = [U]$
3. Form [Z]: $[Z] = [M]\ [Y]$
4. Solve for [V]: $[L]\ [V] = [Z]$
5. Form [W]: $[W] = [V]\ [T^*]$ and estimate λ_i (see below for definition of $[T^*]$)
6. Form $[\bar{U}]$ by Schmidt orthogonalization of [W]
7. Test $\|U-\bar{U}\| < \varepsilon$
8. If test of Step 7 passes, then solve $[L]^T\ [X] = [\bar{U}]$ and print the eigenvectors [X] and eigenvalues λ_i. If test of Step 7 fails, then set $[U] = [\bar{U}]$ and go to Step 2.

The key step in the method is a matrix iteration of the form $[A]\ [U] = [V]$ where [A] is a symmetric matrix, [U] is an n by m matrix of iterated vectors. Note that all modes of interest are simultaneously iterated. In practice, it is necessary to use about twice as many trial vectors as the number of vectors desired. The SIMIT method differs from the usual matrix iteration method in that a sweeping matrix is not required. Also, the $[K]^{-1}[M]$ matrix is never formed.

As stated above, the matrix [A] must be symmetric. An important step in the SIMIT technique is to transform the eigenvalue problem of equation (3.50) to the form

$$[A]\{q\} = \lambda\{q\} \tag{3.52}$$

where [A] is symmetric, which has the eigensolutions (λ_i, q_i), $i = 1,\ldots,n$. This can be accomplished by defining

$$[A] = [L]^{-1}[M][L]^{-T} \tag{3.53a}$$

$$\{q\} = [L]^T\{x\} \tag{3.53b}$$

where $[K] = [L][L]^T$. Note that [A] so defined is symmetric and that the eigenvalue problem described by Equations (3.52) and (3.53) is equivalent to equation (3.50).

In practice, the matrix [A] is never explicitly formed. Instead, for a given set of trial vectors [U], the product [A][U] is formed in the following steps:

1. Solve $[L]^T[Y] = [U]$ for [Y] by back substitution
2. Form [Z] = [M][Y] by premultiplication of [Y] by [M]
3. Solve [L][V] = [Z] for [V] by forward substitution.

It is easily verified that the above steps which make use of the properties of the [L] matrix are equivalent to forming the matrix product [A][U]. In the ADDRESS program, [L] is stored in "skyline" or variable bandwidth form.

The diagonal terms of $[U]^T[V]$ are used as the first estimates of the eigenvalues. The eigenvectors must be modified before the next step, since they would otherwise all converge to the vector corresponding to the largest eigenvalue. In the terminology of Reference 29, an "interaction analysis" is performed on the vector which decouples them. The decoupled vectors, [W], follow from the matrix multiplication

$$[W] = [V][T^*] \tag{3.54}$$

where [T*] has unit diagonal terms and skew-symmetric off-diagonal terms given by

$$t^*_{ij} = 2b_{ij}/c_{ij} \tag{3.55}$$

where b_{ij} are the elements of the "interaction matrix"

$$[B] = [U]^T[V] \tag{3.56}$$

and

and

$$c_{ij} = b_{ii} - b_{jj} + S\sqrt{(b_{ii}-b_{jj})^2+16b_{ij}^2} \qquad (3.57)$$

with S equal to the sign of $b_{ii}-b_{jj}$. The [W] vectors are then made orthogonal by the usual Grahm Schmidt orthogonalization process. By efficient use of storage registers, it is not necessary to have separate storage for the [B] and [T*] matrices.

The orthogonalized vectors $[\overline{U}]$, obtained from the [W] matrix and then stored in [U] and the iteration is continued. The process is completed by performing either a specific number of iterations or by achieving a given small error on the Euclidean norm of $[U]-[\overline{U}]$.

The final step of the procedure is to use back substitution to recover the mode shapes for the original vibration problem of equation (3.50). This is accomplished by solving equation (3.53b) where the columns of the converged [U] are the $\{q_i\}$ vectors.

A number of investigators have used SIMIT (see Reference 29) on large sized problems. Although the basis for the interaction analysis as presented in Reference 29 is somewhat empirical, numerical results have been consistently good.

In the case of unrestrained structures, the [K] matrix will not be positive definite. In this case, use can be made of the eigenvalue shifting technique. The quantity $\mu[M]\{x_i\}$ is added to both sides of equation (3.50) where μ is a predetermined positive constant. Hence, the "shifted problem" becomes

$$[K]\{x\} = \eta[M]\{x\} \qquad (3.58a)$$

where

$$[K] = [K] + \mu[M] \qquad (3.58b)$$

$$\eta = \lambda + \mu \qquad (3.58c)$$

For the work herein, μ is selected as

$$\mu = \min_{j} \left(K_{jj}/M_{jj}\right) \qquad (3.58d)$$

where K_{jj} and M_{jj} are the diagonal terms of the stiffness and mass matrices, respectively. Hence, for unrestrained modal calculations, equation (3.58a) is solved by the SIMIT technique, and the desired eigenvalues are then recovered by solving equation (3.58c) for λ_i. It is important to note that even the zero frequency node shapes are obtained in the solution of equation (3.58a).

3.5 FREQUENCY AND MODE SHAPE REANALYSIS

A number of papers have been written on the rates of change of eigenvalues and eigenvectors with respect to system parameters (see References 19-23, for example). Hemming, et al.[24] have developed a technique specifically for the analysis of damaged structures. The eigenvalues are determined from a Rayleigh quotient procedure for the frequency calculation; however, the modified vectors are iteratively determined from solving a system of equations based on the decomposition of the stiffness matrix for the undamaged structure.

The reanalysis procedure is derived by first considering the vibration problem for the undamaged structure

$$[K]\{x_i\} = \lambda_i [M]\{x_i\} \qquad i = 1,\ldots,m \qquad (3.59)$$

and a particular damage case

$$[\bar{K}]\{\bar{x}_i\} = \bar{\lambda}_i [\bar{M}]\{\bar{x}_i\} \qquad i = 1,\ldots,m \qquad (3.60)$$

where

$$[\bar{M}] = [M] - [M_1] = \text{modified mass matrix}$$
$$\{\bar{x}_i\} = \{x_i\} - \{x_{i1}\} = \text{modified eigenvectors}$$
$$\bar{\lambda}_i = \lambda_i - \lambda_{i1} = \text{modified eigenvalues}$$

and [K] is given by equation (3.17).

The iteration equation for the $i^{\underline{th}}$ modified eigenvalue has been selected to be the Rayleigh quotient for equation (3.60),

$$\lambda_i^{(\nu)} = \left\{\bar{x}_i^{(\nu)}\right\}^T [\bar{K}]\left\{\bar{x}_i^{(\nu)}\right\} \Big/ \left\{\bar{x}_i^{(\nu)}\right\}^T [\bar{M}]\left\{\bar{x}_i^{(\nu)}\right\} \tag{3.61}$$

where (ν) denotes the iteration counter. The starting mode shapes on the right side of equation (3.61) are taken to be the mode shapes of the undamaged system. The iteration equations for the i^{th} eigenvector are obtained by substituting equation (3.61) into (3.60) and rewriting in the iterative form

$$[K]\left\{\bar{x}_i^{(\nu+1)}\right\} = (\bar{\lambda}_i^{(\nu)} [\bar{M}] + [K_1]) \left\{\bar{x}_i^{(\nu)}\right\} \tag{3.62}$$

The flow of calculations is then as follows:

1. Solve equation (3.59) by simultaneous iteration and save the decomposition of the stiffness matrix.

2. Evaluate equation (3.61) to get the first estimates of the eigenvalues.

3. Solve equation (3.62) using the decomposition of the stiffness matrix determined in Step 1. Iterate this equation several times until the norm of the vectors changes less than some specified amount.

4. Orthogonalize the last set of iterated vectors from Step 3 with respect to the modified stiffness matrix.

5. Repeat Steps 2, 3, and 4 a prespecified number of times. Each time Step 2 is performed, use the last set of eigenvectors obtained from Step 4 as input.

The iteration scheme used herein is similar to that of Rudisill and Chu.[22] In their work, however, they are considering the <u>derivative</u> problem rather than the <u>perturbation</u> problem. In Reference 22, the eigenproblem is differentiated and terms are rearranged so that eigenvector derivatives appear on both sides

of the equation. This form is then used as the basis for a fixed-point iteration scheme.

Several key questions arise in the use of iteration expressions such as these:

1. Do the iterations converge?
2. Do they converge to a unique solution?
3. Is it the correct solution?

Reference 23 deals with such questions for the Rudisill-Chu iteration method. The method converges for the dominant eigenvector/eigenvalue; however, in other cases the solution characteristics can depend on the initial guess for the eigenvector derivative.

For the perturbation method used herein, satisfactory results have been obtained when the mass and stiffness changes are small. This implies that mode shape changes are not large. Numerical results are presented in Section 5 herein.

3.6 OPTIMIZATION FOR STRESS AND DEFLECTION REQUIREMENTS

Following a development similar to the optimality criterion approach of Reference 30, the object of the optimization process is to provide a structure which is satisfactory from a stress and deflection standpoint and has minimum total weight. It is further required that the structure also satisfy these requirements in its damaged configuration or configurations.

The total structural weight of a finite element model with "m" elements is

$$W = \sum_{i=1}^{m} \rho_i \, A_i \, \ell_i \tag{3.63}$$

where ρ_i is the mass density and $A_i \ell_i$ is volume of the i^{th} element. If the elements are bars, then A_i is the cross-sectional area and ℓ_i is the length. For membrane and shear panels the A_i and ℓ_i are the thickness and area, respectively. The beam element variables are the same as for the bars.

A necessary condition for an optimal design is that the function

$$\phi = \sum_{i=1}^{m} \rho_i A_i \ell_i - \lambda Z \tag{3.64}$$

be stationary with respect to the design variables, A_i, where λ is a Lagrange multiplier and Z is a stiffness requirement. When Z is selected as the strain energy of the structure, it can be shown that the stationary conditions lead to the following statement of the optimality criterion for the generalized stiffness requirement:

> "The optimum structure for a generalized stiffness requirement is the one in which the ratio of the average strain energy density to its mass density is the same for all elements."

When a displacement constraint is present, the stiffness requirement has the form of the virtual work expression

$$Z = \{F\}^T \{r\} \tag{3.65}$$

where {F} is a unit load vector and {r} is the generalized displacement vector. The unit load vector contains zeroes except in the unit entry corresponding to the displacement constraint. Again, from the stationary condition of the ϕ function, the following statement of the optimality criterion is given as follows:

> "The optimum structure for a specified displacement is the one in which the ratio of average virtual strain energy density to the mass density is the same for all elements."

Damage cases are handled in the same way that multiple loading conditions are treated. The optimality conditions then take the form

$$\lambda_1 e_i^{(1)} + \lambda_2 e_i^{(2)} + \ldots + \lambda_p e_i^{(p)} = 1 \quad ; \quad i = 1,\ldots,m \tag{3.66}$$

where

$$e_i^{(j)} = \begin{cases} \frac{1}{2} \{r\}^T [K_i] \{r_j\} \; / \; \rho_i A_i \ell_i & \text{(Stress)} \\ \{f_j\}^T [K_i] \{r_j\} \; / \; \rho_i A_i \ell_i & \text{(Deflection)} \end{cases} \tag{3.67}$$

and $\{f_j\}$ is the displacement vector corresponding to the j^{th} unit load vector. The $[K_i]$ matrices are the stiffness contributions of the elements for i=1,...,m. The index p equals the number of damage cases times one plus the number of loading conditions.

Resizing of the element areas takes place in accordance with formulas of the type

$$(\alpha_i \Lambda)_{\nu+1} = (\alpha_i)\nu \sqrt{E_i} \tag{3.68}$$

where α_i is the normalized member size, Λ is a scale factor, ν denotes the iteration, and E_i is a weighted average of the strain energy density in the i^{th} element. The scale factor can be exactly determined for stress and deflection constraints.

In the ADDRESS computer code, resizing takes place first for the stress requirements and then for displacements. A specified number of resizings take place to make the strain energy density uniform in each element when subjected to the load case/damage conditions. The design is scaled so that all the stress and deflection requirements (if any) are satisfied. Resizing is terminated in the energy mode (i.e., stress constraints) if the weight increases. Resizing then takes place for the displacement requirements and checks are made on stress levels and appropriate scalings of member sizes are made. The algorithm is very similar to the ØPTSTAT[25] program except that additonal "pseudo load cases" (i.e., damage cases) are included.

3.7 OPTIMIZATION FOR VIBRATION REQUIREMENTS

Reference 31 develops an optimality criterion approach to the minimum weight design of structures subjected to dynamic loads. In many design problems, it is possible to characterize the dynamic load problem as a requirement that a given natural frequency not be lower than some specified value. Such frequency constraint problems are solvable by direct search techniques which involve the calculation of frequency gradients.

The optimality criterion approach does not treat a frequency as a formal constraint as indicated above, but rather the object is to obtain minimum weight with maximum stiffness. The optimality criterion is that difference between the strain energy density and the kinetic energy density (Lagrangian density) be uniform for all the elements when the structure is vibrating in its mode of interest. The resizing formula is the case in equation (3.68) where E_i is the Lagrangian density. The procedure[31] for using the resizing formula is as follows:

1. With an assumed relative design vector (such as $\alpha_1 = \alpha_2 = \ldots = \alpha_m = 1.0$), the desired normal mode and corresponding frequency ω_p are determined.

2. The relative strain energy and kinetic energy of each element in this mode is determined.

3. Each design variable for the next iteration is determined by substituting the relative energies in equation (3.68).

4. The design vector is normalized with respect to the largest variable. This normalization eliminates the need for determining the constant of proportionality, Λ. (The next section is concerned with determining this constant.)

5. The procedure is repeated until the optimality criterion is attained or a prespecified number of iterations have taken place.

Experience with the ADDRESS code has indicated that in the case of damage with small nonstructural mass, a frequency requirement is not a meaningful constraint. It is of interest, however, to

check the frequencies before and after damage. The frequencies of the optimal structure which is designed for stress, deflection, and damage tolerance under multiple loads does not have frequencies which are sensitive to changes in design variables.

If the structure is designed from only a frequency standpoint, it may be possible that the particular mode being tracked is no longer the mode with the smallest eigenvalue. For example, a uniform wing design may have its lowest frequency in the first bending mode. After several resizings, it may be possible for the first torsion mode frequency to be below the bending frequency. At this point the algorithm must shift to computing energies for the displacement pattern of the torsion mode. Although such conditions were not noted in the current study, they are of some potential importance. Eigenvalue solutions (see Reference 32, for example) should contain a Sturm sequence check in this case. This matter is further discussed in Section 7.

3.8 DESIGN SCALING

The process for determining the scale factor Λ in equation (3.68) is trivial in the case of stress and deflection constraints. Stresses and deflections are simply inversely proportional to the member sizes. For constraints on natural frequencies, the situation is not as simple. This can be seen by observing that when the mass and stiffness matrices are scaled in the Rayleigh quotient

$$\omega_i^2 = \frac{\{x_i\}^T[K]\{x_i\}}{\{x_i\}^T[M]\{x_i\}} \tag{3.69}$$

the frequency will remain unchanged. This problem was noted by Kuisalaas in Reference 33.

Frequencies can be modified, however, by scaling a portion of the mass and stiffness matrices. Assume that the global mass and stiffness matrices have the forms

$$[M] = [M_o] + \sum_{i=1}^{m} \alpha_i [M_i] \tag{3.70a}$$

$$[K] = [K_o] + \sum_{i=1}^{m} \alpha_i [K_i] \tag{3.70b}$$

where the $[M_o]$ and $[K_o]$ matrices correspond to mass and stiffnesses which remain fixed during the design scaling and optimization process. The α_i's are a set of relative design variables which are to be scaled by Λ to achieve a required natural frequency, ω_R.

Introduction of the unknown scale factor creates a new eigenvalue problem with Λ as the eigenvalue. Rearrangement of equation (3.69) using equations (3.70) and $\omega_i = \omega_R$, $\{x_i\} = \{x_R\}$ gives

$$\Lambda[A]\{x_R\} = [B]\{x_R\} \tag{3.71a}$$

where

$$[A] = \sum_{i=1}^{m} \alpha_i (\omega_R^2 [M_i] - [K_i]) \tag{3.71b}$$

and

$$[B] = [K_o] - \omega_R^2 [M_o] \tag{3.71c}$$

The smallest real eigenvalue, Λ^*, of the above problem (if one exists) will be the design scale factor which places the design exactly on the constraint boundary, $\omega_i - \omega_R = 0$.

To demonstrate the above scaling procedure, the optimal design of a tapered bar with a tip mass was studied. Figure 3.4 shows both a continuous model and a discrete model of the bar. Reference 34 gives the optimal mass distribution as

$$M(x) = M_o \cosh^2(\beta_1 L) \Big/ \cosh^2(\beta_1 x) \tag{3.72}$$

where M_o is the tip mass, L is the length, $\beta_1^2 = \omega_R \rho / E$, with ρ

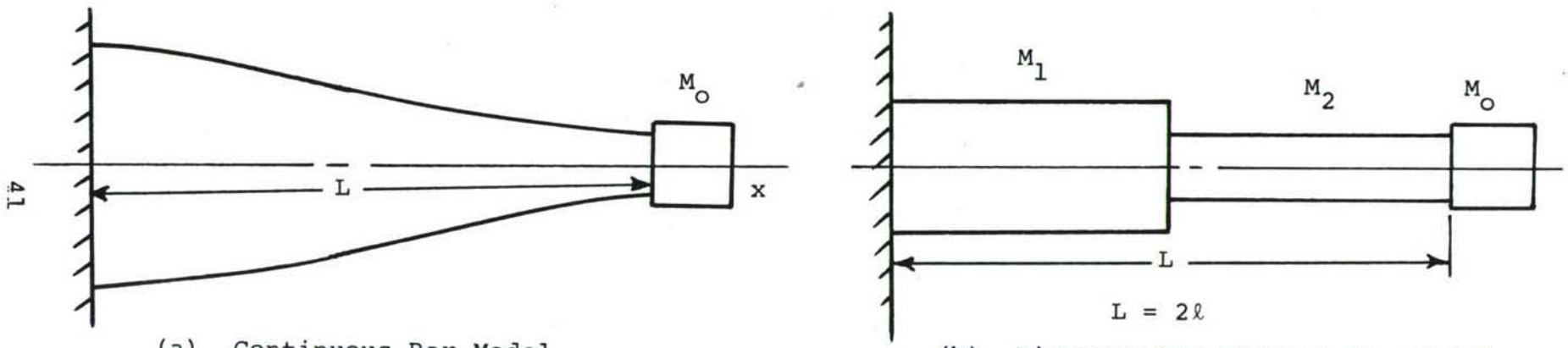

(a) Continuous Bar Model

(b) Discrete Two Element Bar Model

Figure 3.4. Tapered Bar with Tip Mass.

being the mass density and E is Young's modulus. The fundamental frequency, ω_R, is fixed. The total optimal mass of the continuous bar is

$$M_T = M_o \sinh^2(\beta_1 L) \tag{3.73}$$

which is the integral of equation (3.72). For illustrative purposes, the following data: L = 90 in., M_o = .05 lb.-sec.^{2}/in., $\rho = 2.59 \times 10^{-4}$ lb.-sec.^{2}/in.^{4}, $E = 10.3 \times 10^6$ psi, ω_R - 2578 rad/sec are used. Use of these values gives M_T = .104 lb.-sec.^{2}/in. The discrete model of Figure 3.4(b) consists of two axial bar elements of equal length.

Using the above material properties, constraint curves can be generated for various choices of the fundamental frequency, ω_R. Figure 3.5 shows frequency contours in the M_1 - M_2 design space for various choices of the eigenvalue $\lambda_1 = \rho\omega_R^2\ell^2/6E$. The λ_1 = .056 curve corresponds to the Reference 34 value of ω_R. For convex feasible regions such as those indicated by Figure 3.5, the scaling of the design along a vector from the origin to a feasible point is a well defined process.

Figure 3.6 shows contours of constant eigenvalues in the second mode. In this case the optimal design will be controlled by side constraints on M_1 and M_2 as well as the eigenvalue requirement. Thus, trends that are noted for the fundamental mode may not carry over for higher modes.

The value of the fixed mass, M_o, also strongly affects the frequency constraint. In Figure 3.7 three values of M_o were selected (.05, .10, and .20) and the contours of λ_1 = .056 were determined. For M_o = .05 the optimal design is M_1 = .076, M_2 = .034 and hence M_T = .110 which is about six percent higher than the continuous case. As M_o approaches zero, the optimal design problem becomes meaningless without side constraints.

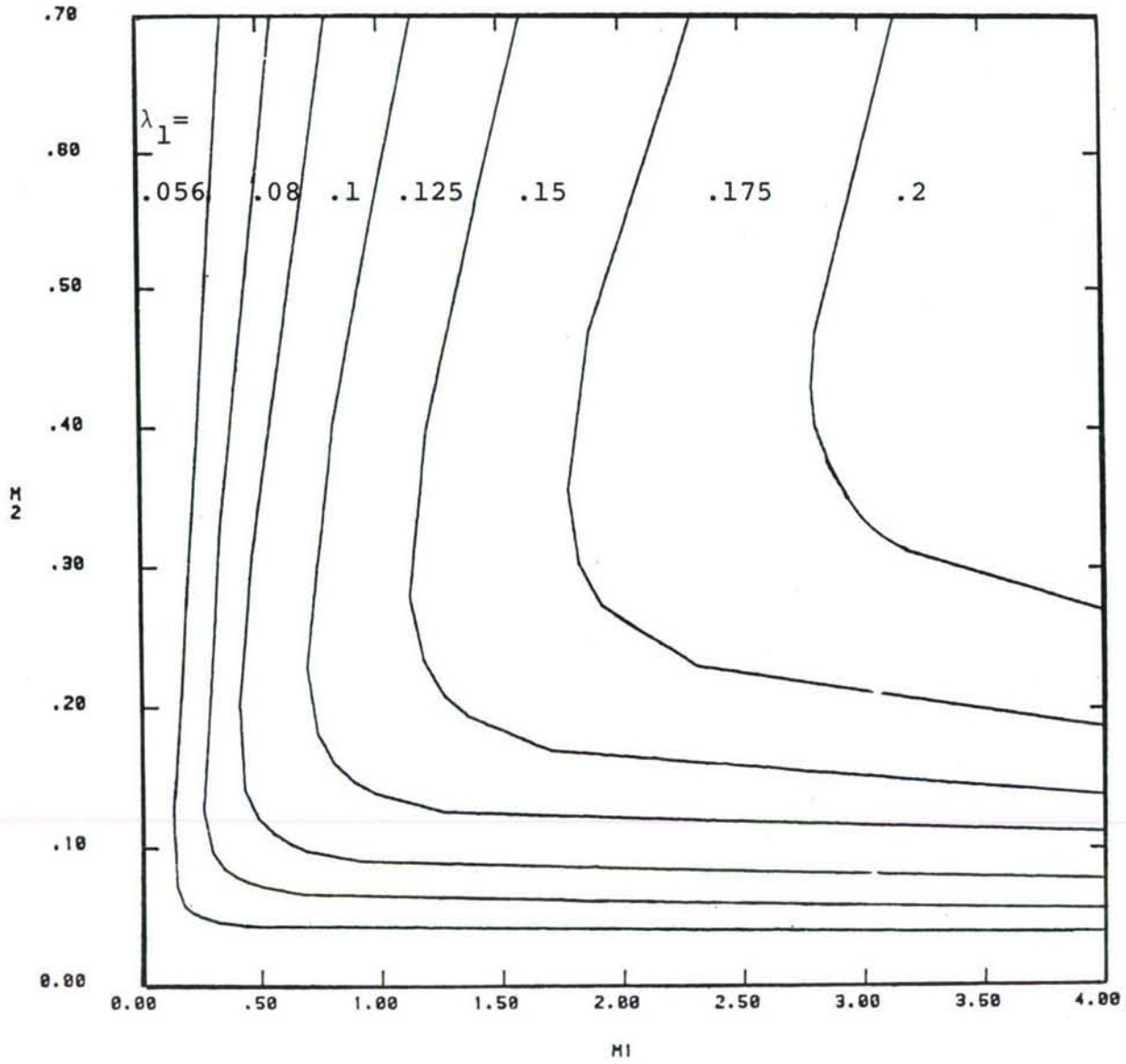

Figure 3.5. Mode 1 Eigenvalue Contours for Two Element Bar.

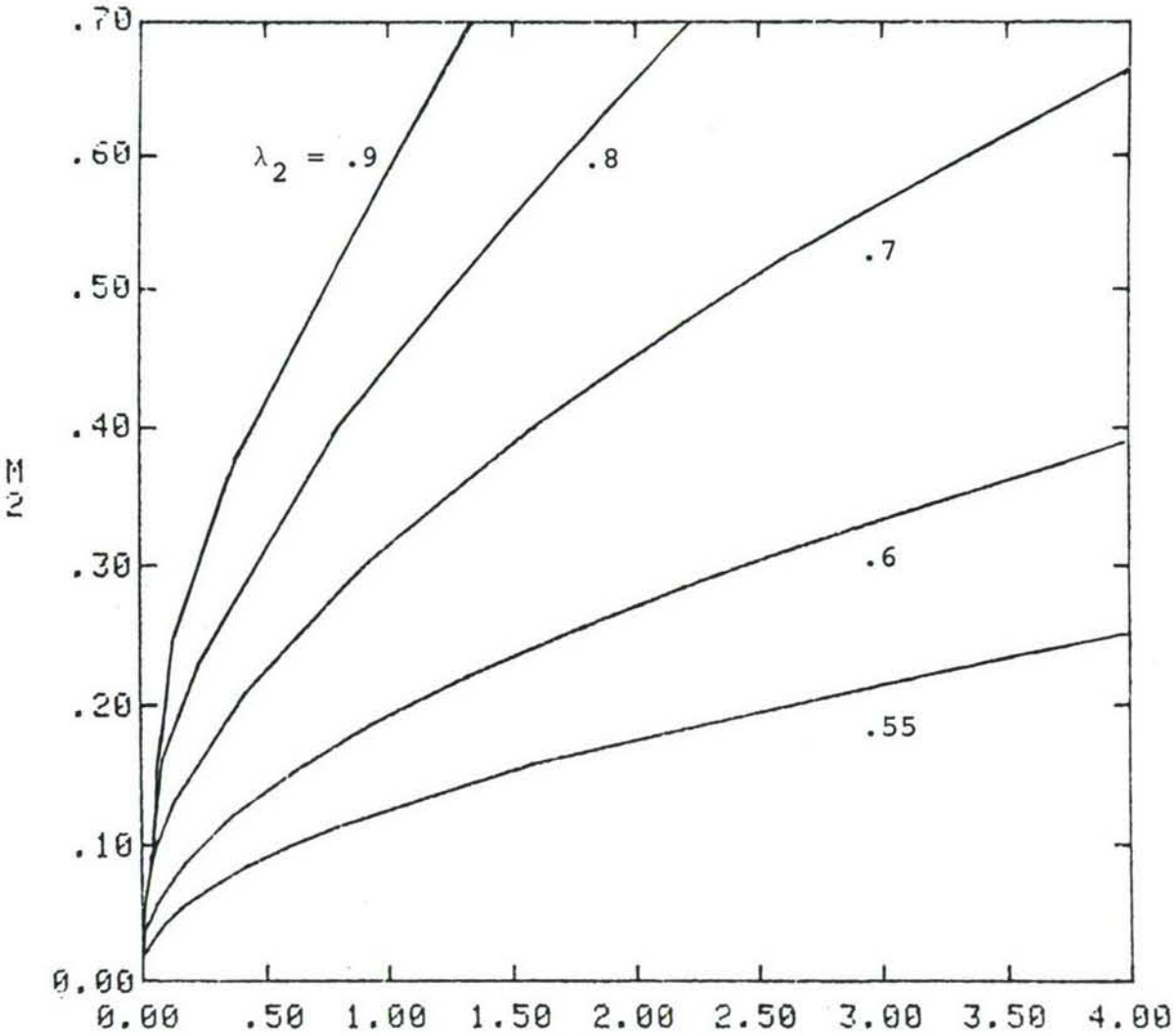

Figure 3.6. Mode 2 Eigenvalue Contours for Two Element Bar.

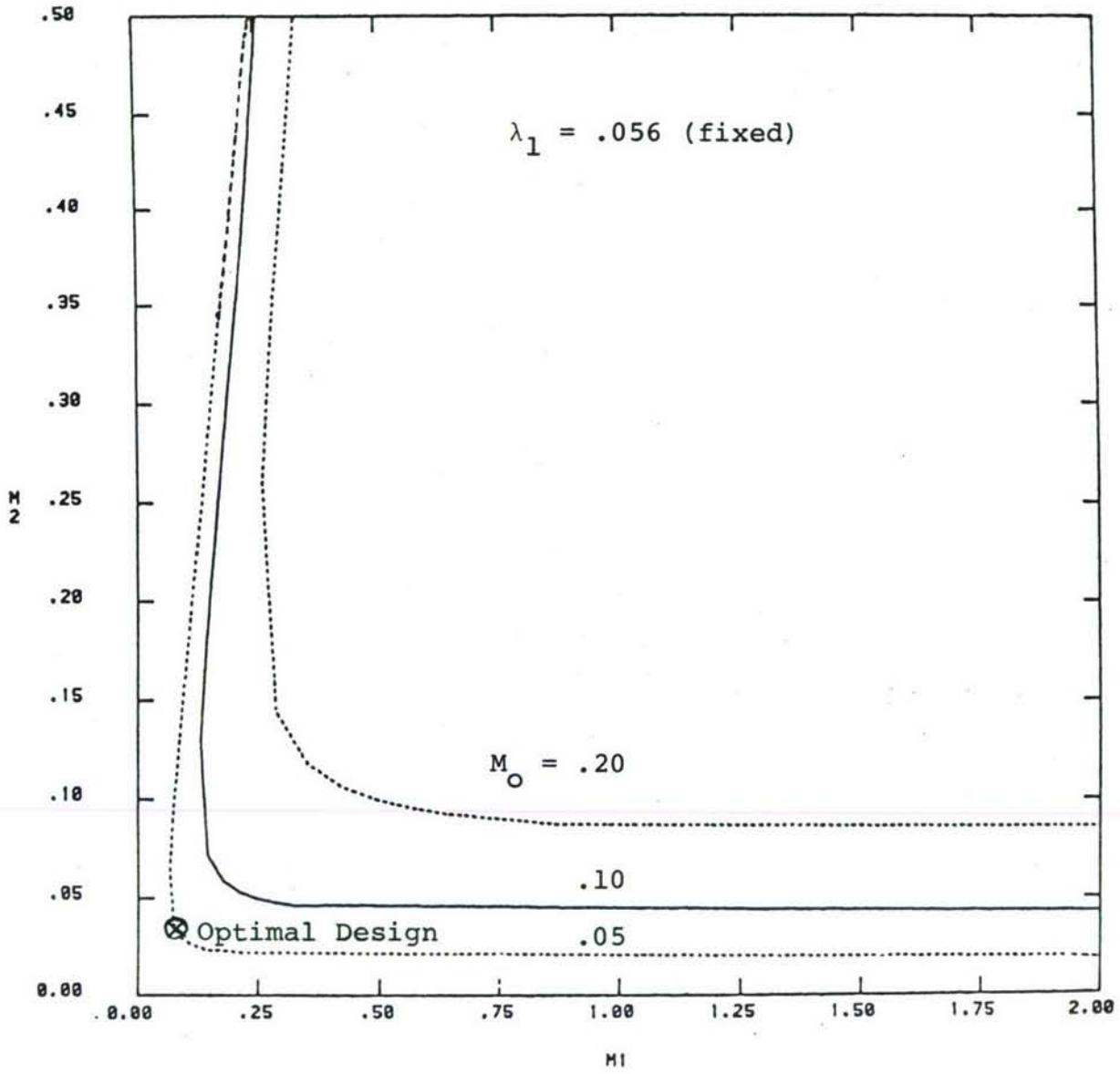

Figure 3.7. Effect of Tip Mass Variations on Mode 1 Eigenvalue for Two Element Bar.

The following design strategy achieves minimum weight for a given fundamental frequency requirement:

1. Form the characteristic determinant for the system shown in equation (3.71), treating Λ as the eigenvalue.

2. Find the smallest positive root Λ^* and the corresponding eigenvector $\{X_R^*\}$.

3. Compute the weight using Λ^* as the scale factor.

4. Compute the Lagrangian densities, e_i, for each element.

5. Resize according to $M_{i\ new} = M_{i\ old} \sqrt{|e_i|}$

6. Normalize the $M_{i\ new}$ design and go to Step 2.

7. Repeat Steps 2 - 5 a specified number of times or until the weight increases.

The above scaling and resizing procedure tends to equalize the energy (Lagrangian density) in all the elements and at the same time brings the design to the required fundamental frequency. It can be shown that the Lagrangian densities are directly proportional to the rates of change of the eigenvalues with respect to the element names. Thus uniform Lagrangian density implies equal sensitivity to design changes. The energies can sometimes be negative for a given element. This implies that increasing the element causes a reduction in the frequency. Note that the element resizing formula uses the absolute value of the element energies.

In the bar example, the mass and stiffness matrices are tridiagonal. The Sturm sequence of polynomials

$$P_1 = 1$$

$$P_2 = c_1$$

$$P_i = c_{i-1}P_{i-1} - b_{i-2}^2 P_{i-2} \qquad i=2,\ldots,n+1$$

are generated where the c_i's are the diagonal and the b_i's are the upper and lower diagonals. Sign alternations need to be checked to assure that the smallest eigenvalue is obtained. The

root is determined by using the golden section minimization technique[35] on the absolute value of the polynomial P_{n+1}. Reference 32 contains a listing of the eigenroutine. This software package also contains a Givens-Householder[36] routine to reduce equations (3.71) to tridiagonal form for more complex problems which are not tridiagonal. The golden section technique together with Sturm sequence checks is more efficient than the usual bisection or secant procedure.

Figure 3.8 shows scaling and resizing steps in design space for the two element bar. One scaling took the design from point A to point B which lies on the constraint. An energy resizing scaling step then brought the design to point C. Figure 3.9 shows how resizing proceeds from a different starting point. Additional resizings and scalings from point D tend to create a "zig-zag" path in which little additional weight is removed.

The above design scaling technique for frequency requirements needs further testing before it is included in the ADDRESS program. The results in this section are intended to show that frequency requirements can be met in a noniterative manner. The combination of scaling and energy resizing appears to have considerable promise for frequency constraints.

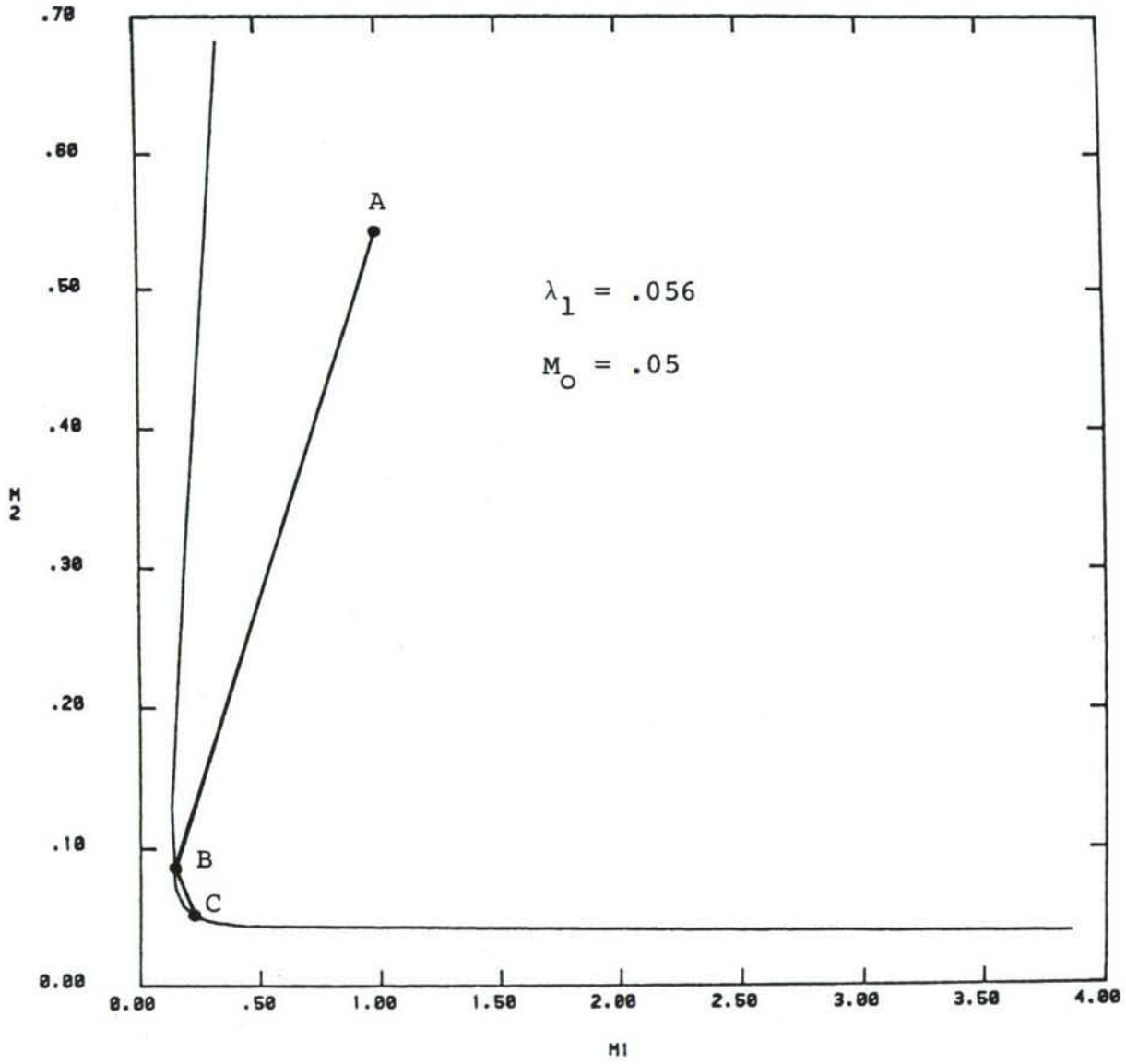

Figure 3.8. Frequency Constraint Resizing of Two Element Bar (One Energy Resizing).

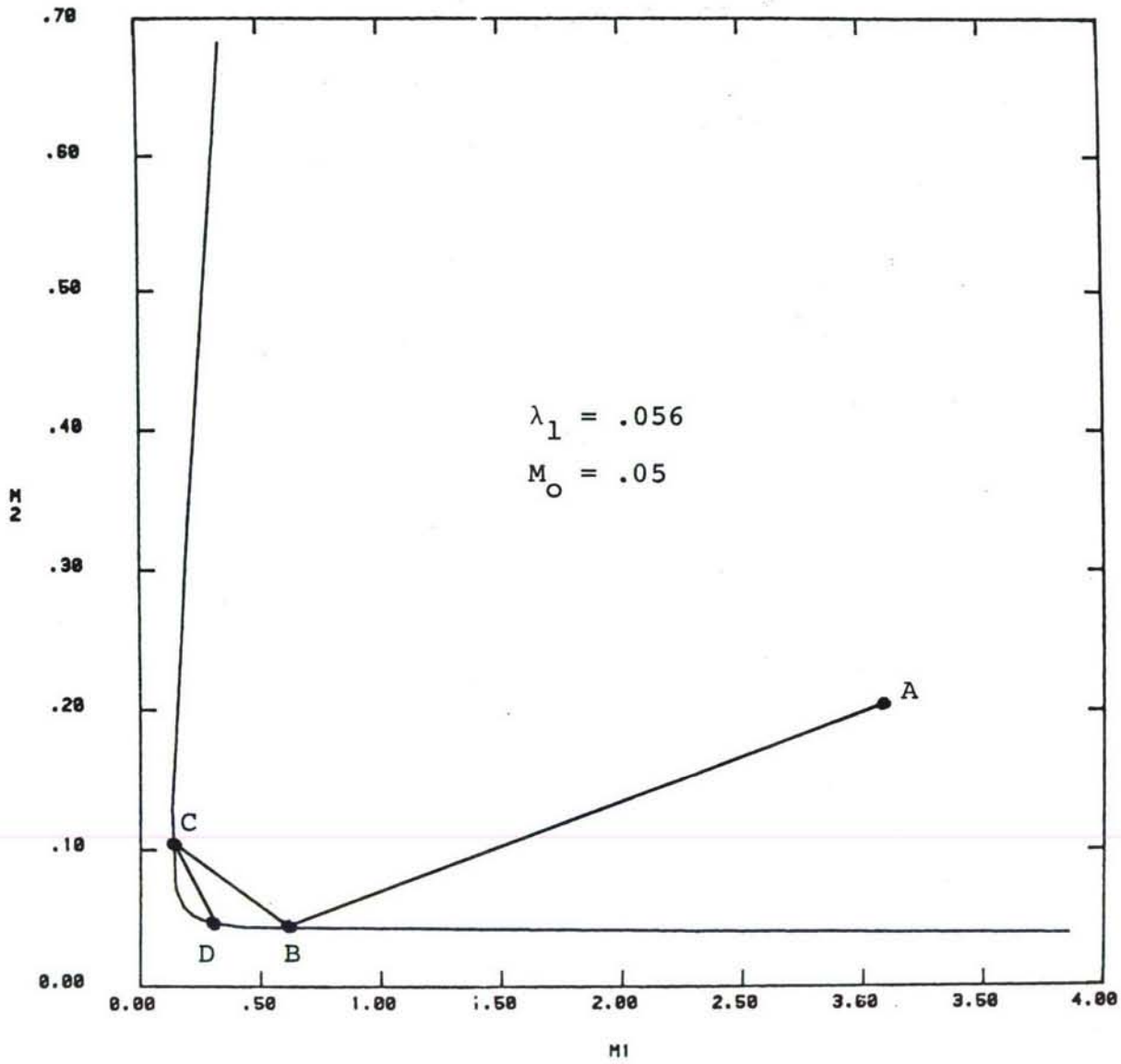

Figure 3.9. Frequency Constraint Resizing of Two Element Bar (Two Energy Resizing).

SECTION 4
ALGORITHM FOR DAMAGE REQUIREMENTS

In this section the algorithm for the optimal design of damage tolerant structures is presented. After the overview of the approach, the organization of the calculations is presented. This is followed by a discussion of the use of reanalysis procedures and a description of the computer code which implements the procedure.

4.1 OVERVIEW OF THE APPROACH

A conventional approach to optimization and damage assessment may proceed along the following steps:

(1) Define the undamaged structure.

(2) Solve the optimized problem -

find $\{d\}$

such that $W(\{d\}) \rightarrow$ minimum

and $G_i\{d\} \geq 0 \qquad i = 1,\ldots,N_c$

where $\{d\}$ = design variable vector

W = merit function (weight)

G_i = i^{th} constraint on undamaged structure

N_c = number of constraints.

(3) Perform vulnerability analysis of damage configuration using the $\{d\}$ determined in (2).

(4) Adjust $\{d\}$ to obtain satisfactory performance of the damaged structure.

The last step could involve engineering judgment and the use of criteria based on experience with similar design problems.

The more general approach taken herein is to include additional constraints for the damage configuration in the problem statement as follows:

(1) Define the undamaged and damaged configurations.

(2) Solve the optimization problem -

$$
\begin{aligned}
&\text{find } \underset{\sim}{d} \\
&\text{such that } W(\underset{\sim}{d}) \rightarrow \text{minimum} \\
&\quad \text{and } G_i(\underset{\sim}{d}) \geq 0 \qquad i = 1,\ldots,N_c \\
&\quad \text{and } g_{1i}(\underset{\sim}{d}) \geq 0 \qquad i = 1,\ldots,N_{c1} \\
&\qquad \vdots \\
&\qquad g_{mi}(\underset{\sim}{d}) \geq 0 \qquad i = 1,\ldots,N_{cm}
\end{aligned}
$$

where g_{ki} = i^{th} constraint on the k^{th} damage model

m = number of damage models

N_{ck} = number of constraints on the k^{th} damage model

and $\underset{\sim}{d}$, W, G_i, N_c are as before. The constraint conditions include requirements on stress, deflection, natural frequency, and limits on member sizes. As shown in Figure 4.1, this general approach also includes the possibility for modification to the applied loads in the damage models.

4.2 ORGANIZATION OF THE CALCULATIONS

Calculations to perform the optimization for damage tolerance requirements are arranged as given in the flow description below for a typical design step:

(1) Assemble stiffness (and mass, if required) for the latest design.

(2) Perform static solutions for all design conditions not containing damage. Save the factored stiffness matrix for use in (4).

(3) If required, perform solutions for natural frequencies and mode shapes of the undamaged structure.

(4) For each design condition containing damage, define the change in stiffness and solve for the response of the damaged structures using reanalysis techniques. Find changes in frequencies and mode shapes of the damaged structures, if required.

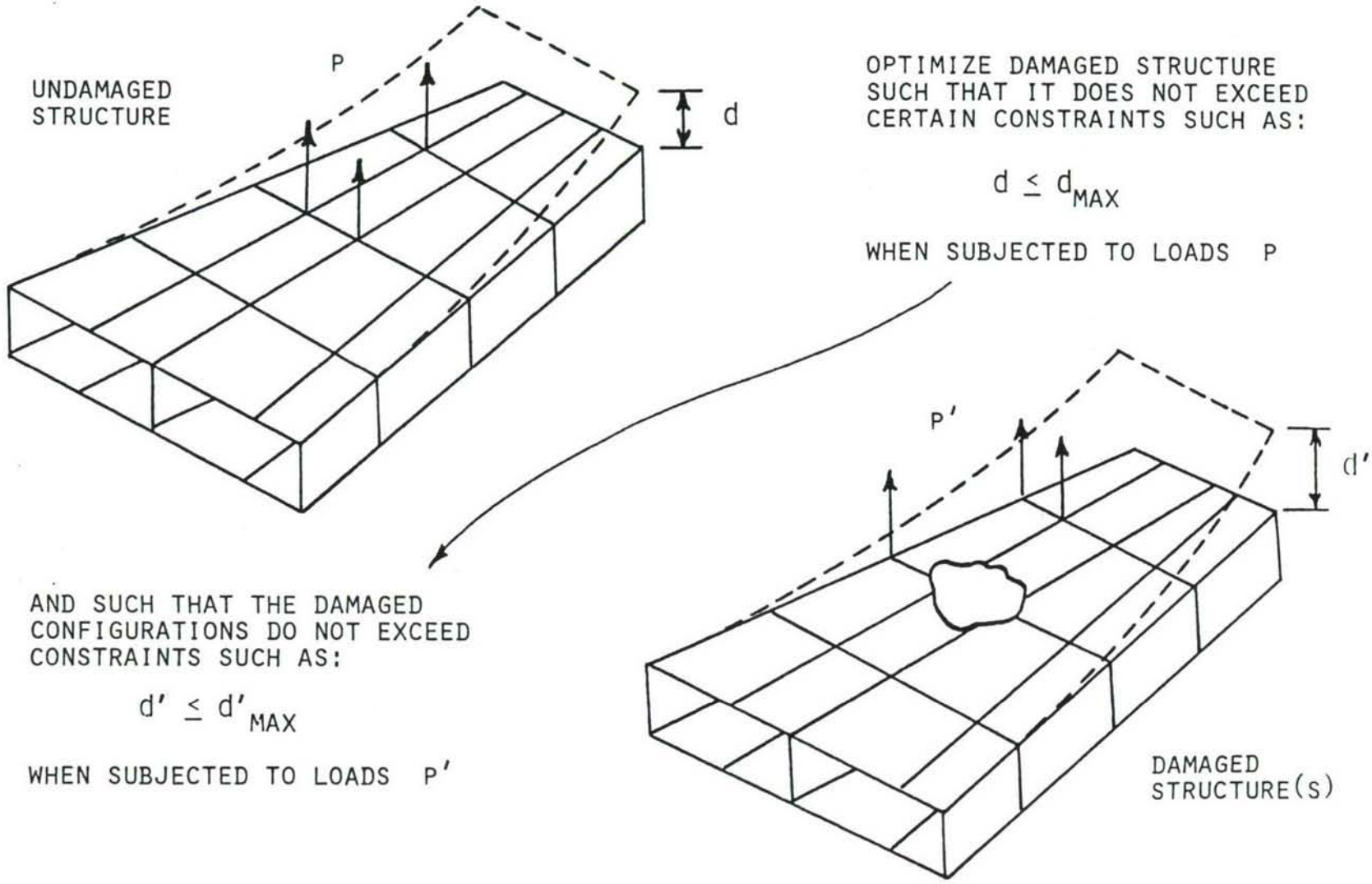

Figure 4.1. Damage Optimization Concept.

(5) Compute element forces, stress, etc. of the undamaged and damaged configurations in preparation for resizing. If an element is damaged in a certain design condition, generate null stress vector (or other appropriate responses) for that condition.

(6) Perform resizing, element by element, using optimality criteria.

(7) Go to (1) to begin the next redesign cycle, if required.

The above computation scheme integrates damage reanalysis into the optimization procedure in such a way that the presence of damage in certain design conditions is transparent to the resizing segment of the program. Solutions for damage conditions are returned as additional response vectors, for which noncritical stress states are to be generated in any damaged elements. Thus, the optimization can proceed as usual with behavioral constraints for damaged design conditions treated in an analogous manner as for additional loading cases in an undamaged structure.

4.3 THE ADDRESS PROGRAM STRUCTURE

The computer program ADDRESS, developed under this project, was designed from the outset to be easily modified and to incorporate state of the art numerical methods. The code was developed in standard ANSI FORTRAN and contains no features which preclude its portability. The code was written in a structured form and arranged in modular routines with liberal use made of internal documentation.

From a conceptual point of view, the overall program control organization is shown in Figure 4.2. The "Executive Control", a main program, calls the "Analytic/Optimization Control" which, in turn, performs the analysis and optimization by calls to the energy (stress), displacement, and frequency control segments. The Executive Control is detailed in Figure 4.3. Its primary functions are to set up the structural model (both original and damaged) and to control the optimization process.

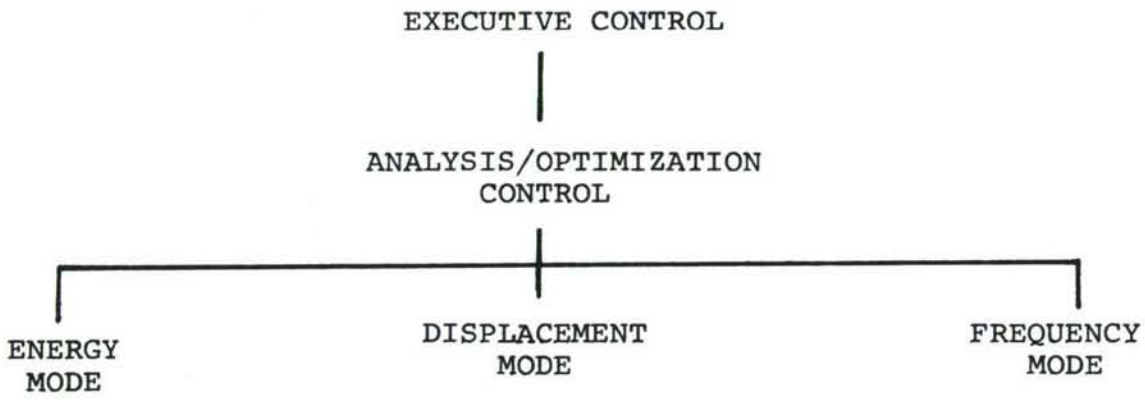

Figure 4.2. Overall Control Organization of the ADDRESS Program.

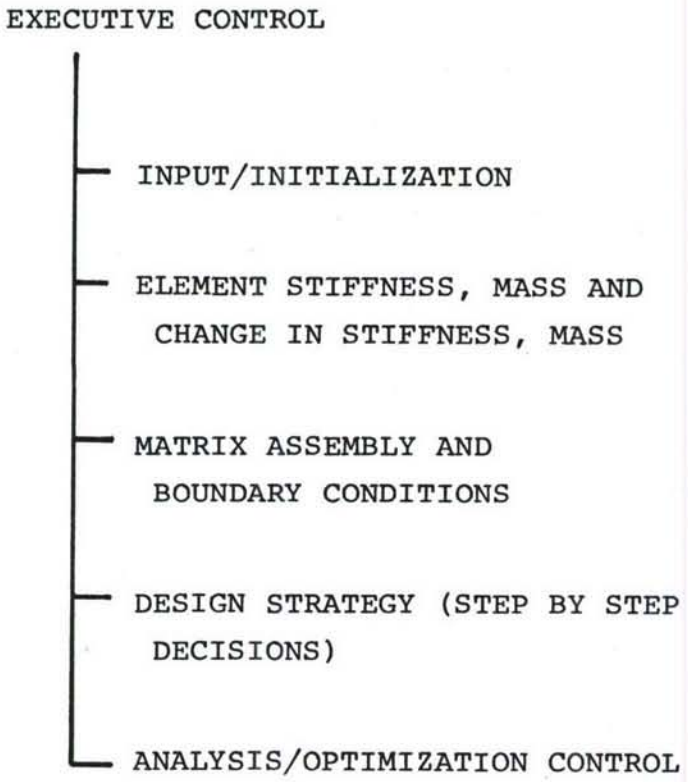

Figure 4.3. ADDRESS Executive Control.

The design strategy, shown in Figure 4.4, currently consists of a preselected number of cycles of energy mode resizing, followed by displacement mode resizing if required. Frequencies are checked at each step. Stress and deflection scaling takes place to assume a feasible design after each step.

Details of the energy, displacement, and frequency mode controls are given in Figures 4.5, 4.6, and 4.7, respectively. The energy and displacement modes are nearly identical to the strategy of the OPTSTATCOMP program. The frequency mode control involves the use of the SIMIT technique for the undamaged structure and the vibration reanalysis procedure of Section 3.5 herein. Further details of these procedures are given in the ADDRESS User's Manual.

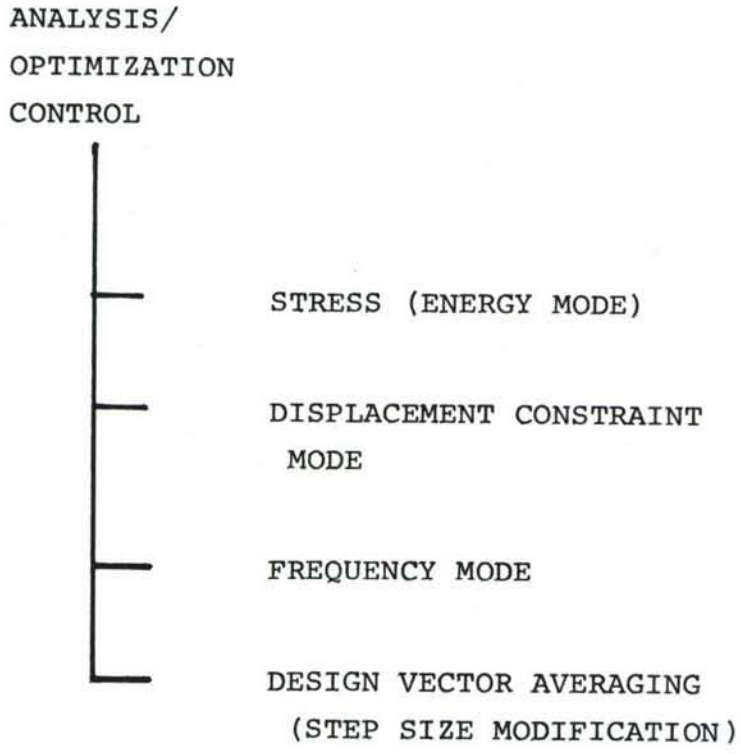

Figure 4.4. ADDRESS Analysis/Optimization Control.

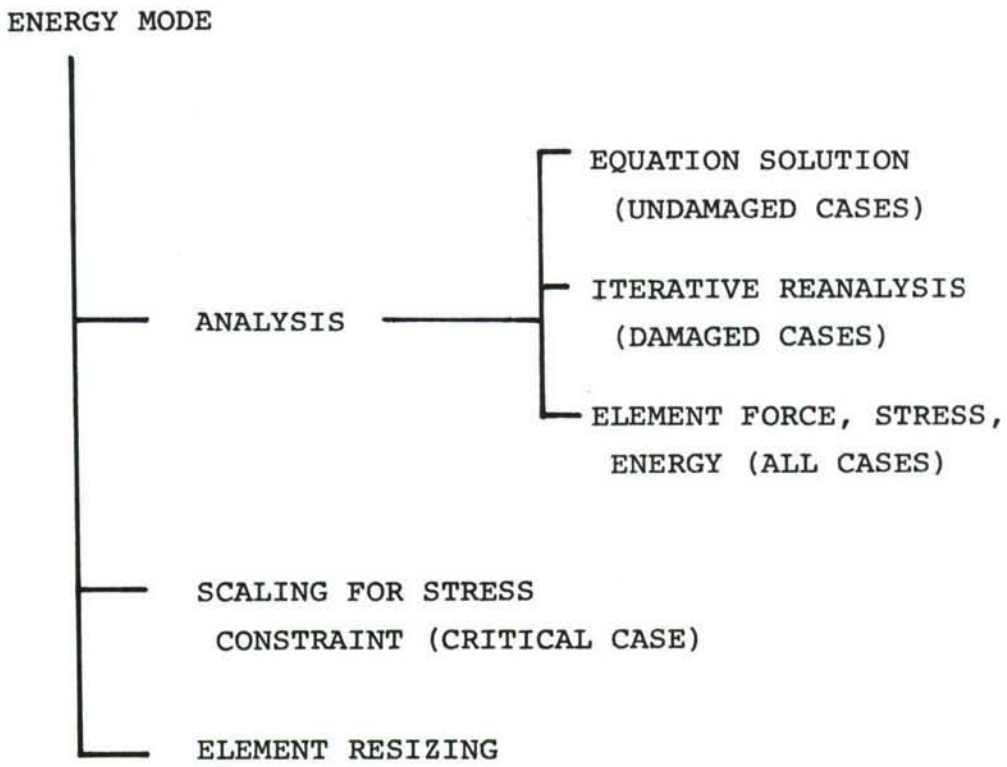

Figure 4.5. ADDRESS Energy Mode Control.

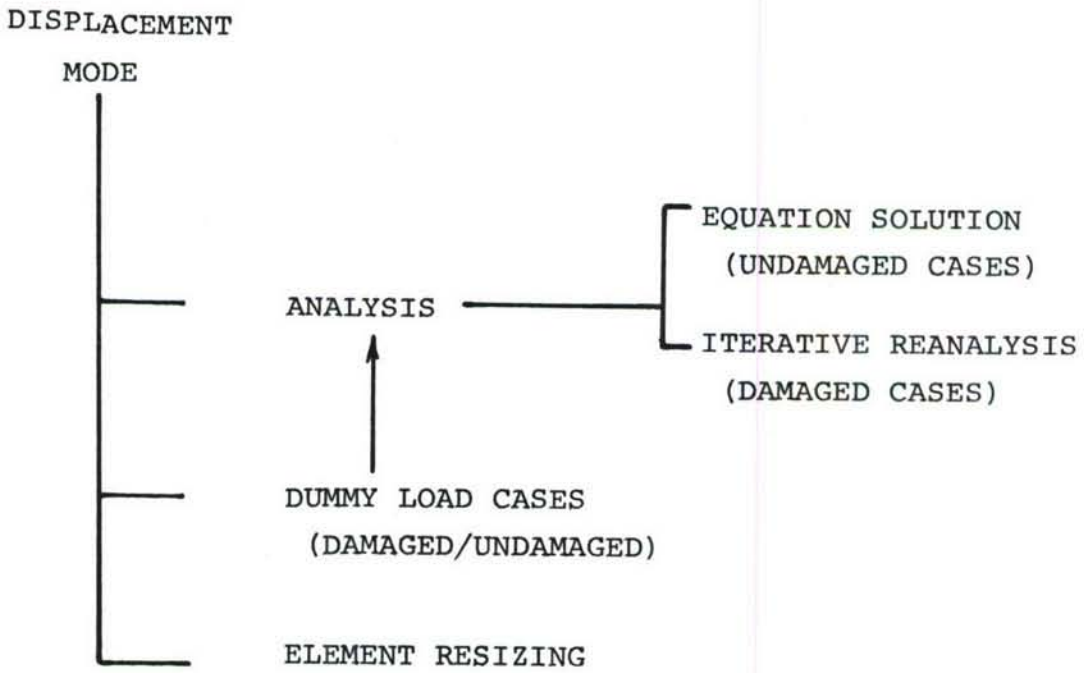

Figure 4.6. ADDRESS Displacement Mode Control.

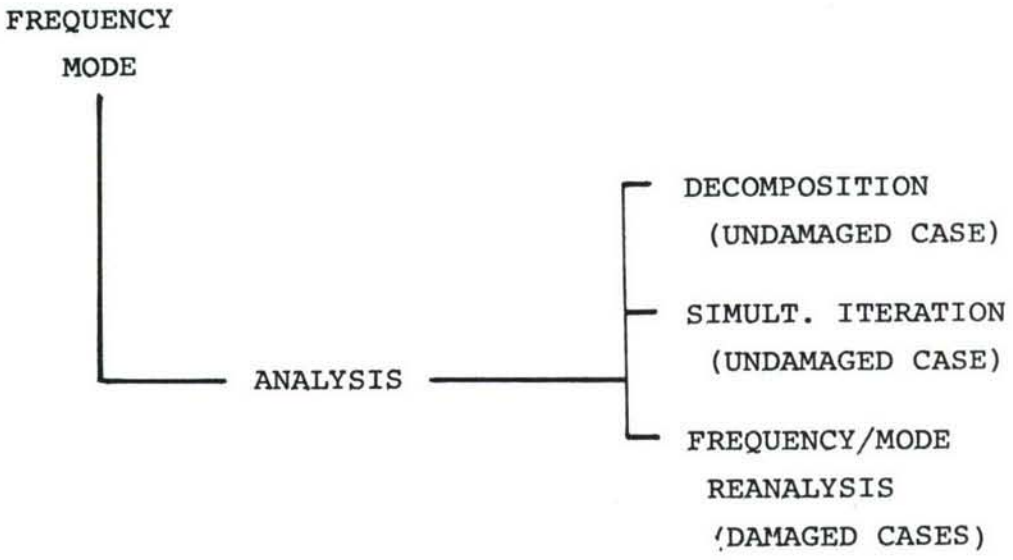

Figure 4.7. ADDRESS Frequency Mode Control.

SECTION 5

APPLICATIONS OF THE ADDRESS PROGRAM TO REPRESENTATIVE STRUCTURES

The ADDRESS program was applied to several representative structures. Analysis, reanalysis, and optimization results are presented in this section. Comparisons are made with programs obtained from the Air Force such as DANALYZ (vibration program) and OPTSTATCOMP (optimization program with composites capability). The effects of damage on the structural response and the optimal member sizes are noted. Results are presented for the following structures:

- Ten bar truss
- Simple wing box
- Intermediate complexity wing (ICW)

A major design and analysis study of the A-7 outer wing panel was also conducted. These results are given in the next section.

5.1 TRUSS RESULTS

The optimal design of the ten bar truss shown in Figure 5.1 has been studied in detail by a number of investigators (see Reference 30, for example). Two independent load cases (LC1, LC2) shown in Figure 5.2 are applied together with the two damage cases (DC1, DC2) shown in Figure 5.3.

The constraints are that member stresses not exceed 20,000 psi and that nodal deflections be less than or equal to 2.0 inches. In the first damage case, 95% of the material is removed from member 9, and in the second case 95% of the stiffness in members 2, 5, and 6 is removed. The material properties are based on aluminum.

Six truss designs were studied as shown in Table 5.1. The first truss design has all the member sizes equal and is the lowest weight uniform design which satisfies all the constraints

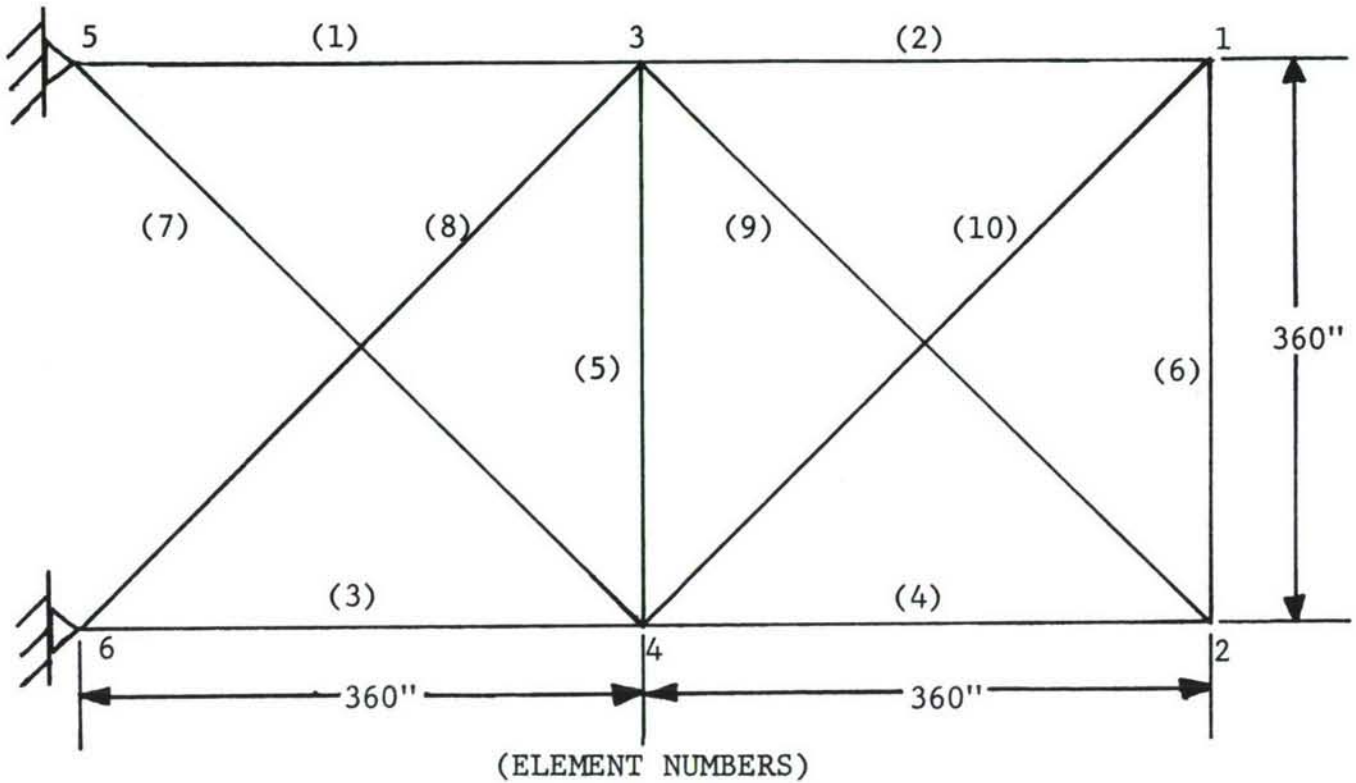

Figure 5.1. Ten-Bar Truss Geometry.

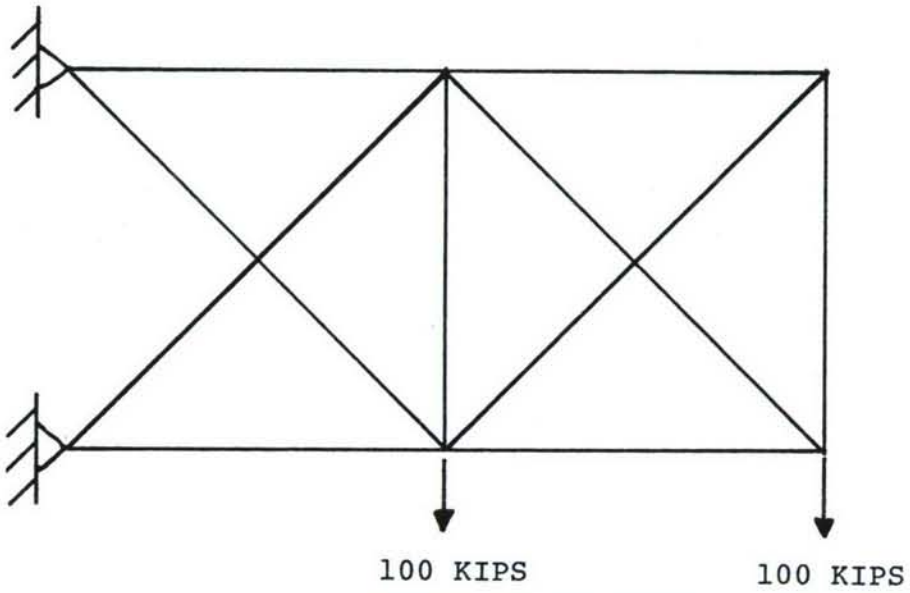

(a) Load Case 1 (LC1)

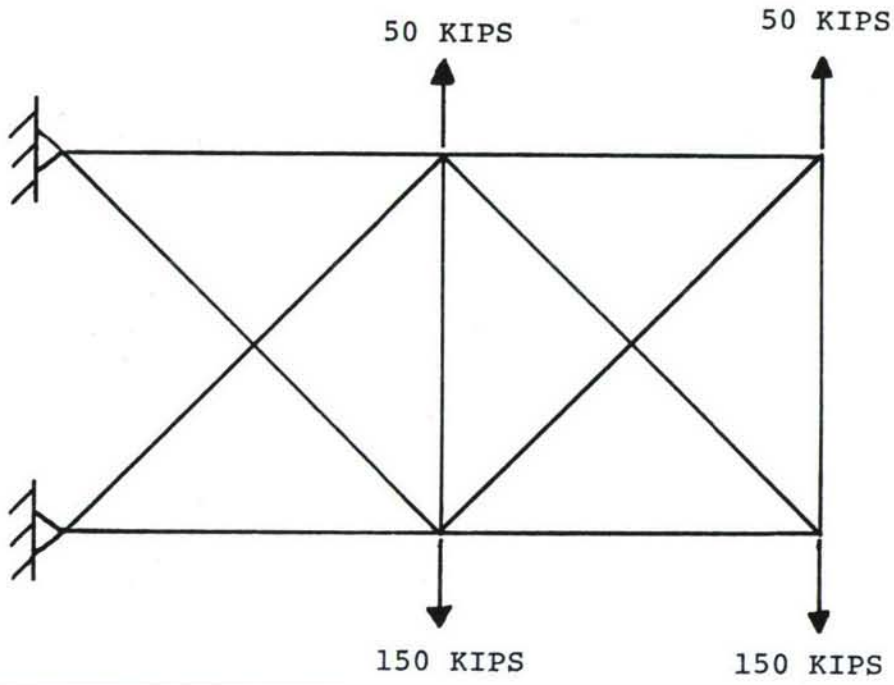

(b) Load Case 2 (LC2)

Figure 5.2. Ten-Bar Truss Load Cases.

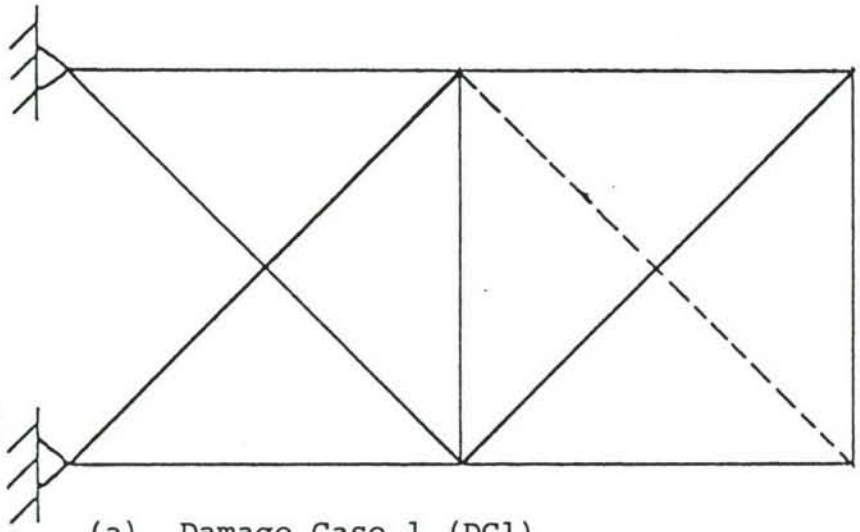

(a) Damage Case 1 (DC1)
95% of Member 9 Removed

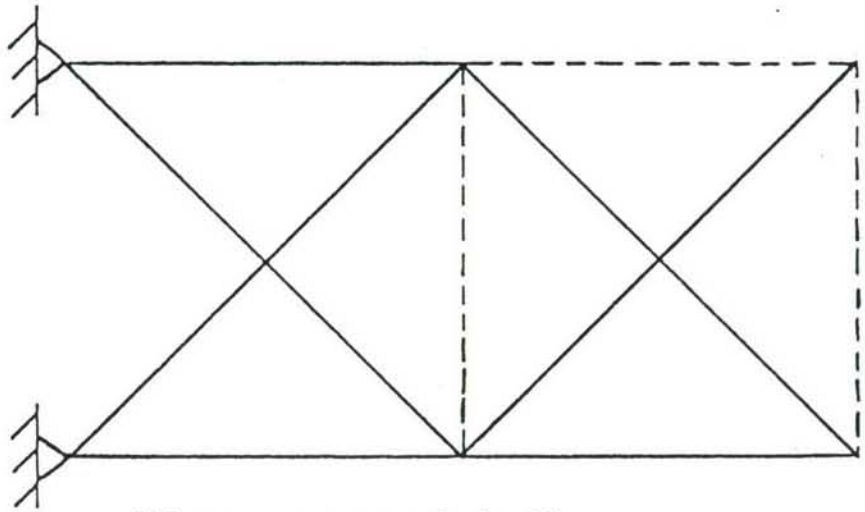

(b) Damage Case 2 (DC2)
95% of Members 2, 5 and 6 Removed

Figure 5.3. Ten-Bar Truss Damage Cases.

TABLE 5.1

DESCRIPTION OF TRUSS DESIGNS

Truss Design	Description	Weight (lb)
1	Uniform	8267
2	Optimal for LC1	5077
3	Optimal for LC2	4823
4	Optimal for LC1, 2	5455
5	Optimal for LC1, DC1	6866
6	Optimal for LC1, DC1, 2	9581

TABLE 5.2

SUMMARY OF TRUSS RESULTS

δ_{max} = Maximum Deflection

NOE = Number of Overstressed Elements

TD	LC	DC	NOE	δ_{max} (in)	TD	LC	DC	NOE	δ_{max} (in)
1	1	1	0	2.5	4	1	1	5	5.6
		2	0	2.3			2	0	2.1
	2	1	0	2.6		2	1	6	6.2
		2	1	2.2			2	4	-9.4
2	1	1	5	10.8	5	1	1	0	2.0
		2	1	2.0			2	7	15.2
	2	1	6	11.6		2	1	3	-10.4
		2	5	-283.5			2	7	14.3
3	1	1	3	8.9	6	1	1	0	1.9
		2	0	2.4			2	0	1.7
	2	1	5	8.9		2	1	0	2.0
		2	4	-7.8			2	1	1.6

under the first load case. Designs 2, 3, and 4 are optimal for the load cases indicated without damage to any of the members. The fifth and sixth designs include the indicated damage conditions when the structure is loaded under the first condition. As can be seen from the table, the addition of damage considerations causes an increase in weight, just as multiple load cases increase the weight of the optimal design.

Table 5.2 is a summary of load and damage tolerance studies performed on the six truss designs. The uniform design performs quite well compared to the optimal designs which do not include damage tolerance. The designs which are optimal for only one load case are quite sensitive to changes in loading or addition of damage. The sixth design, which is optimal for the first load case and both damage conditions, is also satisfactory under the second load case when only the first damage is imposed.

The above calculations were performed with the aid of a small scale computer program which is documented in Appendix E of the ADDRESS User's Manual. Its primary purpose is to reanalyze the damaged truss structure using simple iteration. Insight was gained into the number of iterations required to obtain convergence. In general, no more than five iterations are required to achieve stress and displacements within 5% of those obtained from an exact analysis. This applies to damages of the level used in this problem. For damages which introduce a kinematic instability in the truss, the iterations diverge.

5.2 SIMPLE WING BOX

To check the efficiency of the ADDRESS calculations, a small-scale finite element model of a straight, rectangular wing box was developed. The model is shown in Figure 5.4 and is composed of 24 bar, shear panel, and membrane cover elements. There are a total of 48 unrestrained degrees of freedom in the model corresponding to the three degrees of freedom at each of the

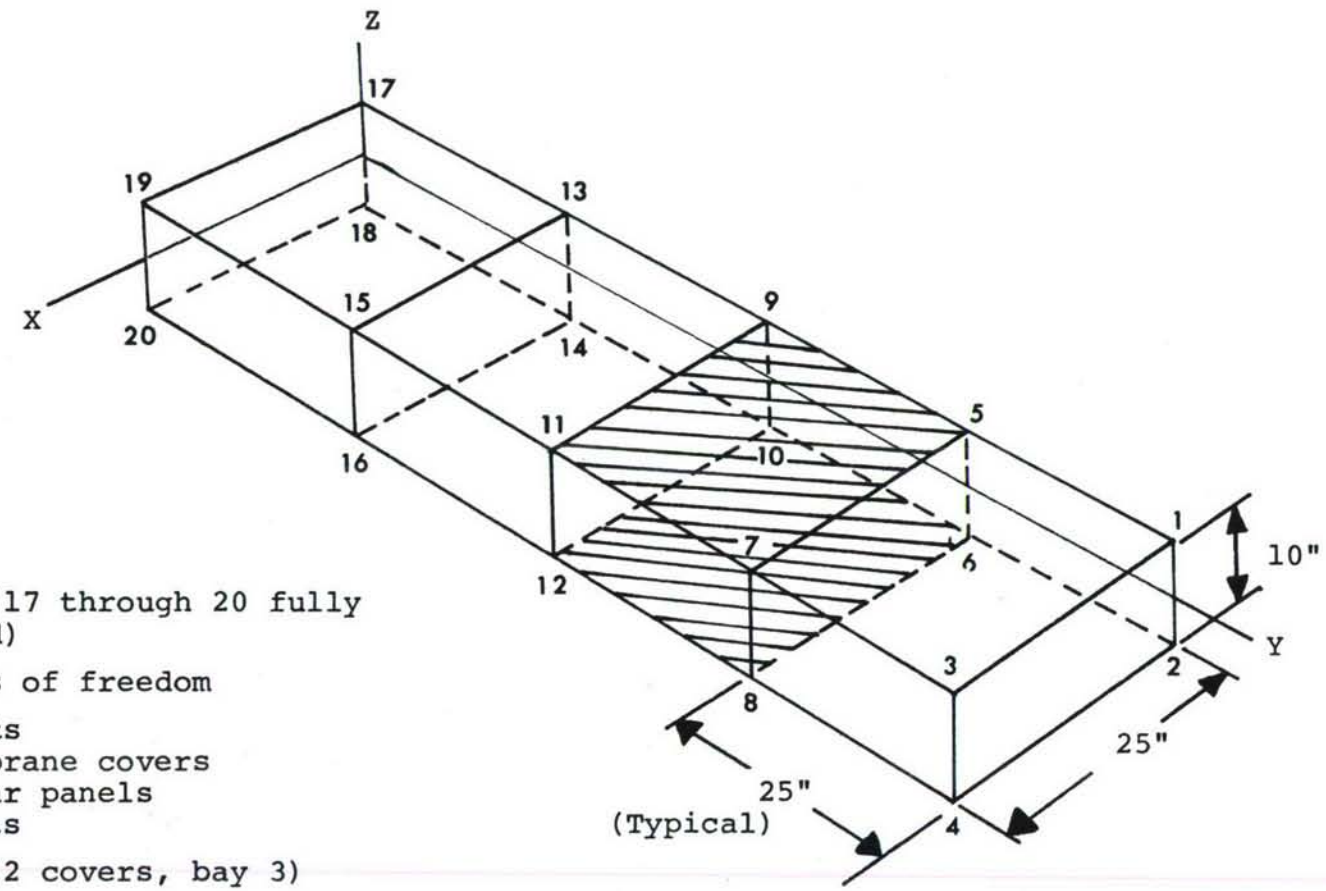

- 20 nodes (17 through 20 fully restrained)
- 48 degrees of freedom
- 24 elements
  - 8 membrane covers
  - 8 shear panels
  - 8 posts
- 1 damage (2 covers, bay 3)

Figure 5.4. Simple Wing Box Finite Element Model.

sixteen unrestrained nodes. The covers in bay 3 were reduced in mass by 25% and in stiffness by 50% to simulate a ballistic damage.

The wing was subjected to loads of 10,000 lb. at the four tip nodes in the negative z-direction. Constraints consisted of the requirement that no member have stresses in excess of 20,000 psi and that displacements be no greater than 2.0 inches. The structure is designed for minimum weight such that the stress and deflection requirements are not exceeded for the original or the damaged wing box.

Three cycles of energy resizing were employed with scaling to meet the constraints. The element weights are shown in Table 5.3. Elements were linked such that top and bottom covers are of the same thickness, shear panels vary together, and bars (posts) are all the same. The results show that after one iteration the weight has reached a near constant value of 307 lb.

Table 5.4 gives comparisons between using a complete analysis at each step and using the reanalysis techniques discussed in Section 3. An accuracy requirement of 0.005 on both the displacements and the mode shapes was required. The table shows that although the computing times are small, the computing time is reduced by 75% for the static analysis and by over 50% for the vibration analysis.

5.3 INTERMEDIATE COMPLEXITY WING

The intermediate complexity wing model of Reference 30 is shown in Figure 5.5. It contains a total of 158 membrane, bar, and shear panel elements. To test the convergence of the static and vibration reanalysis iterations, 25 elements were damaged in the leading edge tip area as shown in the figure. Two separate load conditions corresponding to a subsonic, forward center of pressure load and a supersonic, near uniform pressure loading were assumed. The maximum deflection occurred at the indicated deflection control point for the supersonic loading.

TABLE 5.3

SIMPLE WING BOX WEIGHTS FOR ENERGY AND DISPLACEMENT RESIZING

Element Number	Type	Connectivity				Initial Weight	Cycle 1 Weight	Cycle 2 Weight	Cycle 3 Weight
		MA	MB	MC	MD				
1	C	1	3	7	5	37.088	8.177	7.537	7.505
2	C	2	4	8	6	↓	8.177	7.537	7.505
3	C	5	7	11	9	↓	30.542	30.935	30.979
4	C	6	8	12	10	↓	30.542	30.935	30.979
5	C	9	11	15	13	↓	37.719	37.493	37.463
6	C	10	12	16	14	↓	37.719	37.493	37.463
7	C	13	15	19	17	↓	50.250	50.634	50.650
8	C	14	16	20	18	↓	50.250	50.634	50.653
9	SP	1	2	6	5	14.835	6.730	6.745	6.745
10	SP	3	4	8	7	↓	↓	↓	↓
11	SP	5	6	10	9	↓	↓	↓	↓
12	SP	7	8	12	11	↓	↓	↓	↓
13	SP	9	10	14	13	↓	↓	↓	↓
14	SP	11	12	16	15	↓	↓	↓	↓
15	SP	13	14	18	17	↓	↓	↓	↓
16	SP	15	16	20	19	↓	↓	↓	↓
17	B	1	2	0	0	.593	.014	.010	.010
18	B	3	4	0	0	↓	↓	↓	↓
19	B	5	6	0	0	↓	↓	↓	↓
20	B	7	8	0	0	↓	↓	↓	↓
21	B	9	10	0	0	↓	↓	↓	↓
22	B	11	12	0	0	↓	↓	↓	↓
23	B	13	14	0	0	↓	↓	↓	↓
24	B	15	16	0	0	↓	↓	↓	↓
Total Weights (all elements)						420.128	307.328	307.238	307.234

C = Cover
SP = Shear Panel
B = Bar

TABLE 5.4

COMPARISONS OF ANALYSIS AND REANALYSIS
COMPUTER TIMES FOR SIMPLE WING BOX

Calculation	Computing Time (sec)				
	Initial	Cycle 1	Cycle 2	Cycle 3	Total
Static Analysis (sec)	.31	.30	.30	.29	1.20
Static Reanalysis (sec)	.08	.07	.07	.06	.28
Eigen Analysis (sec)	.21	.24	.24	.25	.94
Eigen Reanalysis (sec)	.11	.10	.10	.09	.40

- 88 Nodes
- 234 Degrees of Freedom
- 158 Elements
- 1 Damage Zone

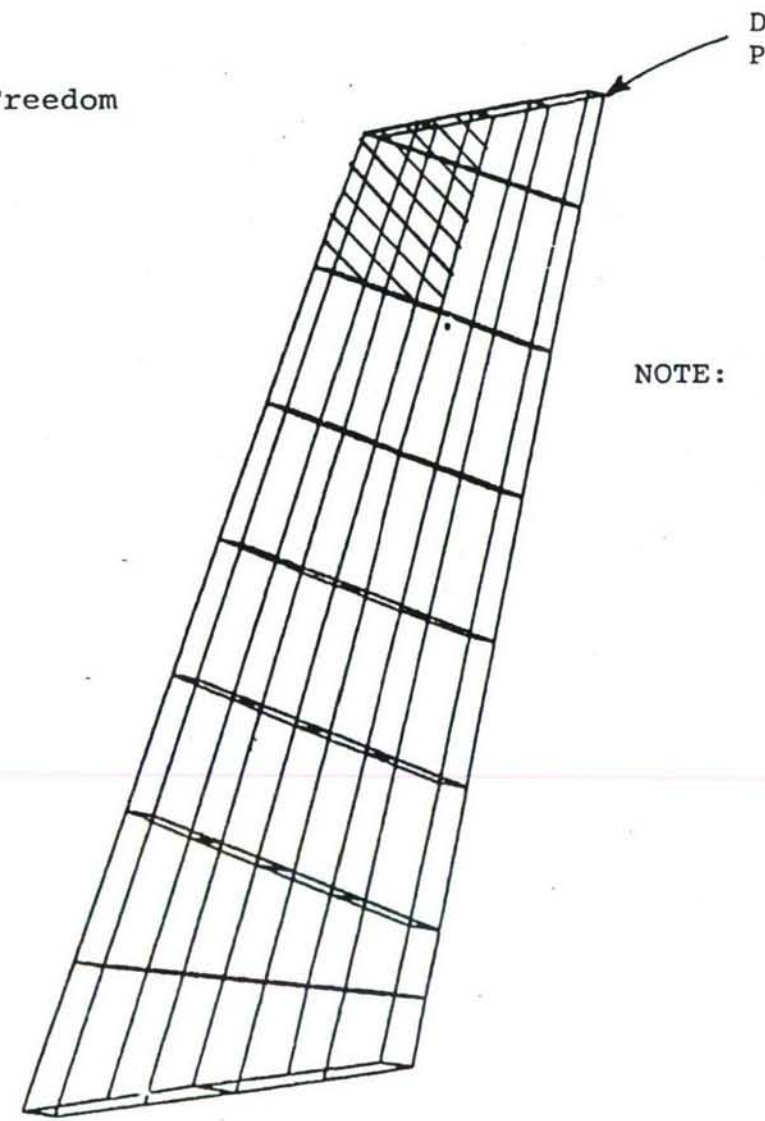

NOTE: All 25 elements in damage zero were reduced in stiffness by 75%.

Figure 5.5. Wing Model for Static Reanalysis (Reference 30).

Table 5.5 shows the iteration history and compares it to the "exact" analysis of the damaged structure. Figure 5.6 shows the error in the tip deflection as a function of computing time. The computing cost for five iterations is seen to be about one-half that of the "exact" analysis. At the same time, the tip deflection determined by the iteration is within 1% of the exact value. The time savings on larger problems is even greater since iteration involves only successive forward and back substitutions.

To check the vibration analysis capability, the ICW model was run using the Air Force's DANALYZ program and compared to the simultaneous iteration (SIMIT) technique used in ADDRESS. Several damages were imposed on the wing covers as shown in Figure 5.7. Table 5.6 summarizes the frequency calculations using DANALYZ and SIMIT to compute the first four modal frequencies. Good correlation was obtained in all cases. Mode shapes compared to three decimal places. Mode shapes appear to be relatively insensitive to structural damage for this problem (see Figures 5.8 through 5.19).

Table 5.7 gives results of the iteration procedure for the ICW damage condition of Figure 5.5. The iteration column of Table 5.7 indicates the number of times which modes and frequencies have been recomputed using the iteration scheme of Section 3. It is interesting to note that not all frequencies converge at the same rate. For mode one and three, one iteration was sufficient to achieve a high degree of accuracy. Mode two, however, required three iterations to achieve similar accuracy. The efficiency of the reanalysis is also quite good. The table shows that computing time can be reduced by over 50% for this problem.

5.4 COMPARISONS WITH OPTSTATCOMP

The efficiency and accuracy of the ADDRESS program was compared with that of OPTSTATCOMP for several of the problems in the previous subsections. In some cases, direct comparisons are not possible since different minimum sizes or number of resizings were used.

TABLE 5.5

CONVERGENCE OF STATIC REANALYSIS FOR ICW
TIP DEFLECTION AT DEFLECTION CONTROL POINT

Iteration Number	Tip Deflection (inches)
undamaged	20.3512
1	21.1567
5	21.6716
10	21.6911
15	21.6916
20	21.6916
exact*	21.7018

*"Exact" in the sense that a complete analysis was performed without iteration.

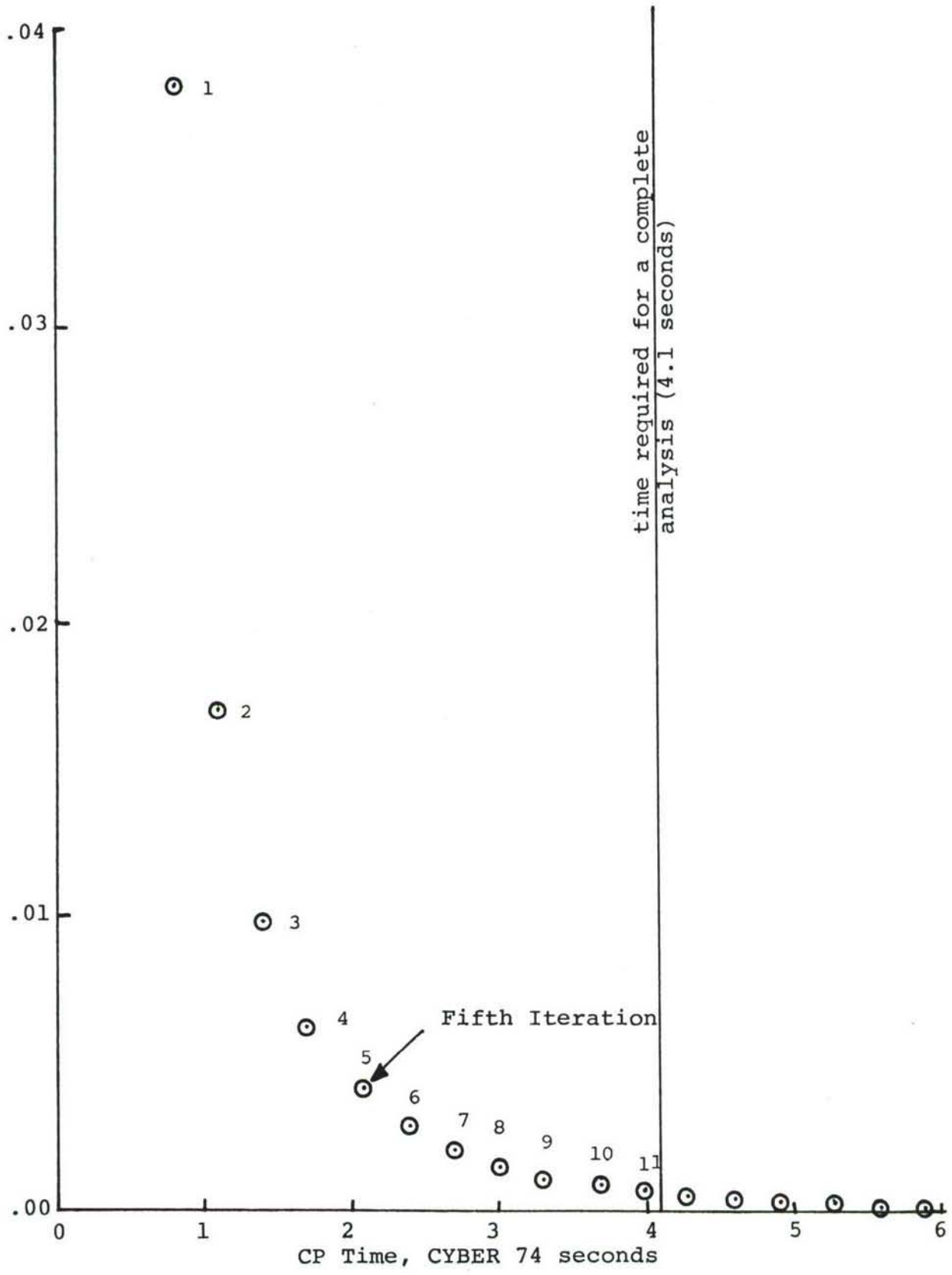

Figure 5.6. Static Reanalysis Computing Times for ICW.

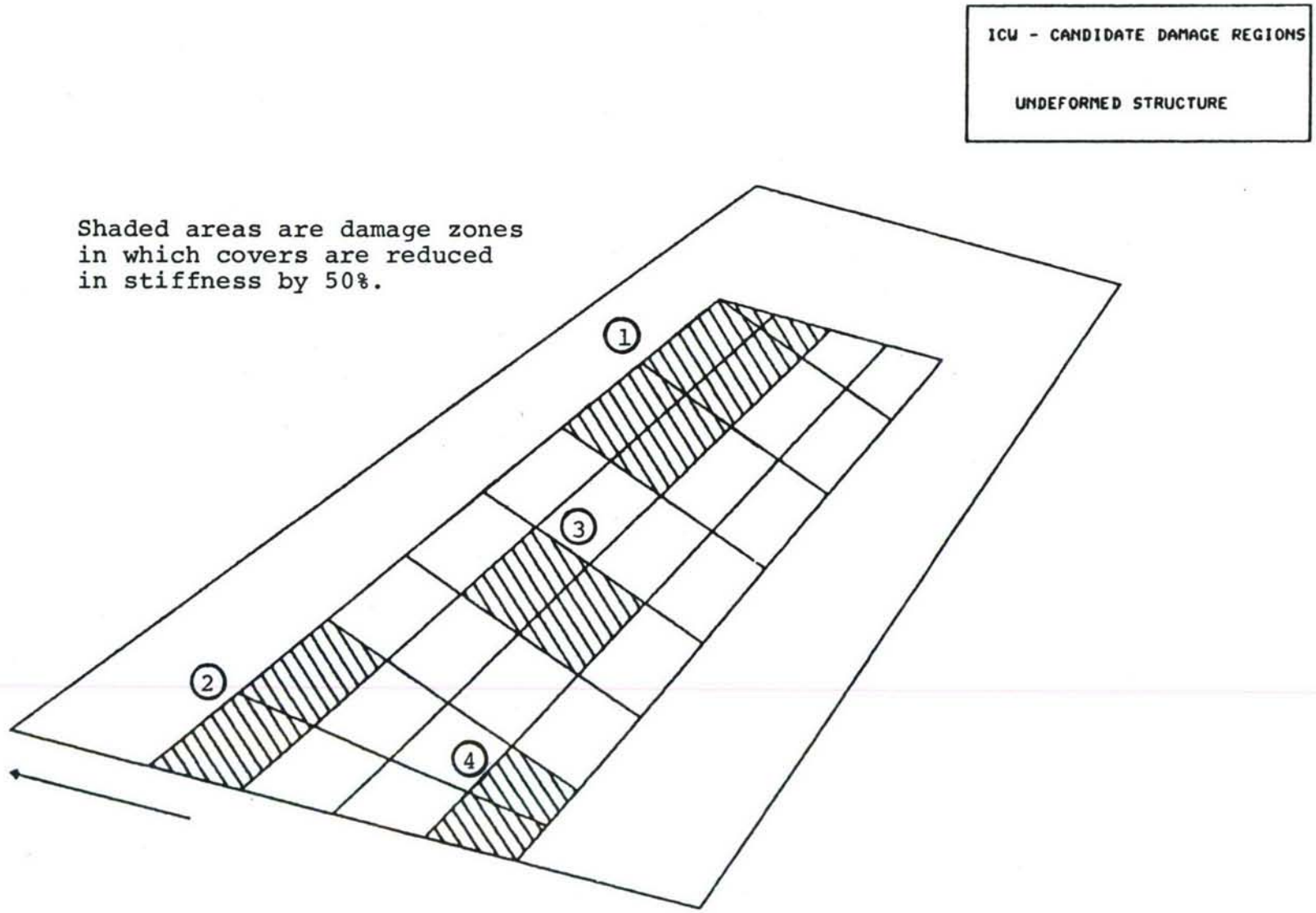

Figure 5.7. Damage Zones on the Intermediate Complexity Wing (ICW).

TABLE 5.6

COMPARISON OF DANALYZ AND SIMIT MODAL FREQUENCIES FOR ICW

Damage	Mode 1 (Hz)		Mode 2 (Hz)		Mode 3 (Hz)		Mode 4 (Hz)	
	DANALYZ	SIMIT	DANALYZ	SIMIT	DANALYZ	SIMIT	DANALYZ	SIMIT
None	42.035	41.943	135.736	135.400	169.553	169.940	264.284	264.370
Zone 1	46.672	45.447	133.726	130.710	189.454	188.300	264.318	260.180
Zones 1 through 4	36.772	35.701	130.336	126.540	145.014	140.790	260.889	253.290

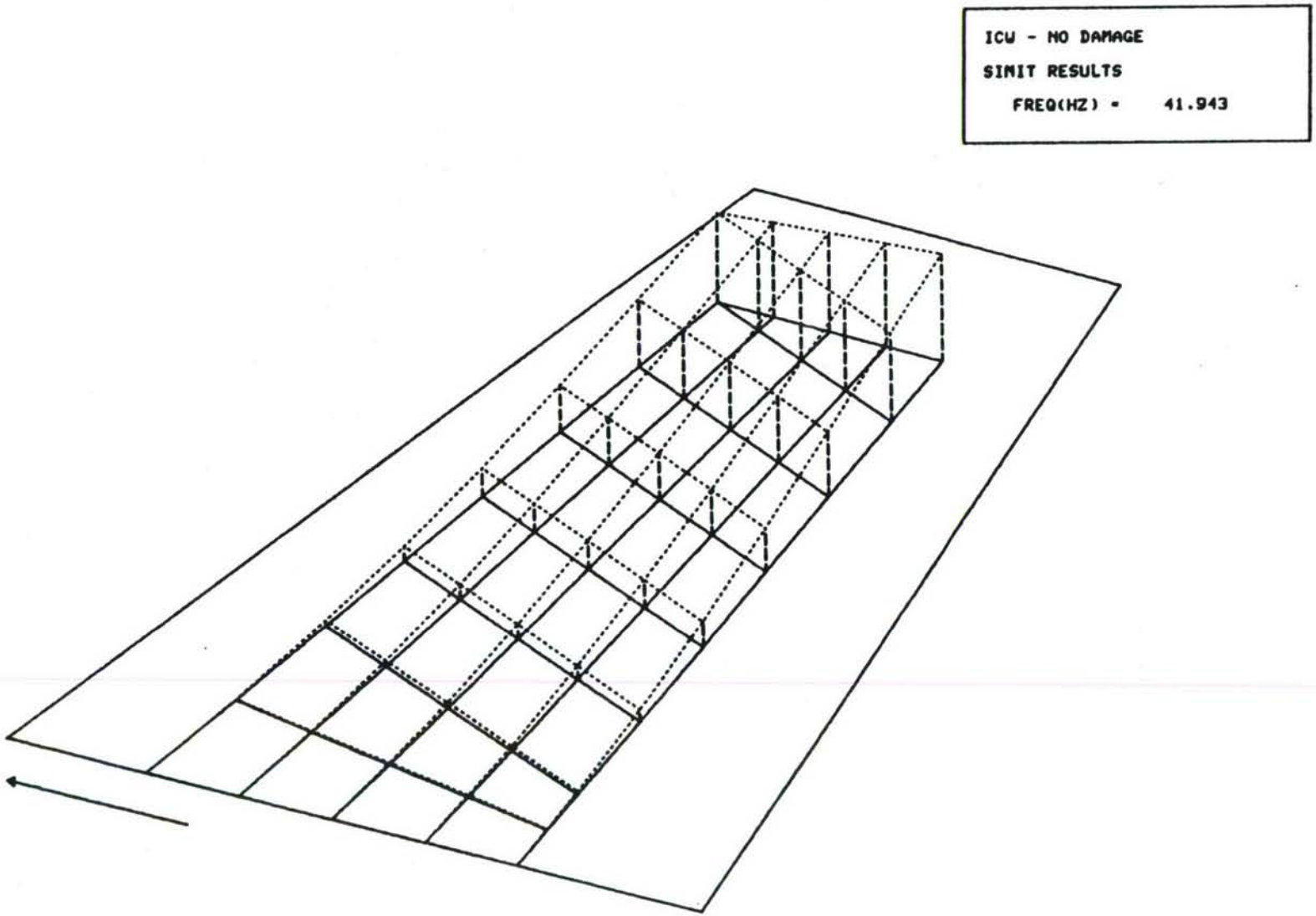

Figure 5.8. First Bending Mode for ICW (No Damage).

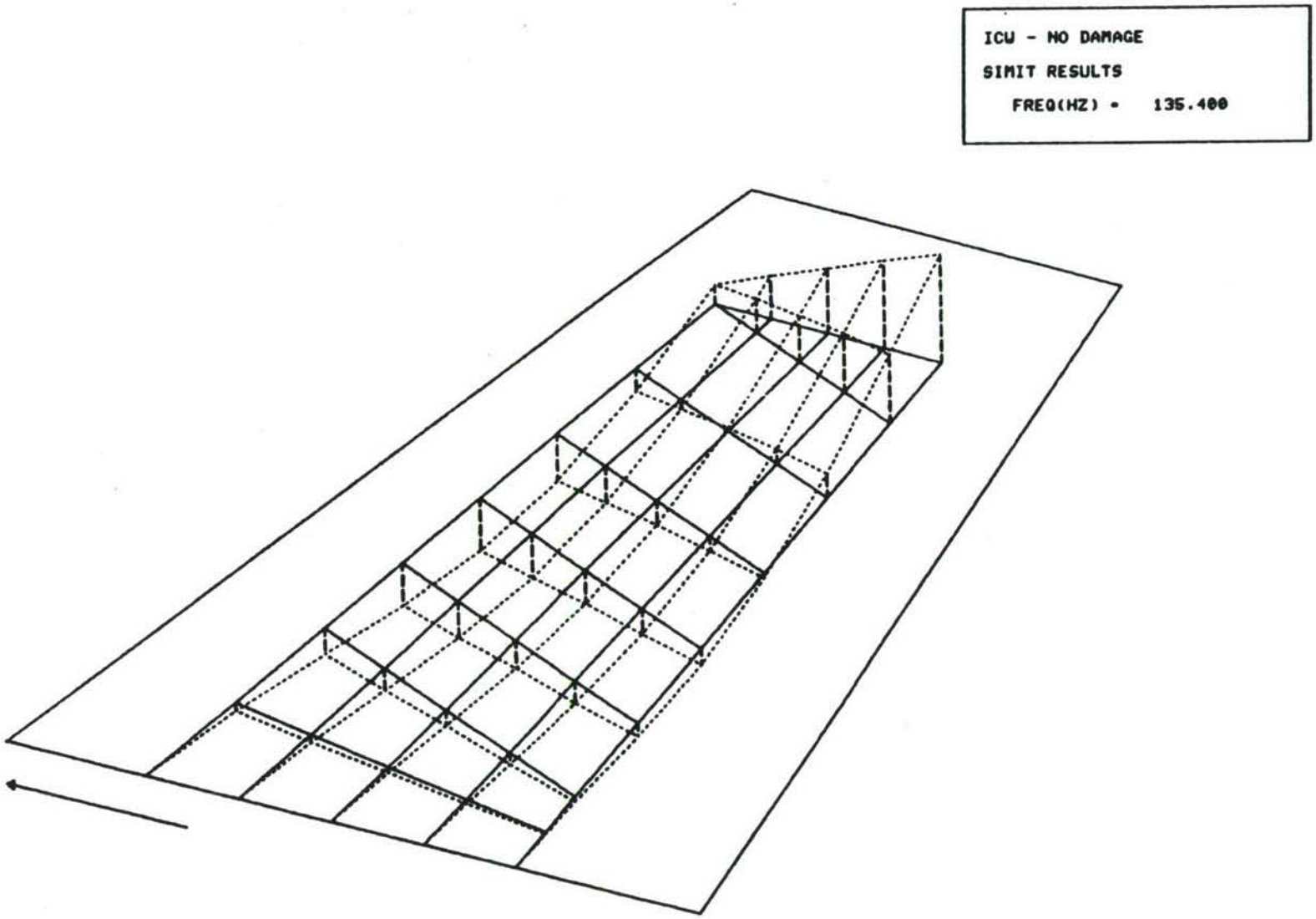

Figure 5.9. Second Bending Mode for ICW (No Damage).

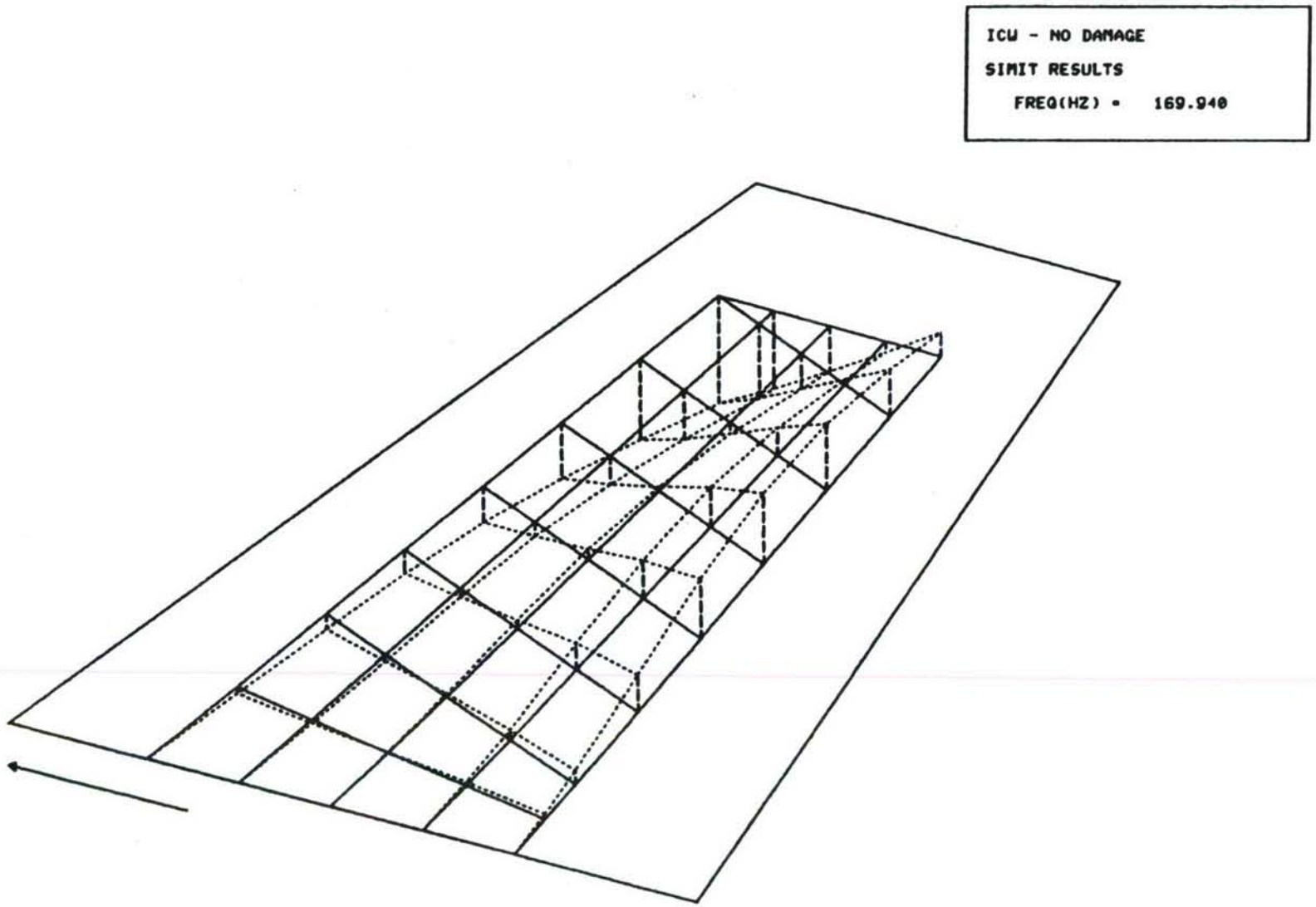

Figure 5.10. First Torsion Mode for ICW (No Damage).

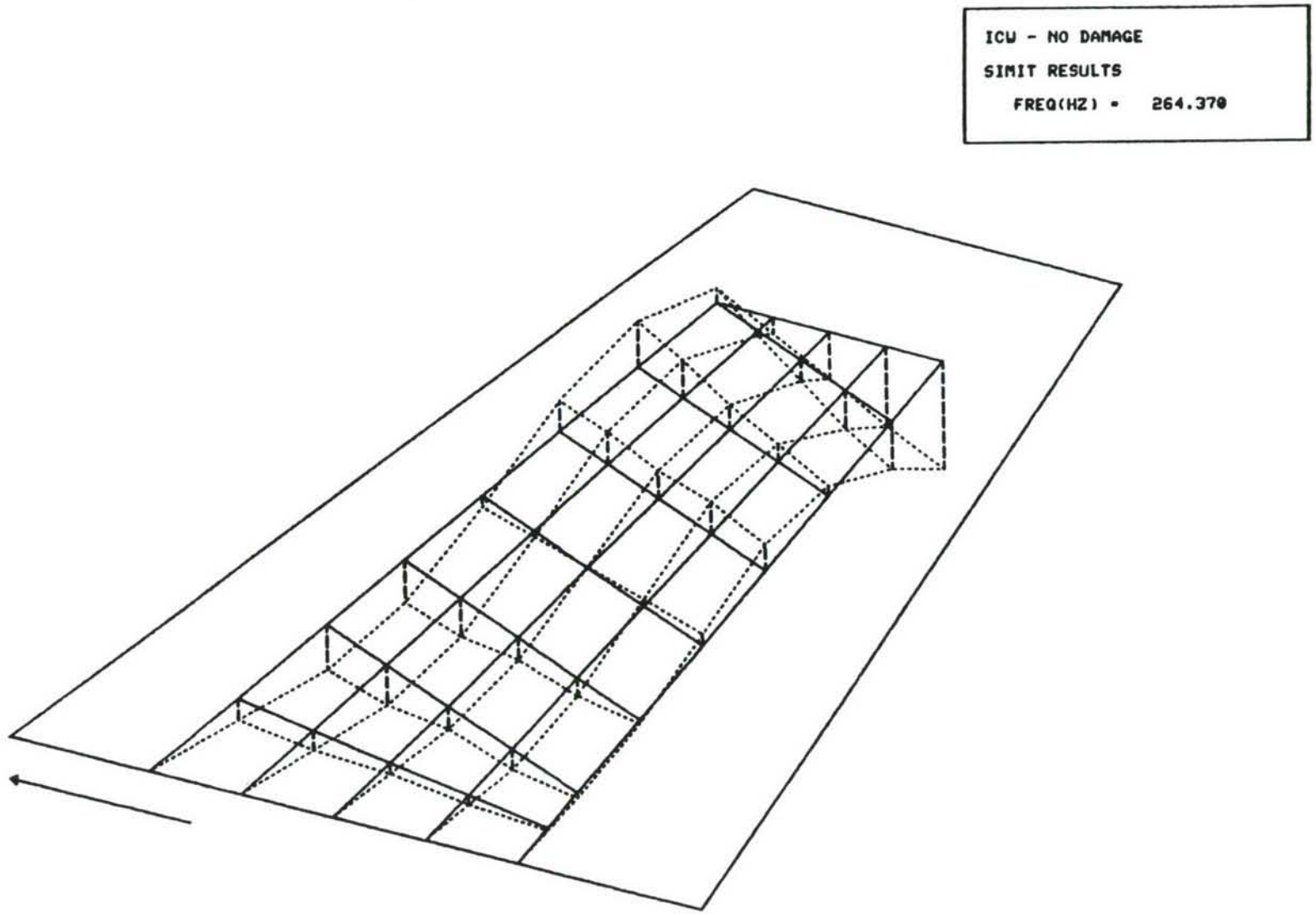

Figure 5.11. Third Bending Mode for ICW (No Damage).

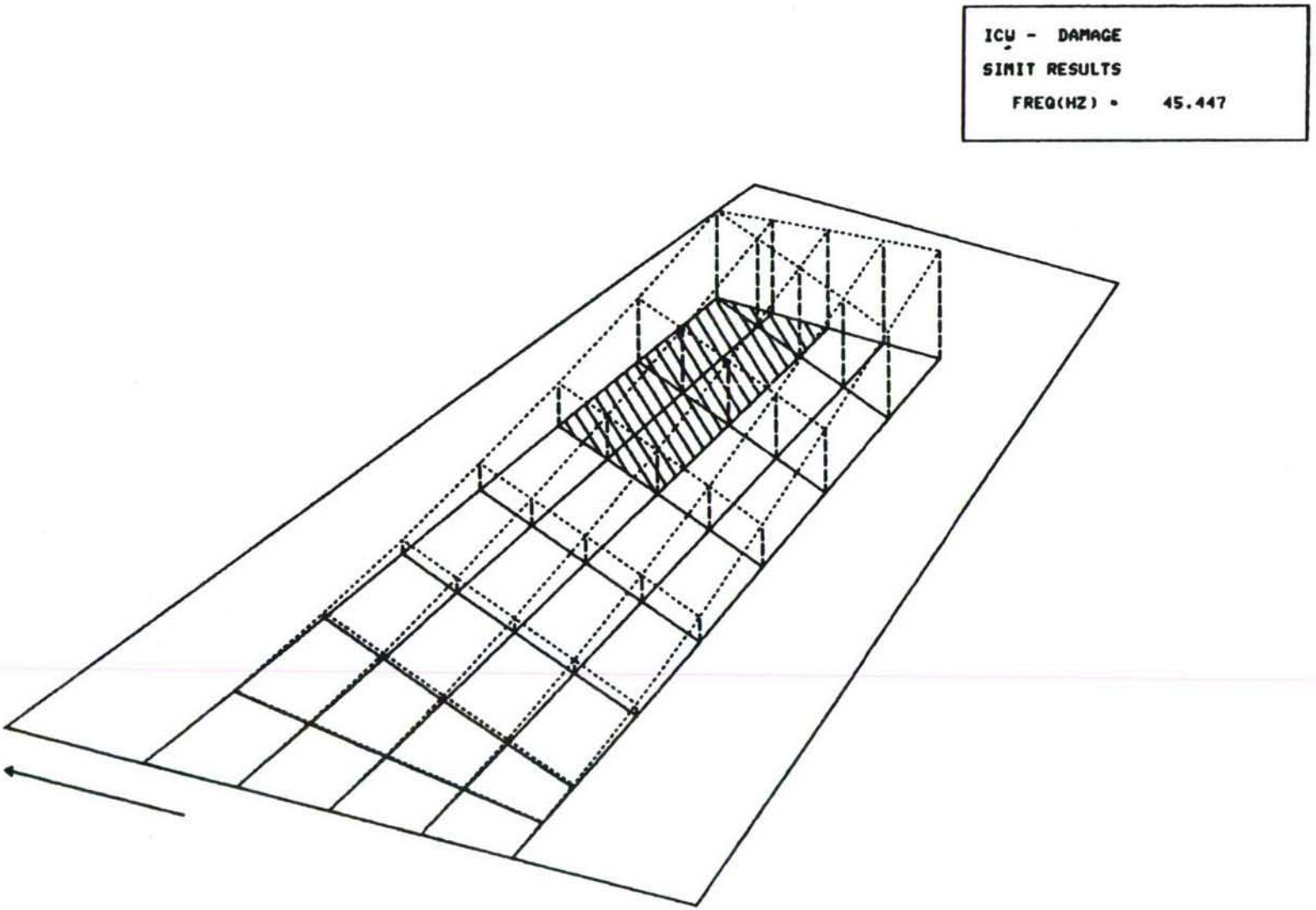

Figure 5.12. First Bending Mode for ICW (Zone 1 Damage).

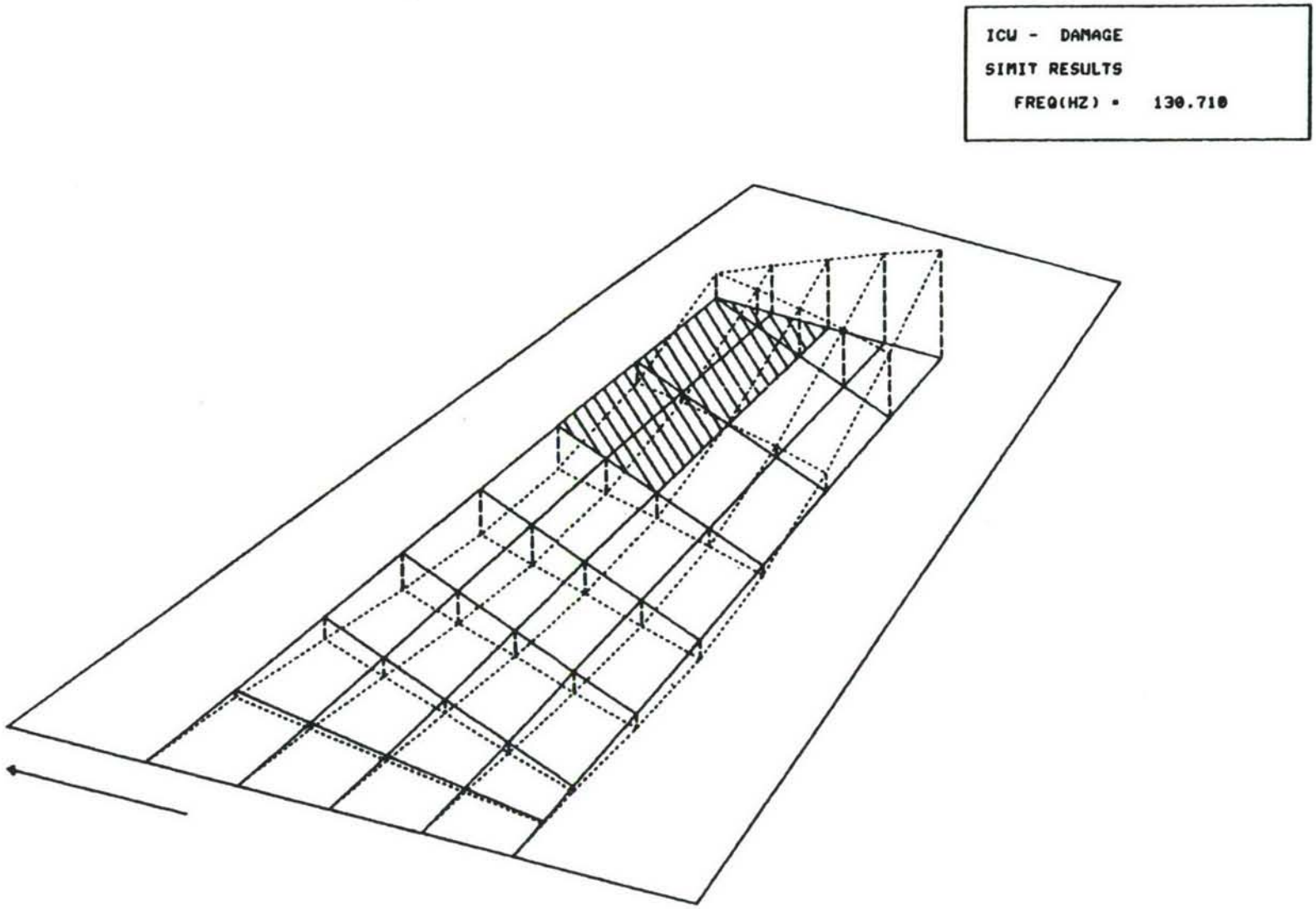

Figure 5.13. Second Bending Mode for ICW (Zone 1 Damage).

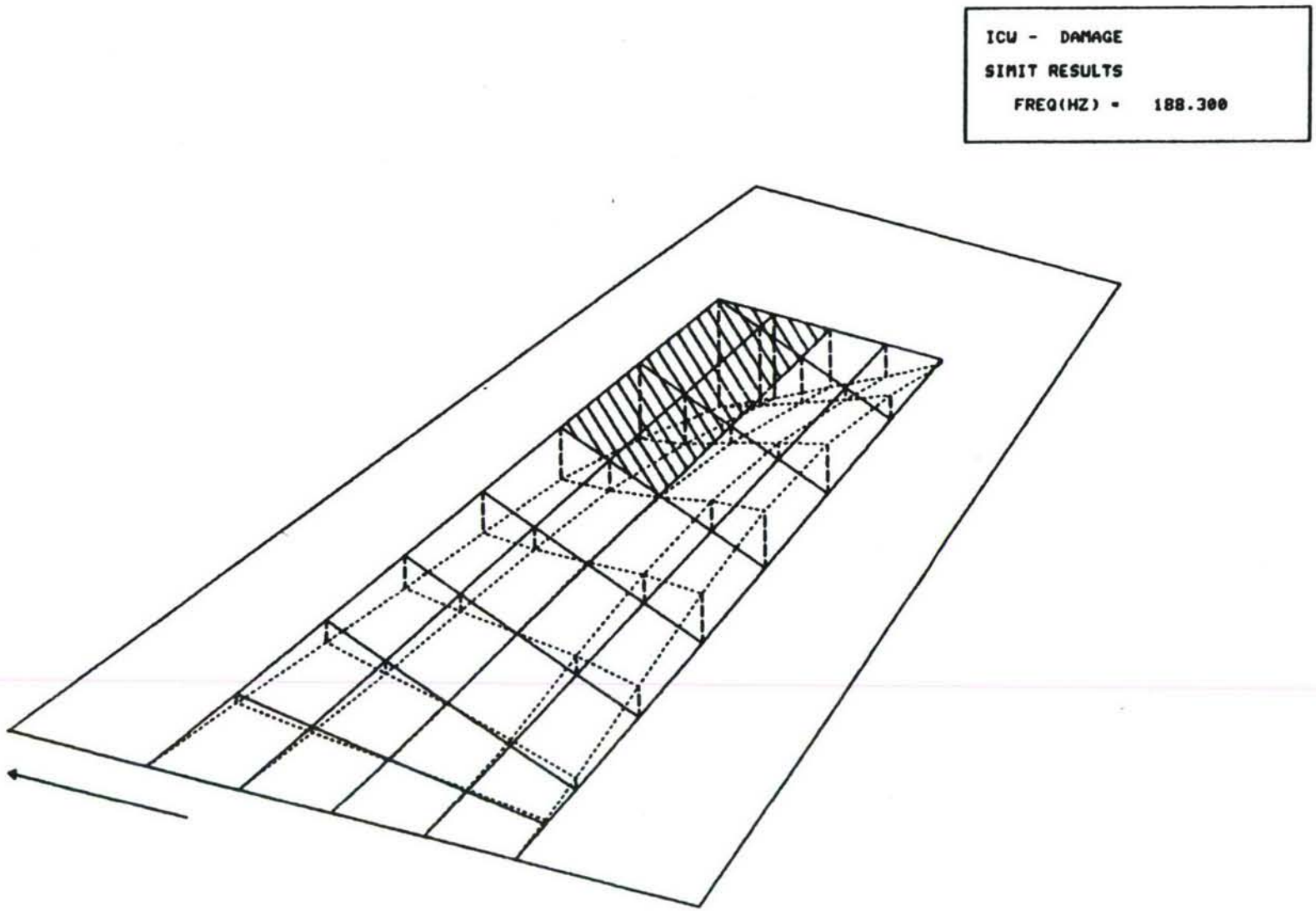

Figure 5.14. First Torsion Mode for ICW (Zone 1 Damage).

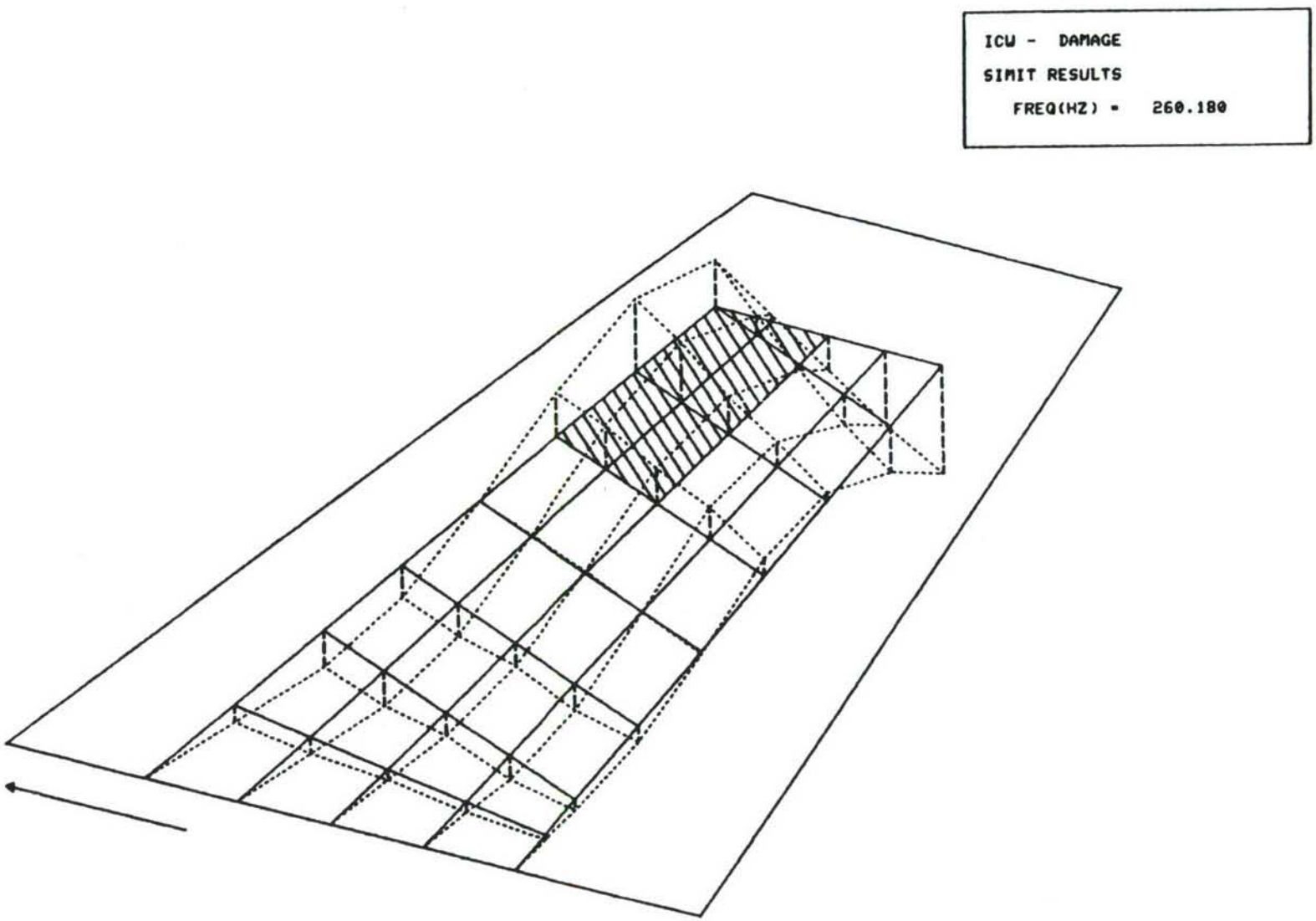

Figure 5.15. Third Bending Mode for ICW (Zone 1 Damage).

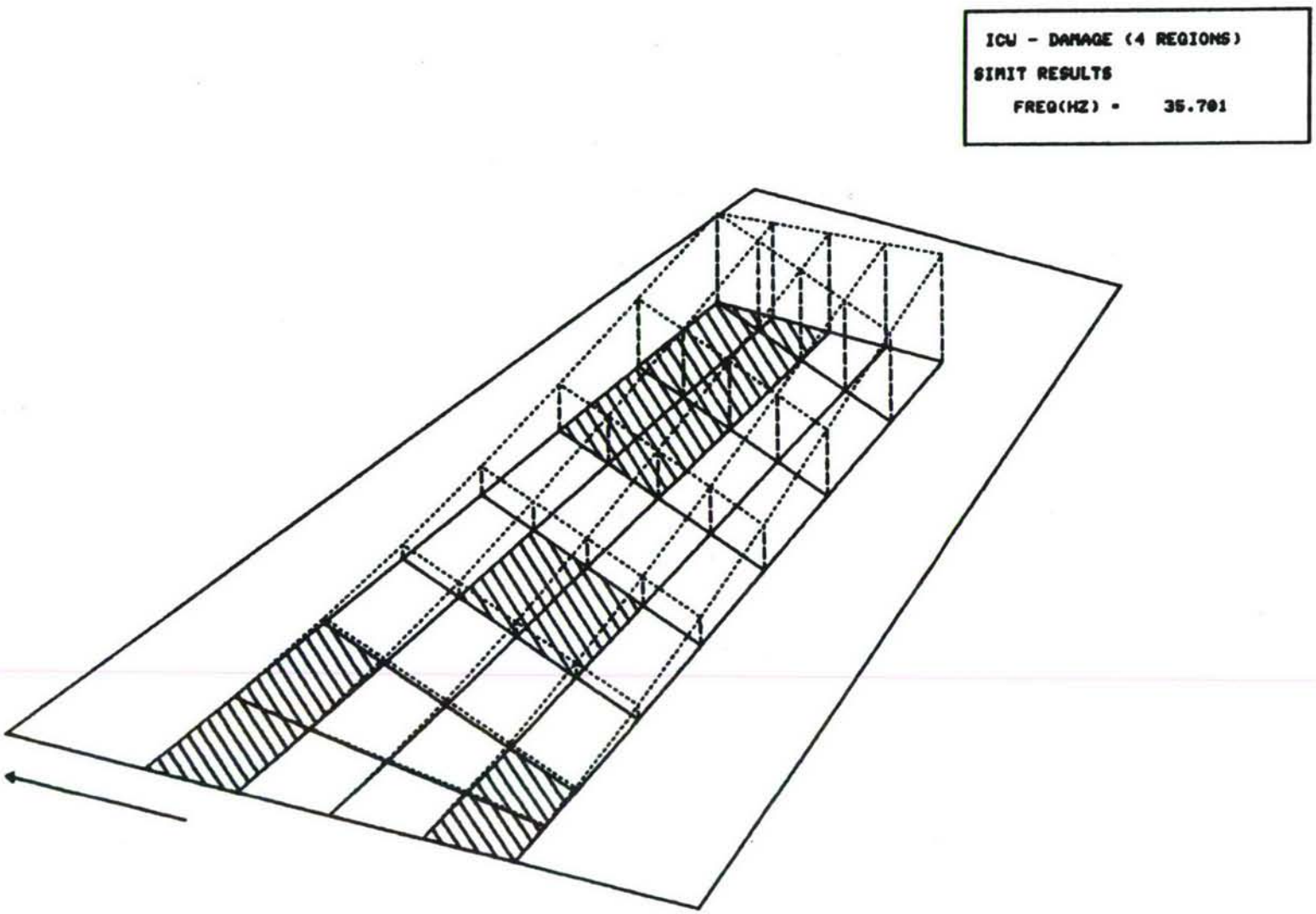

Figure 5.16. First Bending Mode for ICW (Four Damages).

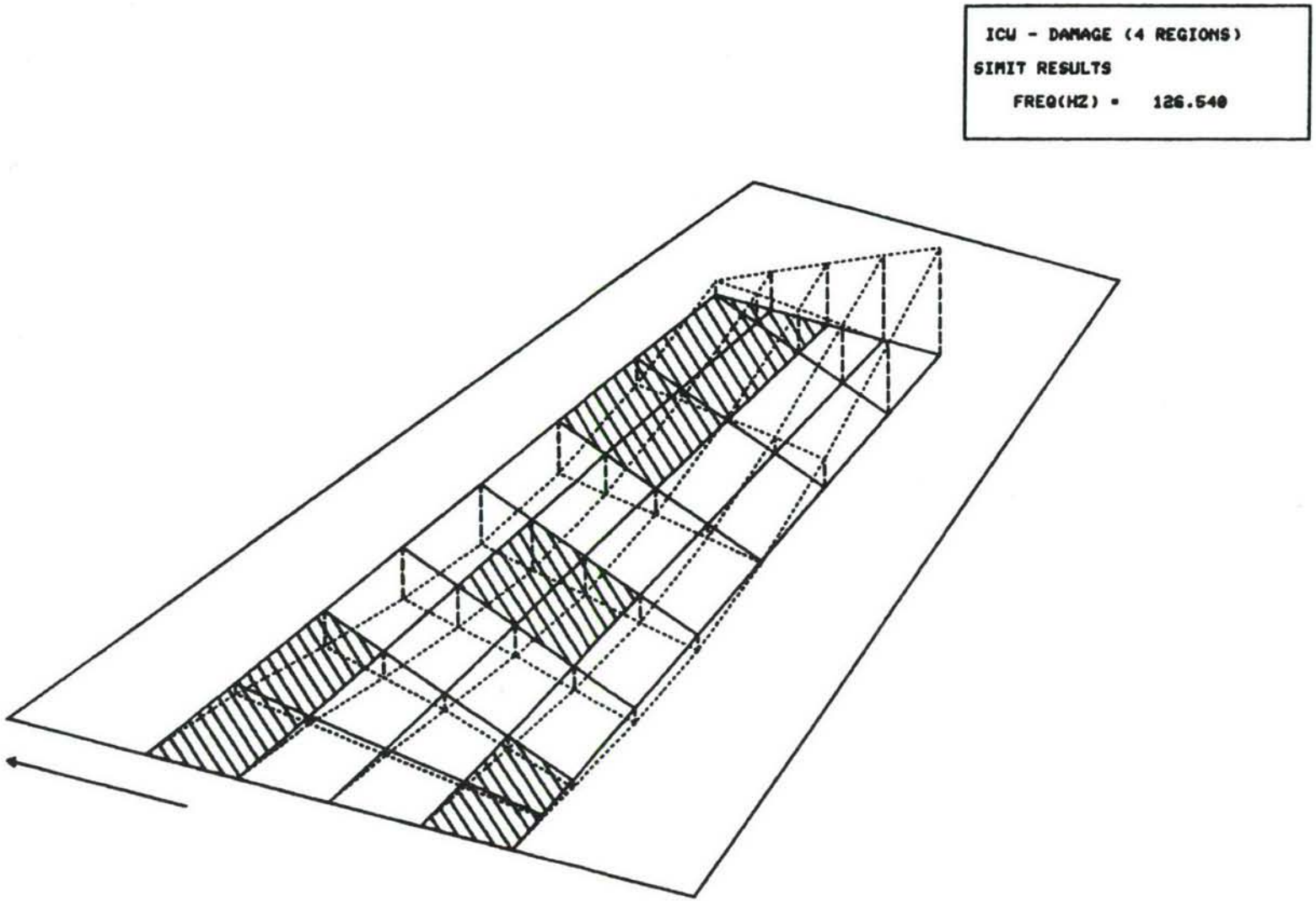

Figure 5.17. Second Bending Mode for ICW (Four Damages).

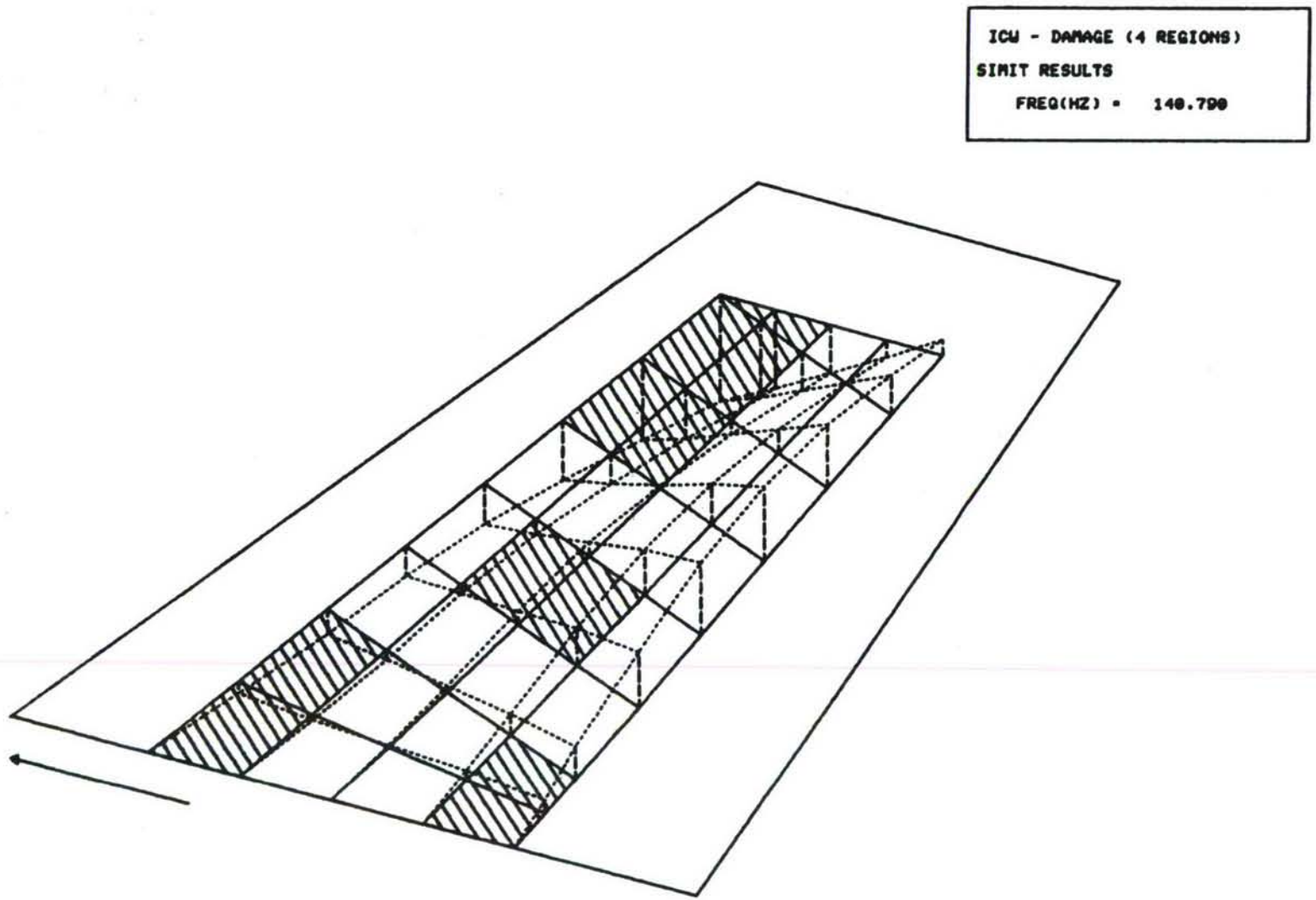

Figure 5.18. First Torsion Mode for ICW (Four Damages).

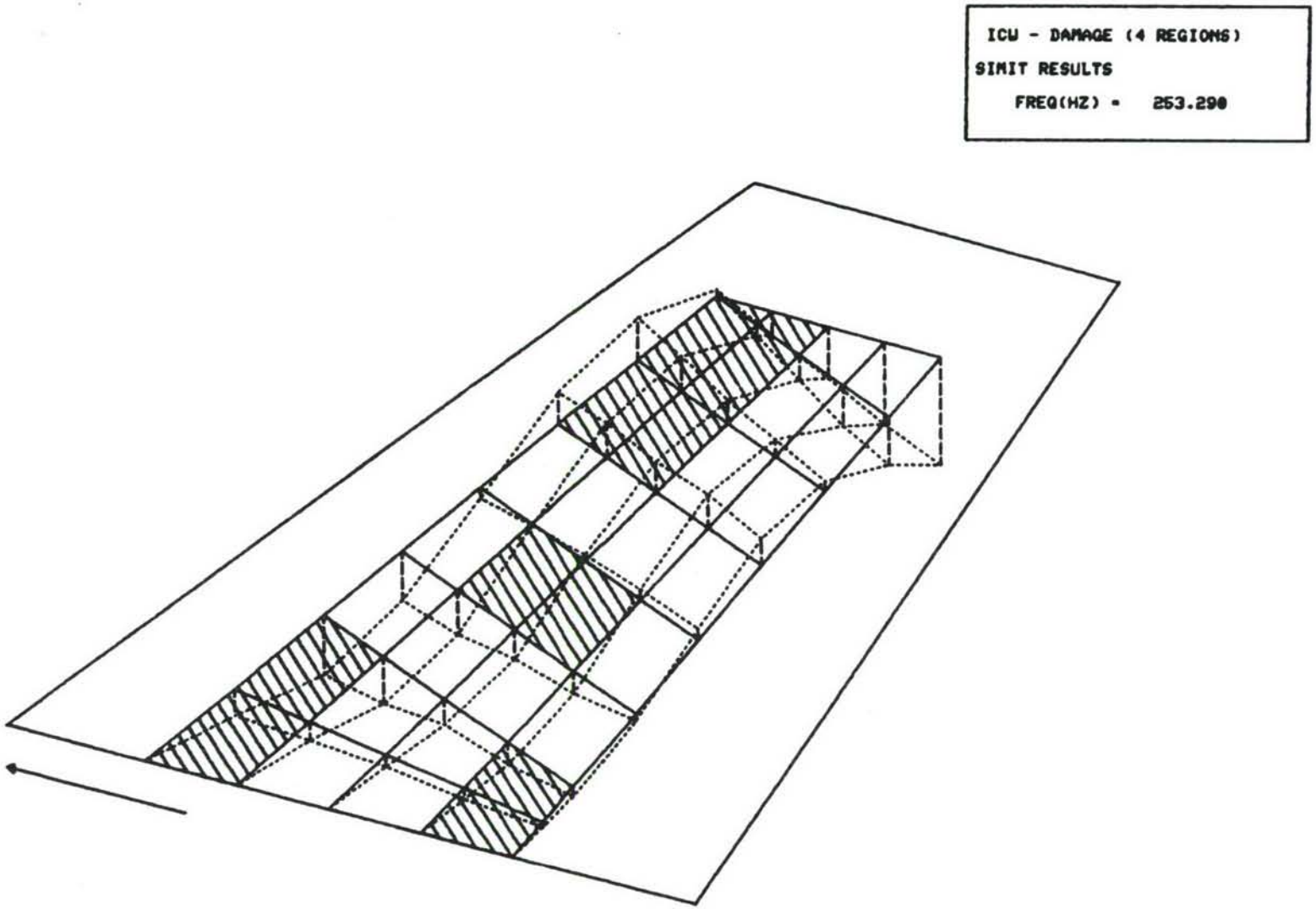

Figure 5.19. Third Bending Mode for ICW (Four Damages).

TABLE 5.7

FREQUENCY REANALYSIS RESULTS FOR ICW

Iteration	CP Sec. (CYBER 74)	f_1 (Hz)	f_2 (Hz)	f_3 (Hz)
0*	-	40.93	132.76	168.63
1	2.42	45.94	132.58	189.03
2	3.58	45.70	131.15	189.80
3	4.74	45.67	130.97	189.59
4	5.90	45.66	130.91	189.56
exact**	12.17	45.66	130.87	189.52

*Frequencies at iteration zero are for the undamaged wing.

**Exact frequencies and CP times for a complete eigen analysis of the damaged structure.

Table 5.8 shows the results for the ten-bar truss example. The ADDRESS program and the OPTSTATCOMP program were both run for five cycles of energy resizing. Reference 30 shows that if more than ten iterations are used, the weight should converge to about 5062 pounds when minimum sizes of 0.1 square inches are used for this load case.

Tables 5.9 and 5.10 show the ADDRESS and OPTSTATCOMP results, respectively, for the metal ICW model discussed earlier. The stress optimization using both programs yields a final design weight after five cycles of approximately 193 pounds. The ADDRESS program seems to produce a slightly lower weight than OPTSTATCOMP after one cycle. Direct stress allowables are taken to be 25 ksi in both tension and compression.

A stress and deflection optimization comparison is shown in Tables 5.11 and 5.12 for the ICW. The first four cycles are based on energy, and the remaining ones are resizing for the deflection requirement. In the ADDRESS program, if the weight more than doubles in the displacement resizing mode, then execution is terminated and the previous design is taken to be the final one. The OPTSTATCOMP program continued to resize for five cycles of displacement calculations, even though the doubling of weight criterion was met. It then returned to the energy based design of cycle 5.

A composite ICW Model based on the data of Reference 19 was also run. Only stress requirements were included. Tables 5.13 and 5.14 show the comparative results. Due to the higher minimum layer requirement used in ADDRESS (.0053) compared to OPTSTATCOMP (.005), the weights of the cover elements shown in Table 5.13 are higher. As with the metal ICW, the composite version was resized for two load conditions.

Figure 5.20 shows the total number of layers in the top and bottom covers obtained from the two programs. In Figure 2.21 the number of layers is broken down into numbers in the 0°, 90°, ±45° directions. The 0° direction is taken to be the direction of the center spar.

TABLE 5.8

COMPARISON OF ADDRESS AND OPTSTATCOMP
TEN-BAR TRUSS DESIGNS

Weight in Pounds

Element Number	ADDRESS Weight	OPTSTATCOMP Weight
1	1106.4	1093.2
2	3.6	17.6
3	861.7	884.1
4	530.5	524.8
5	3.6	.4
6	3.6	24.8
7	434.4	466.5
8	1067.0	1049.8
9	1061.1	1049.7
10	5.1	35.2
Total Weight	5077.0	5146.1

TABLE 5.9

ADDRESS RESULTS FOR METAL ICW WITH STRESS CONSTRAINT*

Weight in Pounds

Element Type	Initial Weight	Cycle 1 Weight	Cycle 2 Weight	Cycle 3 Weight	Cycle 4 Weight	Cycle 5 Weight
Covers	328.98	191.33	189.24	182.29	177.66	171.35
Shear Panels	102.44	23.62	23.09	22.54	22.29	21.78
Bars	6.74	.25	.24	.22	.22	.21
Total Weight (all elements)	438.16	215.20	212.57	205.05	200.17	193.34

TABLE 5.10

OPTSTATCOMP RESULTS FOR METAL ICW WITH STRESS CONSTRAINT*

Weight in Pounds

Element Type	Initial Weight	Cycle 1 Weight	Cycle 2 Weight	Cycle 3 Weight	Cycle 4 Weight	Cycle 5 Weight
Covers	328.98	193.98	189.04	182.20	177.61	171.23
Shear Panels	102.44	23.94	23.04	22.51	22.26	21.75
Bars	6.74	.26	.24	.22	.22	.21
Total Weight (all elements)	438.16	218.18	212.32	204.93	200.09	193.19

*Allowables set at 25 ksi.

TABLE 5.11

ADDRESS RESULTS FOR METAL ICW WITH STRESS* AND DEFLECTION** CONSTRAINTS

Element Type	Initial Weight	Cycle 1 Weight	Cycle 2 Weight	Cycle 3 Weight	Cycle 4 Weight	Cycle 5 Weight	Final Weight
Covers	253.88	232.62	226.66	222.14	218.92	542.18	218.92
Shear Panels	79.08	30.33	28.95	28.83	28.86	44.90	28.86
Bars	5.20	.31	.20	.20	.19	.41	.19
Total Weight (all elements)	338.26	263.26	255.81	251.17	247.97	587.49	247.97

Weight in Pounds

TABLE 5.12

OPTSTATCOMP RESULTS FOR METAL ICW WITH STRESS* AND DEFLECTION** CONSTRAINTS

Element Type	Initial Weight	Cycle 1 Weight	Cycle 2 Weight	Cycle 3 Weight	Cycle 4 Weight	Cycle 5 Weight	Final Weight
Covers	253.98	232.77	226.88	222.41	219.23	525.57	219.23
Shear Panels	79.08	30.34	28.94	28.82	28.83	195.50	28.83
Bars	5.20	.35	.25	.24	.24	.64	.24
Total Weight (all elements)	338.26	263.46	256.07	251.47	248.30	721.71	248.30

Weight in Pounds

*Allowables set at 60 ksi.
**Deflections limited to 4.0 inches in z-direction.

TABLE 5.13

ADDRESS RESULTS FOR COMPOSITE ICW
WITH STRESS CONSTRAINT

Element Type	Initial Weight	Cycle 1 Weight	Cycle 2 Weight	Cycle 3 Weight	Cycle 4 Weight
Covers	124.94	117.13	98.15	93.27	92.89
Shear Panels	70.73	43.42	27.62	27.06	27.38
Bars	4.65	2.75	1.49	1.45	1.47
Total Weight (all elements)	200.33	163.30	127.26	121.78	121.74

Weight in Pounds

TABLE 5.14

OPTSTATCOMP RESULTS FOR COMPOSITE ICW
WITH STRESS CONSTRAINT

Element Type	Initial Weight	Cycle 1 Weight	Cycle 2 Weight	Cycle 3 Weight	Cycle 4 Weight
Covers	124.94	86.03	76.03	71.24	71.24
Shear Panels	70.73	33.80	28.42	27.10	27.59
Bars	4.65	2.02	1.53	1.43	1.47
Total Weight (all elements)	200.33	121.85	105.98	99.77	100.30

Weight in Pounds

NOTE: Top figures are from ADDRESS: bottom figures ( ) are from OPTSTATCOMP.

One OPTSTATCOMP layer = .005 in.

One ADDRESS layer = .0053 in.

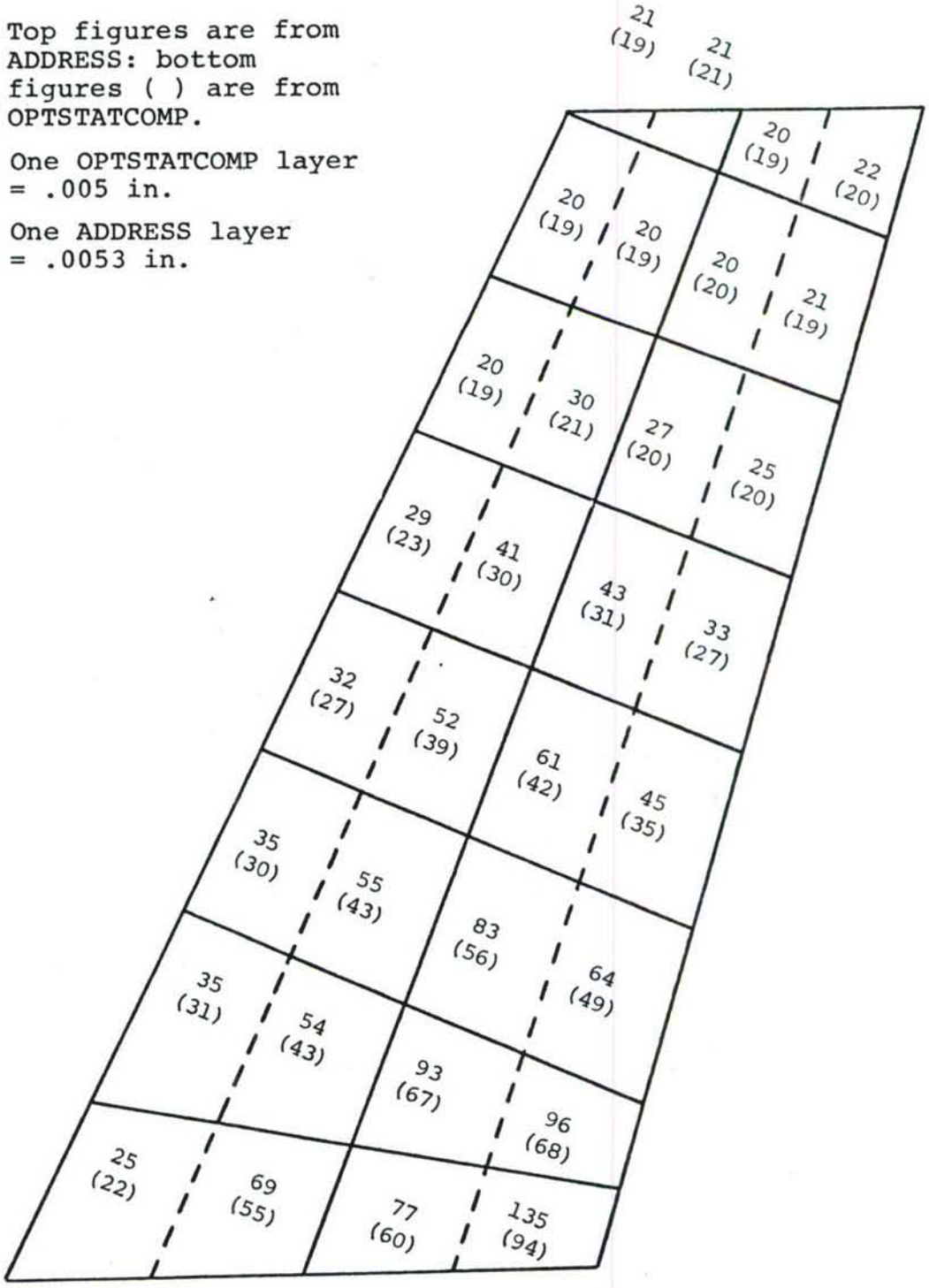

Figure 5.20. Total Number of Layers in the Top Skin of Composite ICW.

NOTE: Top figures are from ADDRESS; bottom figures ( ) are from OPTSTATCOMP.

One OPTSTATCOMP layer = .005 in.

One ADDRESS layer = .0053 in.

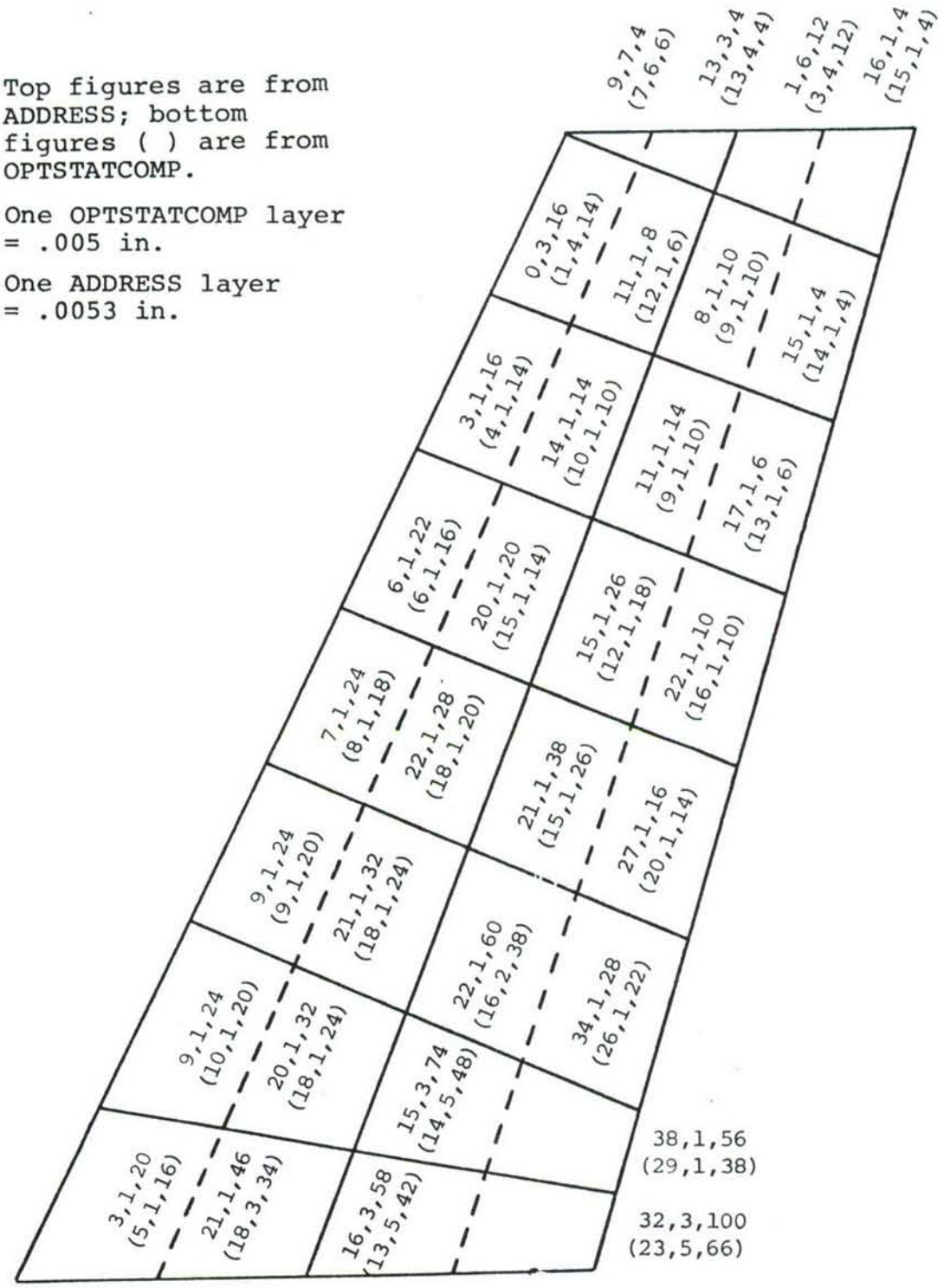

Figure 5.21. Distribution of Fibers in 0°, 90°, ±45° Directions in the Top Skin of Composite ICW.

Table 5.15 summarizes the execution times for the two programs on the problems just discussed. One major reason for the faster ADDRESS time is in the coding of the decomposition of the stiffness matrix. Subroutine GAUSS was replaced with subroutine LLT which has the DO-loops reorganized. This section of code in ADDRESS now runs about four times as fast as the OPTSTATCOMP code. If reanalysis had been used in these examples, the running times would have been improved even more.

TABLE 5.15

EXECUTION TIMES FOR OPTSTATCOMP AND ADDRESS

Problem	Execution Times - CYBER 175	
	OPSTATCOMP	ADDRESS
TEN BAR TRUSS Stress and Displacement Optimization	0.9	0.5
METAL WING Stress Optimization	38.9	23.8
METAL WING Stress and Displacement Optimization	53.5	28.7
COMPOSITE WING Stress Optimization	76.9	51.7

SECTION 6
DESIGN STUDIES FOR A-7D OUTER WING PANEL

To demonstrate the ADDRESS computer program, a major task of this work was to perform a design vulnerability and optimization study on an existing aircraft lifting surface component. This section describes the UDRI and Vought Corporation efforts to model, resize, and further refine the design of an A-7D outer wing panel. Both metal and composite models are considered.

The work described in this section involved several distinct subtasks. Vought, acting as a subcontractor to the UDRI, participated as a consultant in the selection of the A7D outer wing panel as the candidate structure for redesign. During the analysis task Vought supplied UDRI with geometry, loads, material properties, and ballistic damage requirements. The UDRI then set up the finite element model and performed optimization studies using ADDRESS. Member sizes were then supplied to Vought and additional design criteria were applied. The final designs were checked again using the ADDRESS program to obtain final weights and to check the stress levels. A test plan and design drawings were generated by Vought for fabrication and testing purposes. These items are documented as a separate contract item.

6.1 FINITE ELEMENT MODELING OF THE A-7D OUTER WING PANEL

The A-7 aircraft is an attack fighter designed for carrier-based operations. Figure 6.1 shows the overall aircraft arrangement. The portion of the wing structure which was modeled in this study is shaded in the figure.

Figure 6.2 shows the A-7 wing structure in some detail. The portion of the wing inboard of the hinge line is all metal. The outer wing panel can be replaced and is of metal or composite construction. Further structural detail of the outer panel is shown in Figure 6.3. It is this general arrangement of Figure 6.3 which formed the basis of the finite element model.

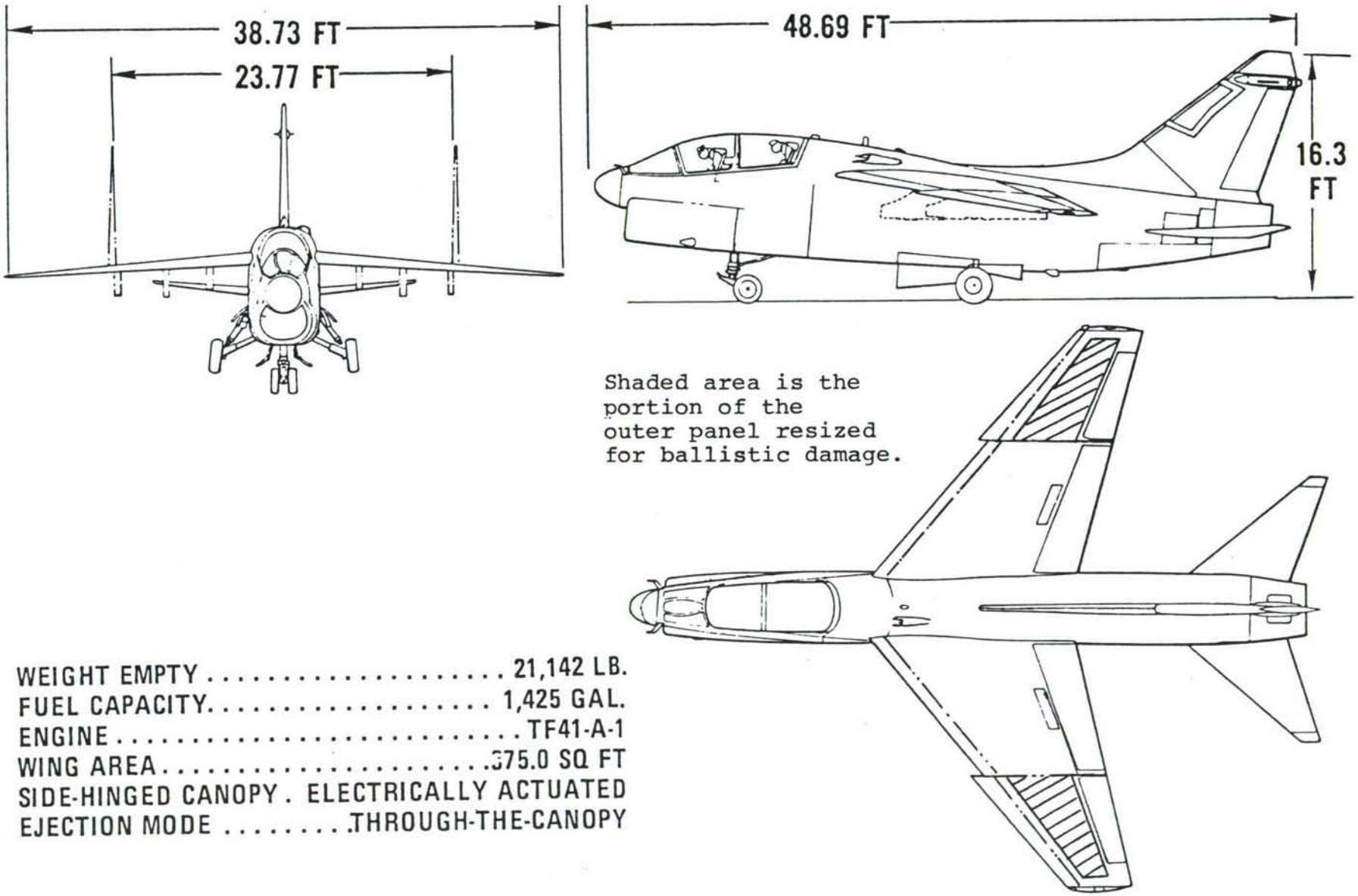

Figure 6.1. A-7 Aircraft General Arrangement.

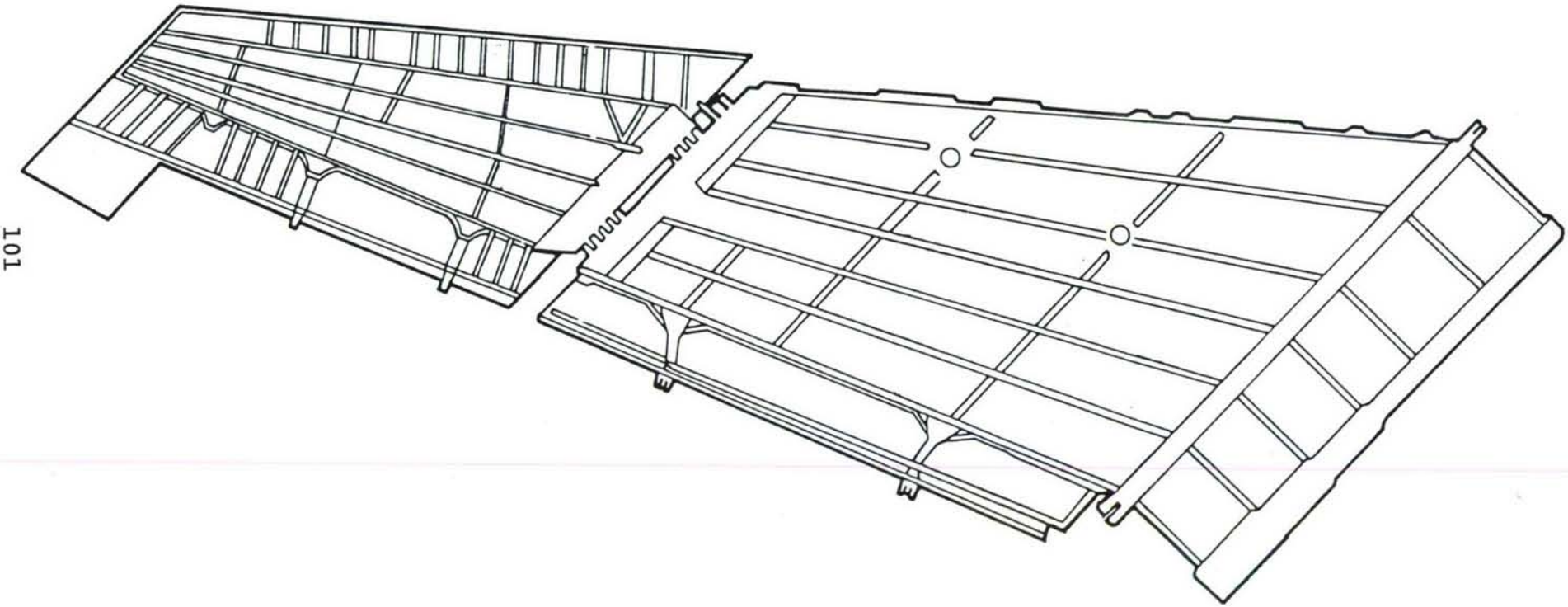

Figure 6.2. A-7 Wing Structural Arrangement.

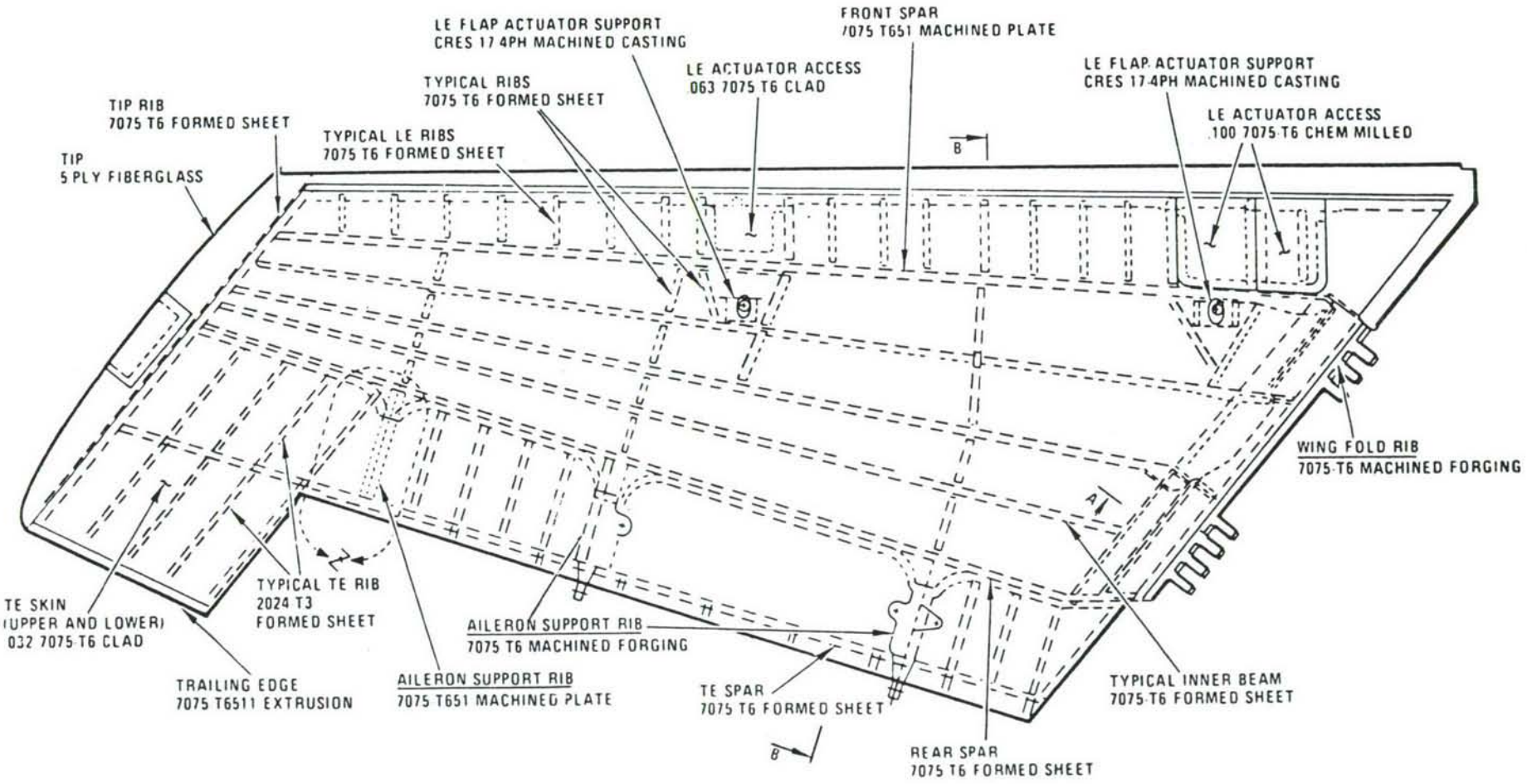

Figure 6.3. A-7 Wing Outer Panel.

The A7 wing structure was tested originally for the static loads described in Table 6.1. A review of these design loads determined that the condition LAD-1 produces the highest skin stresses and was therefore included as a load case. The second loading used was the RPO-2A condition which is primarily a torsion loading.

Figures 6.4 and 6.5 show the shear, moment, and torque diagrams for the LAD-1 and the RPO-2A load cases, respectively. These distributions apply to the entire wing from the fuselage to the tip. Only the portions of the curves outboard of the wing fold line (y_W = 142 in.) were used to generate the discrete loads.

An overview of the UDRI finite element model is shown in Figure 6.6. The seven-spar arrangement was used in both the metal and composite design studies. The model contains 113 nodes and 453 finite elements. Nodes 104 through 113 are fully restrained to simulate a fixed condition at the wing hinge line. The nodes numbered in the figure apply to the top surface with the missing numbers applying to the lower surface. The wing tip tapers to a line of nodes 1 through 7, and hence there are no corresponding lower surfaces at span station 93.

Two damage zones are also indicated in Figure 6.6. Damage zone number one consists of the eight covers (upper and lower) shaded near the tip. The second damage zone is near the root and consists of four covers. Two other cases were also considered for several computer runs. In one of these, rib and spar elements were also damaged as well as the indicated covers. The final damage case consisted of reducing the stiffness of all the covers from root to tip between the third and fifth spar from the leading edge. In all damage cases, 75% of the element thickness was removed to simulate the effect of ballistic damage to the zone.

Table 6.2 shows the nodal coordinates and the three components of the applied loads for both load cases. The point loads were iteratively determined in such a way as to match as closely as

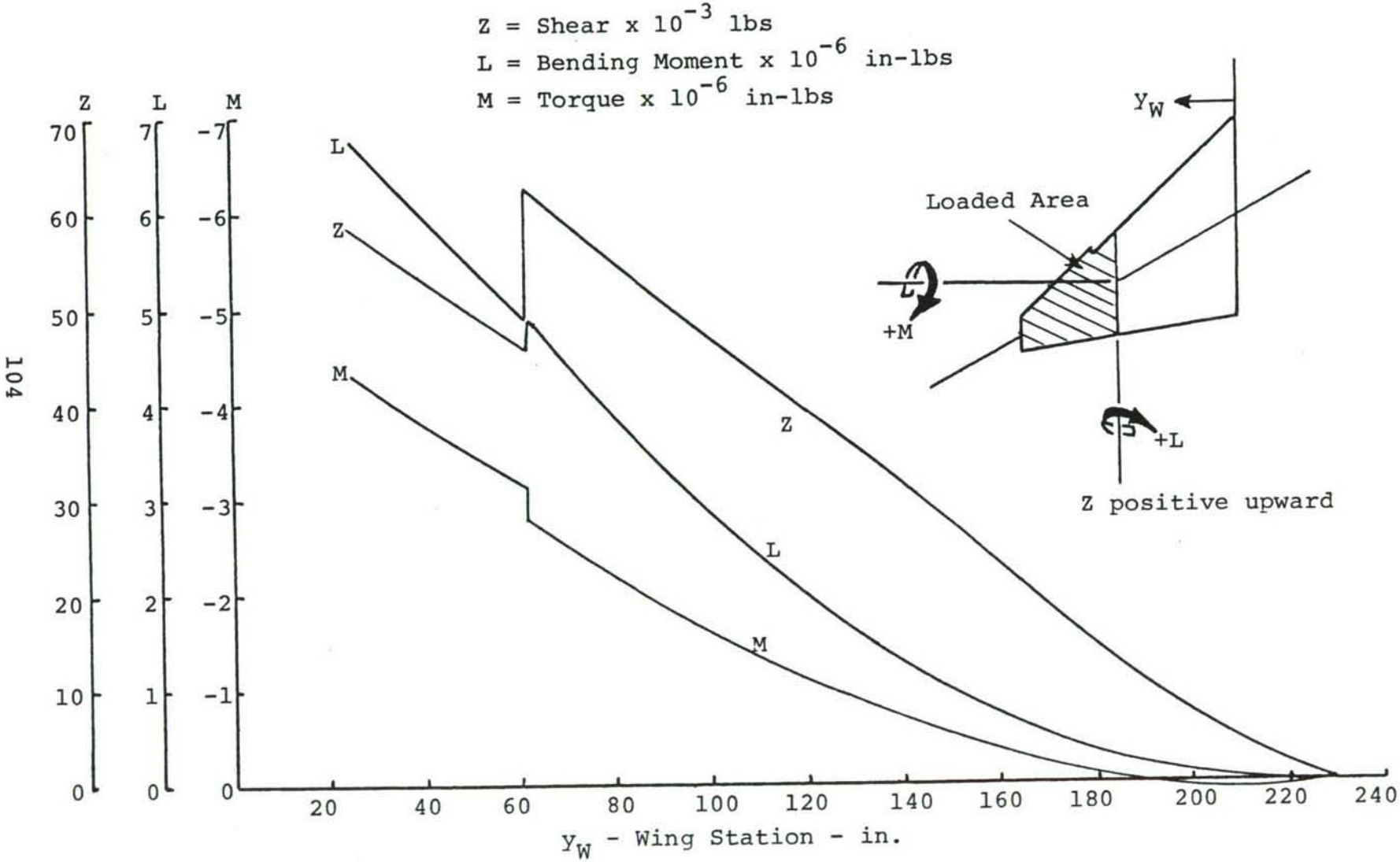

Figure 6.4. A-7 Load Case Number One.

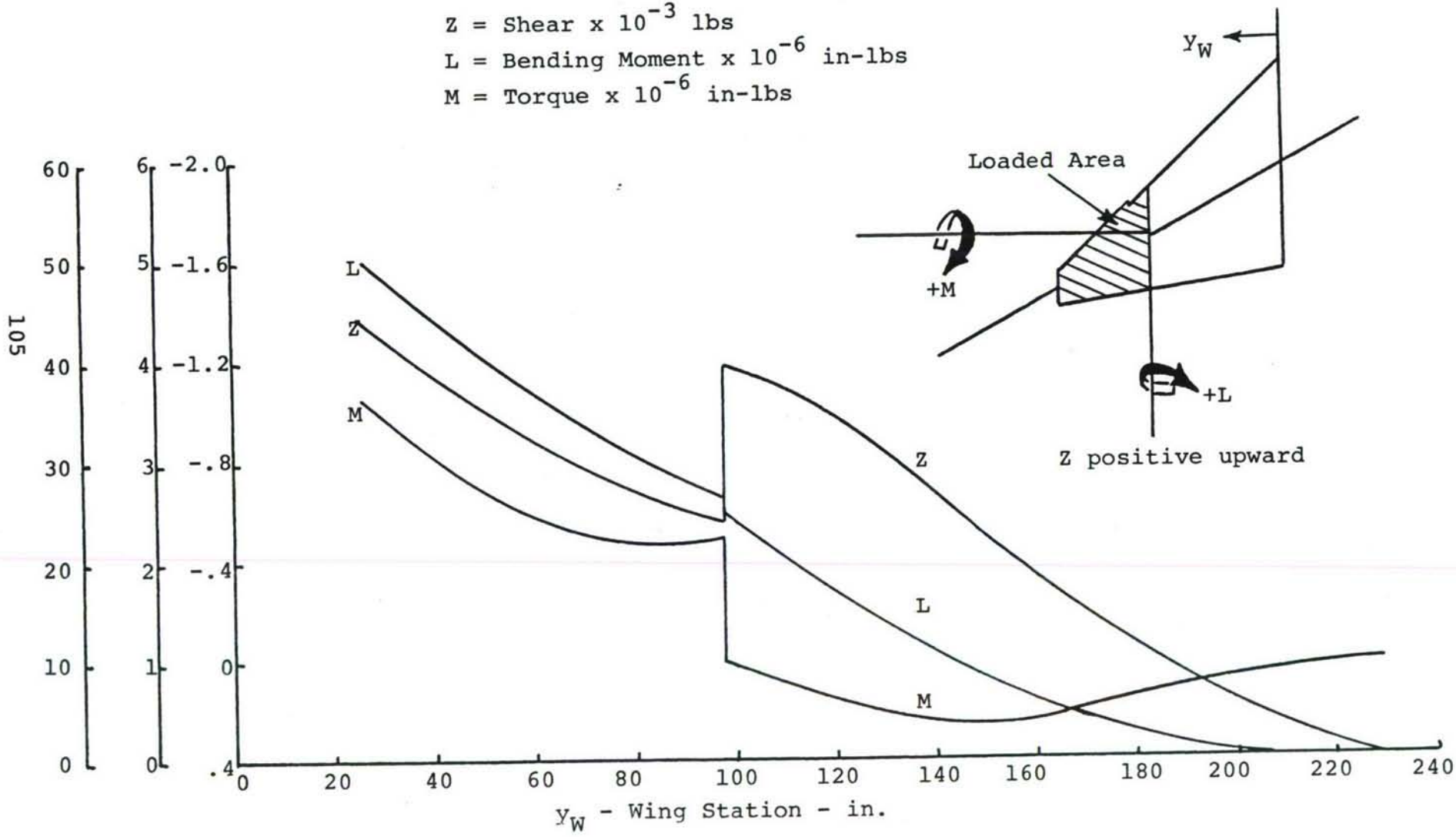

Figure 6.5. A-7 Load Case Number Two.

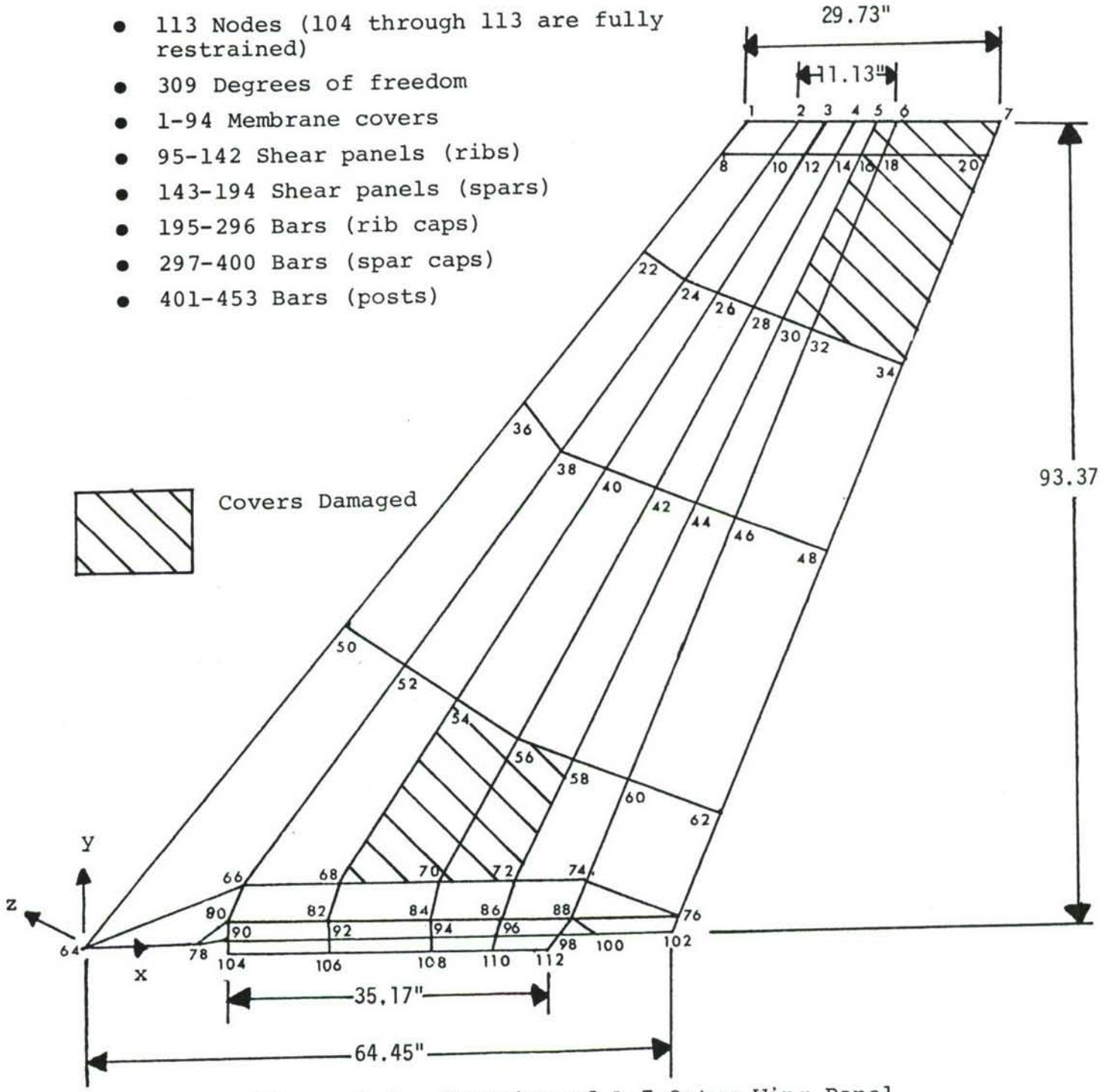

Figure 6.6. Overview of A-7 Outer Wing Panel Finite Element Model.

TABLE 6.1

A-7 STATIC TEST CONDITIONS

CONDITION	DESCRIPTION	N_Z LIMIT	CRITICAL STRUCTURE
LFR-1	UPGOING WING, AILERONS WITH ROLL	0.0	LE RIBS, OUTBOARD RIB, FLAP (DOWN LOAD)
RPO-2A	ROLLING PULLOUT	5.6	MAIN BOX (TORSION), FRONT SPAR, MID SPAR LE (UP LOAD), AILERON (DOWN LOAD)
HAD-1	SYMMETRIC, HIGH ANGLE OF ATTACK, FORWARD cp	7.0	MID SPAR, STUB SPAR, WINGFOLD JOINT
LAD-1	SYMMETRIC, LOW ANGLE OF ATTACK, NORMAL cp	7.0	MAIN BOX SKINS, WINGFOLD JOINT, REAR SPAR, AILERON (UP LOAD)

TABLE 6.2

NODAL AND APPLIED LOAD DATA FOR A-7D OUTER WING PANEL

Node No.	X in	Y in	Z in	F_x - LC1	F_x - LC2	F_y - LC1	F_y - LC2	F_z - LC1	F_z - LC2
1	74.80	92.70	0.00	0.00	0.00	0.00	0.00	17.83	15.26
2	80.89	93.23	0.00					19.77	16.92
3	84.04	93.31	0.00					21.13	18.08
4	87.19	93.39	0.00					22.29	19.08
5	89.61	93.37	0.00					23.07	19.74
6	92.02	93.34	0.00					20.54	17.58
7	104.53	92.99	0.00					16.47	14.10
8	72.00	89.51	0.43					160.47	158.48
9	72.23	89.34	-1.76					160.47	158.48
10	78.07	89.35	1.39					178.12	175.89
11	78.07	89.35	-1.39					178.12	175.89
12	81.54	89.35	1.46					190.47	182.85
13	81.54	89.35	-1.46					190.47	182.85
14	85.00	89.35	1.54					202.83	200.30
15	85.00	89.35	-1.54					202.83	200.30
16	87.71	89.34	1.55					195.77	193.32
17	87.71	89.34	-1.55					195.77	193.32
18	90.42	89.33	1.56					218.71	215.99
19	90.42	89.33	-1.56					218.71	215.99
20	102.97	89.30	1.13					259.30	256.06
21	102.97	89.30	-1.13					259.30	256.06
22	63.26	78.64	.60					528.12	474.33
23	63.52	78.44	-1.95					528.12	474.33
24	67.78	75.18	1.61					475.12	421.24
25	67.78	75.18	-1.62					475.12	421.24
26	71.73	72.67	1.75					427.43	373.45
27	71.73	73.67	-1.75					427.43	373.45
28	75.67	72.16	1.88					474.44	320.35
29	75.67	72.16	-1.88					474.44	320.35
30	79.09	70.80	1.88					342.64	288.49
31	79.09	70.80	-1.88					342.64	288.49
32	82.50	69.44	1.87					300.25	246.02
33	82.50	69.44	-1.87					300.25	246.02
34	92.84	65.30	1.31					178.37	123.89
35	92.84	65.30	-1.31					178.37	123.89
36	49.71	61.79	.74					265.72	775.63
37	49.99	61.56	-2.33					265.72	775.63
38	53.91	56.10	1.94					362.88	667.49
39	53.91	56.10	-1.96					362.88	667.49
40	59.27	53.96	2.12					468.13	571.16
41	59.27	53.96	-2.13					468.13	571.16
42	64.63	51.81	2.29					565.29	473.01
43	64.63	51.81	-2.29					565.29	473.01
44	69.31	49.94	2.23					638.15	399.40
45	69.31	49.94	-2.24					638.15	399.40
46	73.99	48.07	2.18					727.21	309.44
47	73.99	48.07	-2.18					727.21	309.44
48	83.92	44.10	1.58					889.14	109.86

TABLE 6.2 (Continued)

Node No.	X in	Y in	Z in	F_x - LC1	F_x - LC2	F_y - LC1	F_y - LC2	F_z - LC1	F_z - LC2
49	83.92	44.10	-1.58	0.00	0.00	0.00	0.00	889.14	109.86
50	29.80	37.04	.95					-201.38	1213.24
51	30.19	36.75	-2.88					-201.38	1213.24
52	36.27	31.83	2.37					149.15	1038.66
53	36.27	31.83	-2.38					149.15	1038.66
54	42.63	27.41	2.61					499.67	864.09
55	42.63	27.41	-2.62					499.67	864.09
56	48.98	22.98	2.86					850.20	689.51
57	48.98	22.98	-2.86					850.20	689.51
58	55.47	20.43	2.72					1135.00	547.67
59	55.47	20.43	-2.72					1135.00	547.67
60	61.96	17.87	2.57					1463.62	384.00
61	61.96	17.87	-2.57					1463.62	384.00
62	71.25	14.16	1.97					1857.96	187.61
63	71.25	14.16	-1.97					1857.96	187.61
64	0.00	0.00	1.22					-126.60	268.95
65	.56	-.37	-3.84					-126.60	268.95
66	17.85	6.48	2.82					-25.14	214.19
67	17.85	6.48	-2.83					-25.14	214.19
68	28.98	6.48	3.00					63.65	166.23
69	28.98	6.48	-3.05					63.65	166.23
70	40.11	6.48	3.19					143.97	122.93
71	40.11	6.48	-3.26					143.97	122.93
72	48.76	6.48	2.96					207.38	88.70
73	48.76	6.48	-2.99					207.38	88.70
74	57.40	6.48	2.72					270.80	54.47
75	57.40	6.48	-2.72					270.80	54.47
76	66.29	2.39	2.33					346.89	13.40
77	66.29	2.39	-2.33					346.89	13.40
78	13.12	-.02	2.67					-29.36	216.48
79	13.12	-.02	-2.91					-29.36	216.48
80	16.54	2.60	2.84					-16.68	209.98
81	16.54	2.60	-2.80					-16.68	209.98
82	27.86	2.46	3.07					59.42	168.56
83	27.86	2.46	-3.04					59.42	168.56
84	39.18	2.32	3.29					152.43	118.36
85	39.18	2.32	-3.27					152.43	118.36
86	47.01	2.32	3.00					207.38	88.70
87	47.01	2.32	-3.04					207.38	88.70
88	54.83	2.32	2.71					266.57	56.76
89	54.83	2.32	-2.80					266.57	56.76
90	16.54	.58	2.87					-8.22	205.07
91	16.54	.58	-2.84					-8.22	205.07
92	27.86	.58	3.08					76.33	159.43
93	27.86	.58	-3.05					76.33	159.43
94	39.18	.58	3.29					160.88	113.80
95	39.18	.58	-3.27					160.88	113.80

TABLE 6.2 (Continued)

Node No.	X in	Y in	Z in	F_x - LC1	F_x - LC2	F_y - LC1	F_y - LC2	F_z - LC1	F_z - LC2
96	46.23	.58	3.03	0.00	0.00	0.00	0.00	211.61	86.42
97	46.23	.58	-2.98					211.61	86.42
98	53.27	.58	2.77					262.34	59.04
99	53.27	.58	-2.68					262.34	59.04
100	59.37	.47	2.62					304.62	36.22
101	59.37	.47	-2.62					304.62	36.22
102	65.45	.39	2.36					346.89	13.40
103	65.45	.39	-2.36					346.89	13.40
104	16.54	-1.12	2.70					0.00	0.00
105	16.54	-1.12	-2.68						
106	27.86	-1.12	2.99						
107	27.86	-1.12	-2.98						
108	39.18	-1.12	3.28						
109	39.18	-1.12	-3.27						
110	45.45	-1.12	3.00						
111	45.45	-1.12	-2.98						
112	51.71	-1.12	2.72						
113	51.71	-1.12	-2.70						

F_x, F_y, F_z loads are in pounds.
LC1 = Load Case 1
LC2 = Load Case 2

possible the shear, moment, and torque diagrams. The cumulative effect of the loads at the root matches the load diagram exactly; however, due to the skewed pattern of the nodes, the load data in the midsection of the wing matches only to within ±10%.

Figures 6.7 through 6.10 provide further details of the model. The wing taper and tip modeling discussed above can be clearly seen in Figure 6.7. Figure 6.8 shows the cover numbering scheme. The rib and spar panel numbers are shown in Figures 6.9 and 6.10, respectively.

6.2 MATERIAL PROPERTIES AND DAMAGE CASES

Material properties for the metal A7D outer panel were based on typical 7075-T6 aluminum:

E = Young's modulus = 10.3×10^6 psi
ν = Poisson's ratio = .33
ρ = Mass density = .1 lbf/in^3
G = Shear modulus = 3.9×10^6 psi

with the following stress allowables:

σ_{TU} = Allowable stress in tension = 72 ksi
σ_{CY} = Allowable stress in compression = 63 ksi
σ_{CR} = Allowable stress in shear = 43 ksi.

The composite design was based on 5208/T-300 graphite/epoxy tape with a layup consisting of 50% (0° plies), 40% (±45° plies), and 10% (90° plies):

E_1 = 12.2×10^6 psi
E_2 = 4.5×10^6 psi
ν = .4
ρ = .057 lbf/in^3
G = 2.7×10^6 psi

with the following stress allowables:

σ_{TU1} = 102.0 ksi
σ_{TU2} = 15.0 ksi

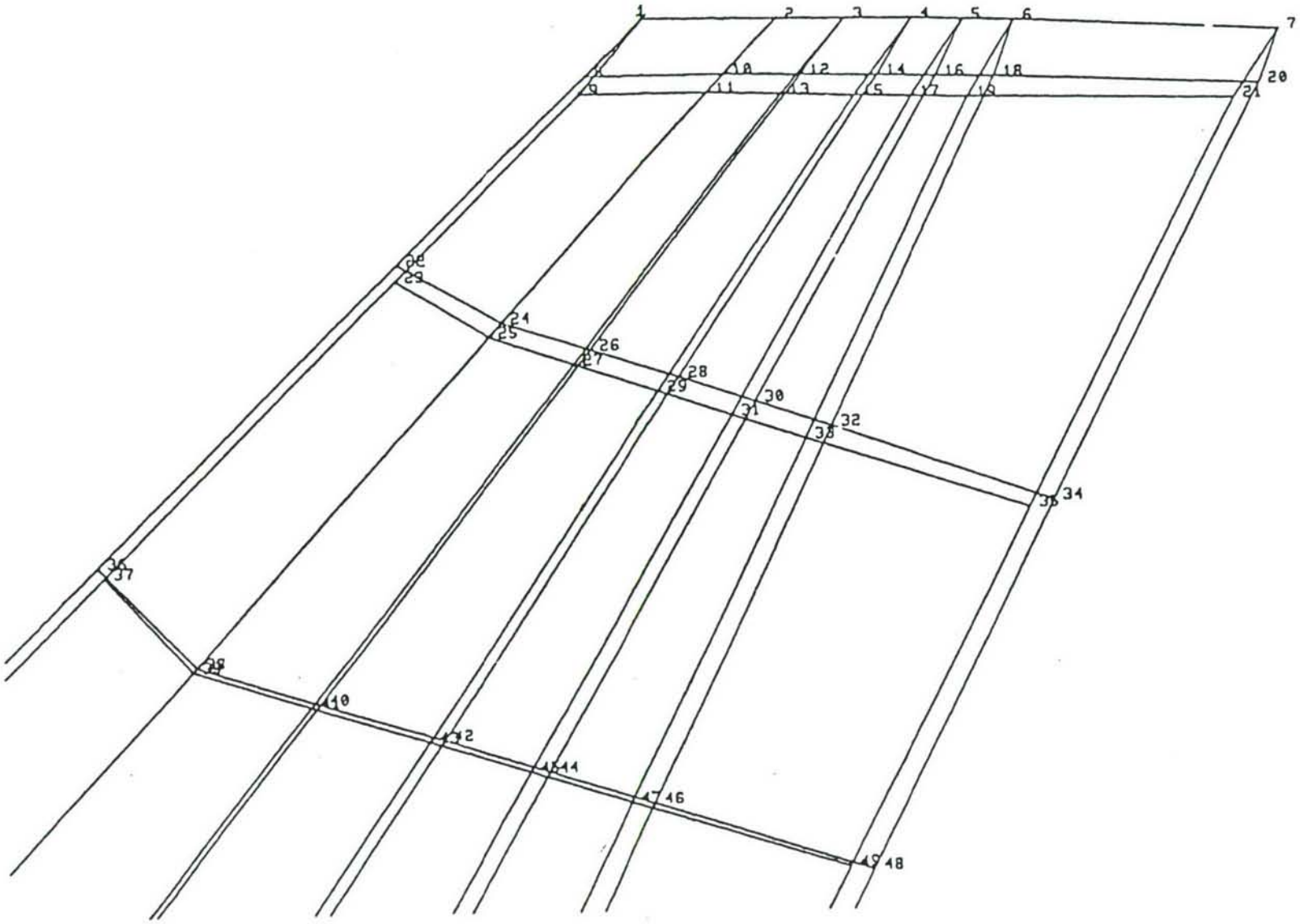

Figure 6.7. A-7 Outer Wing Panel Mode Numbers. (Sheet 1 of 2)

Nodes 104 through
113 are fixed.

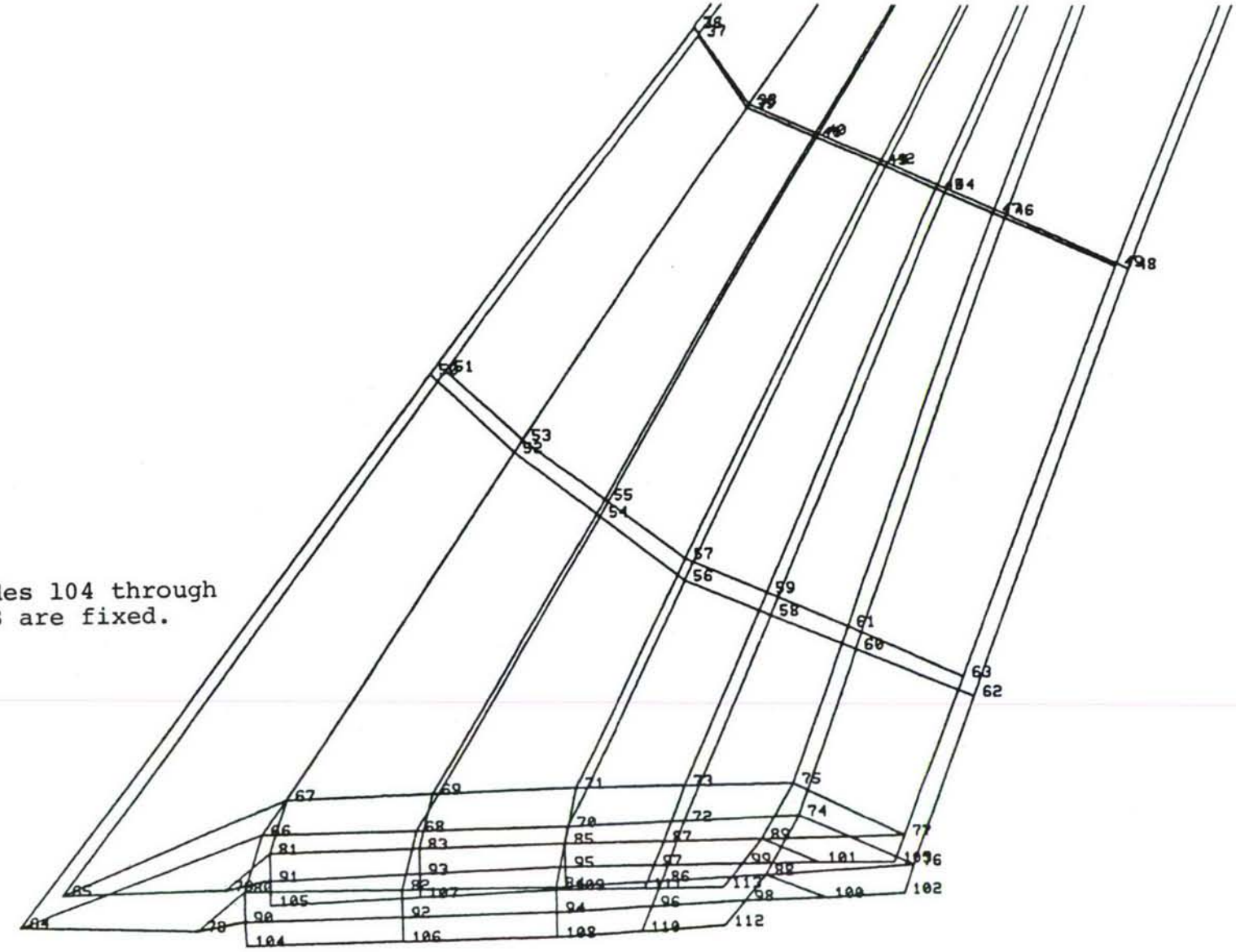

Figure 6.7. A-7 Outer Wing Panel Mode Numbers. (Sheet 2 of 2)

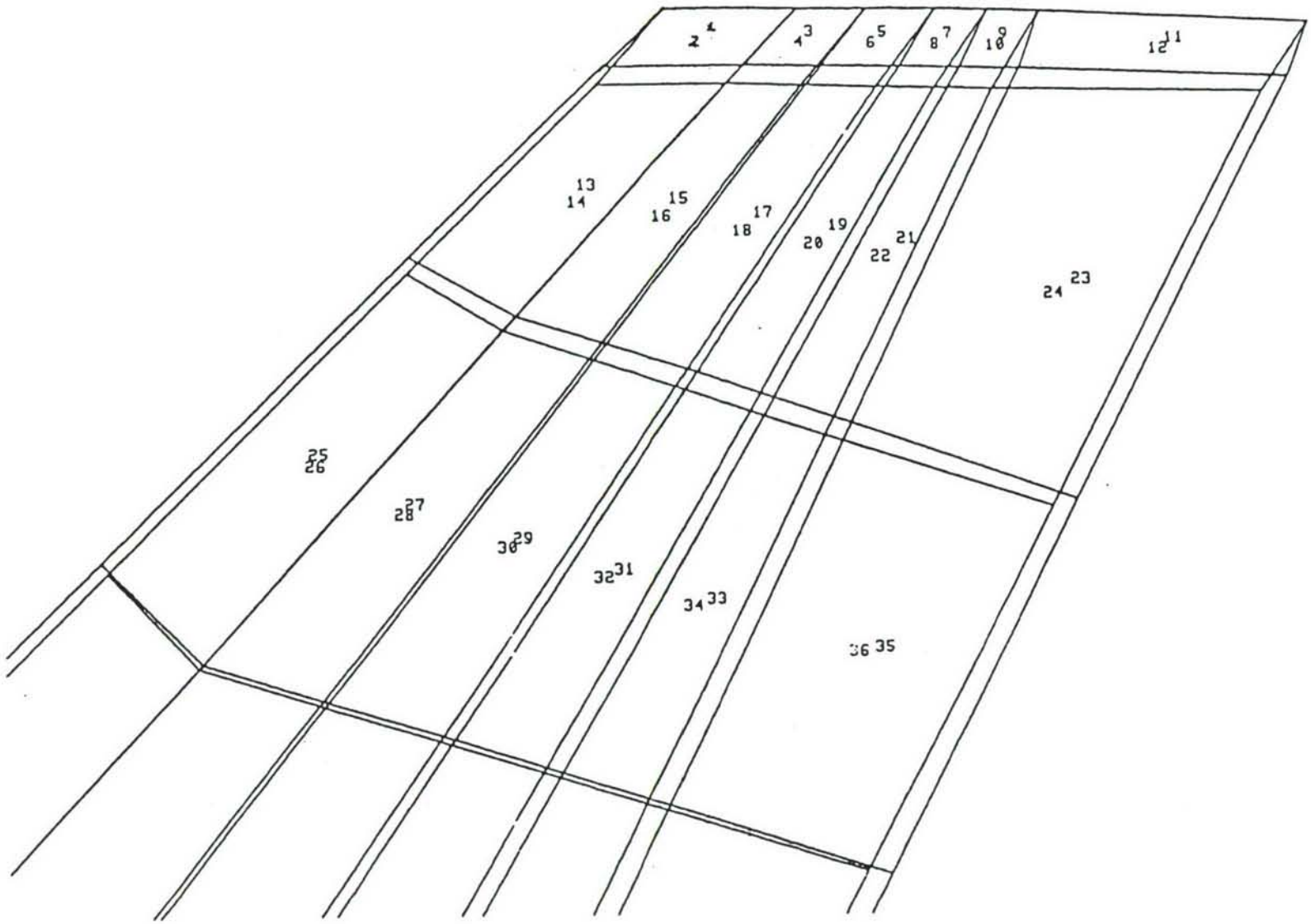

Figure 6.8. A-7 Outer Wing Panel Cover Elements. (Sheet 1 of 2)

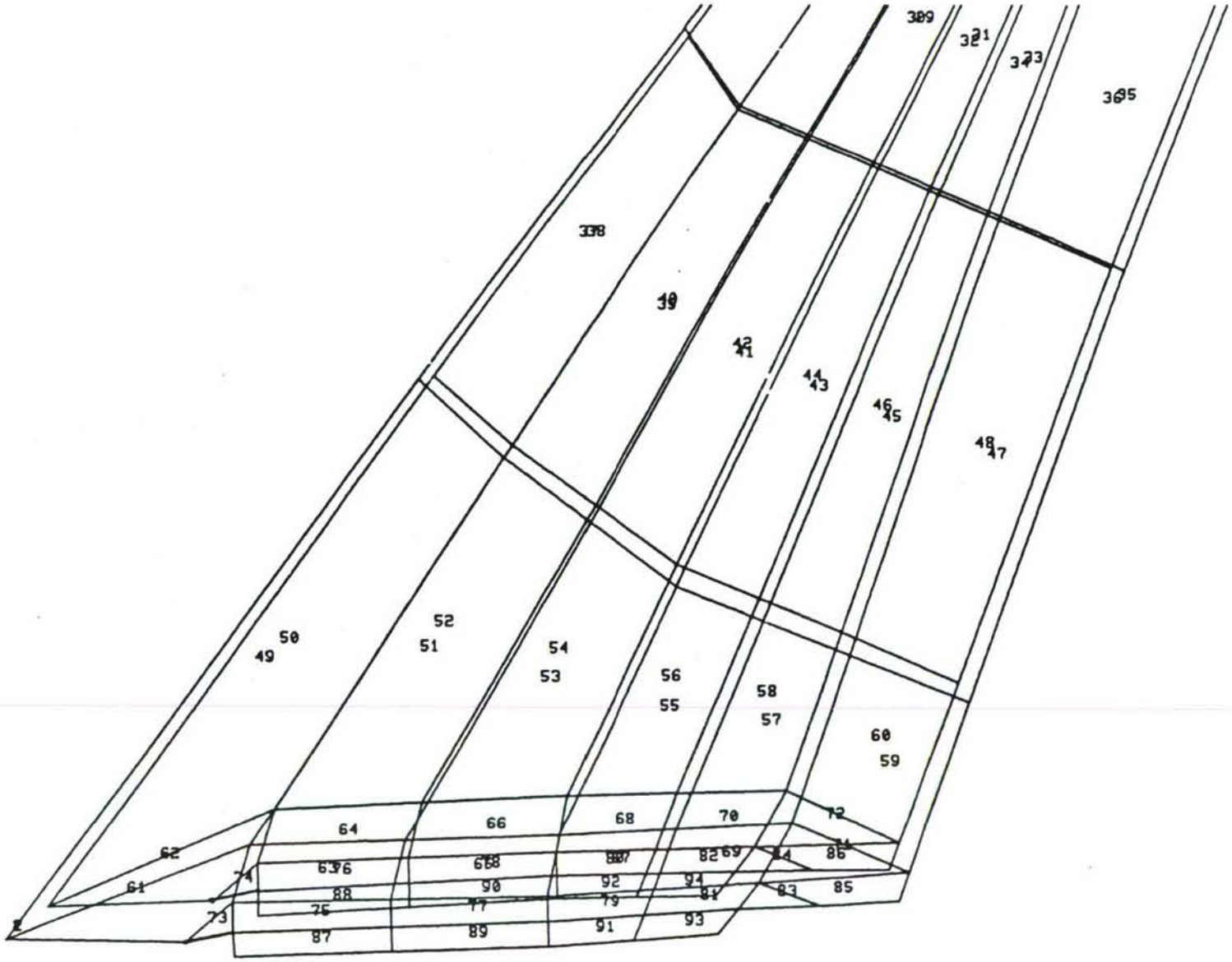

Figure 6.8. A-7 Outer Wing Panel Cover Elements. (Sheet 2 of 2)

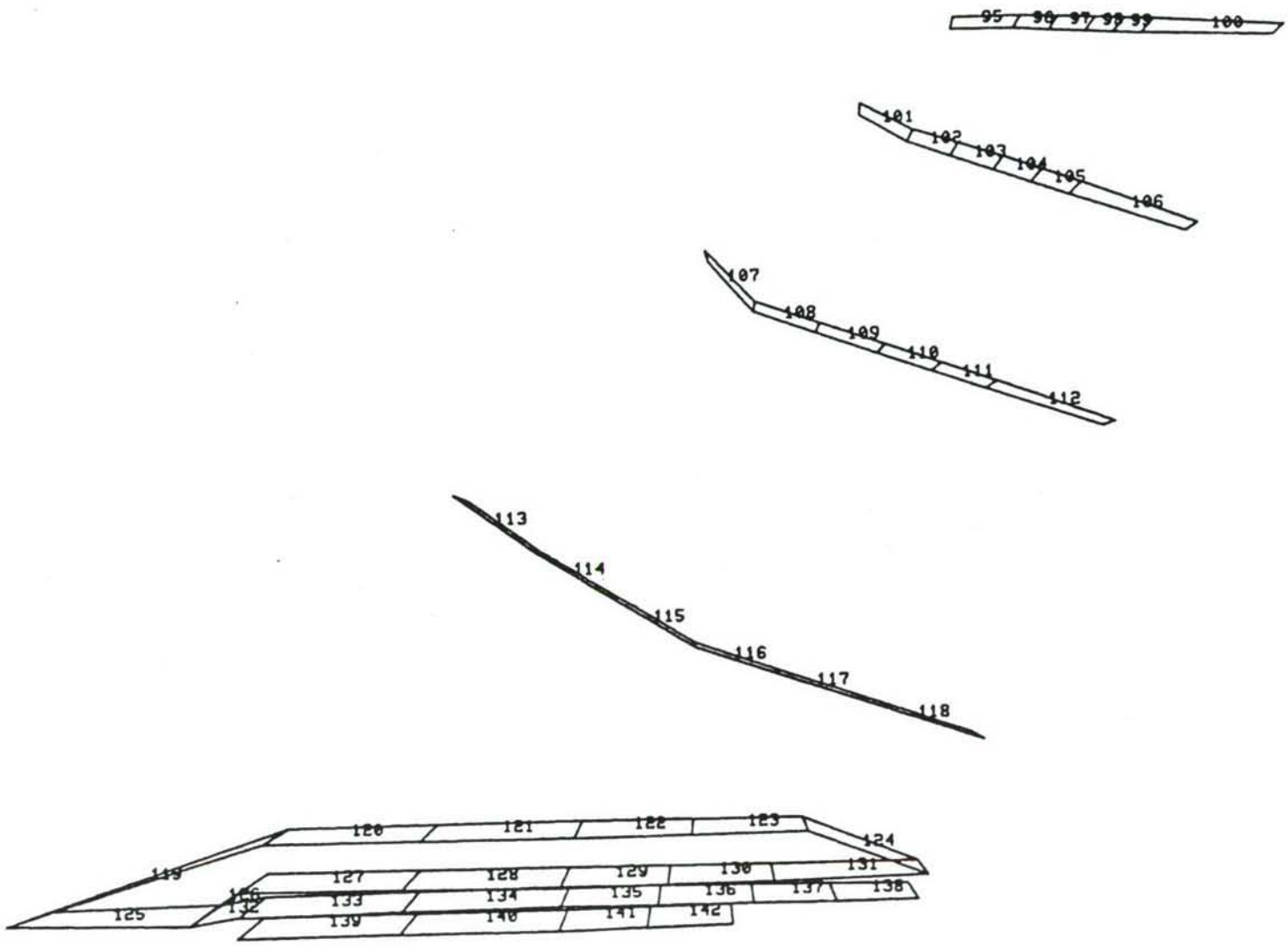

Figure 6.9. A-7 Outer Wing Panel Rib Panel Elements.

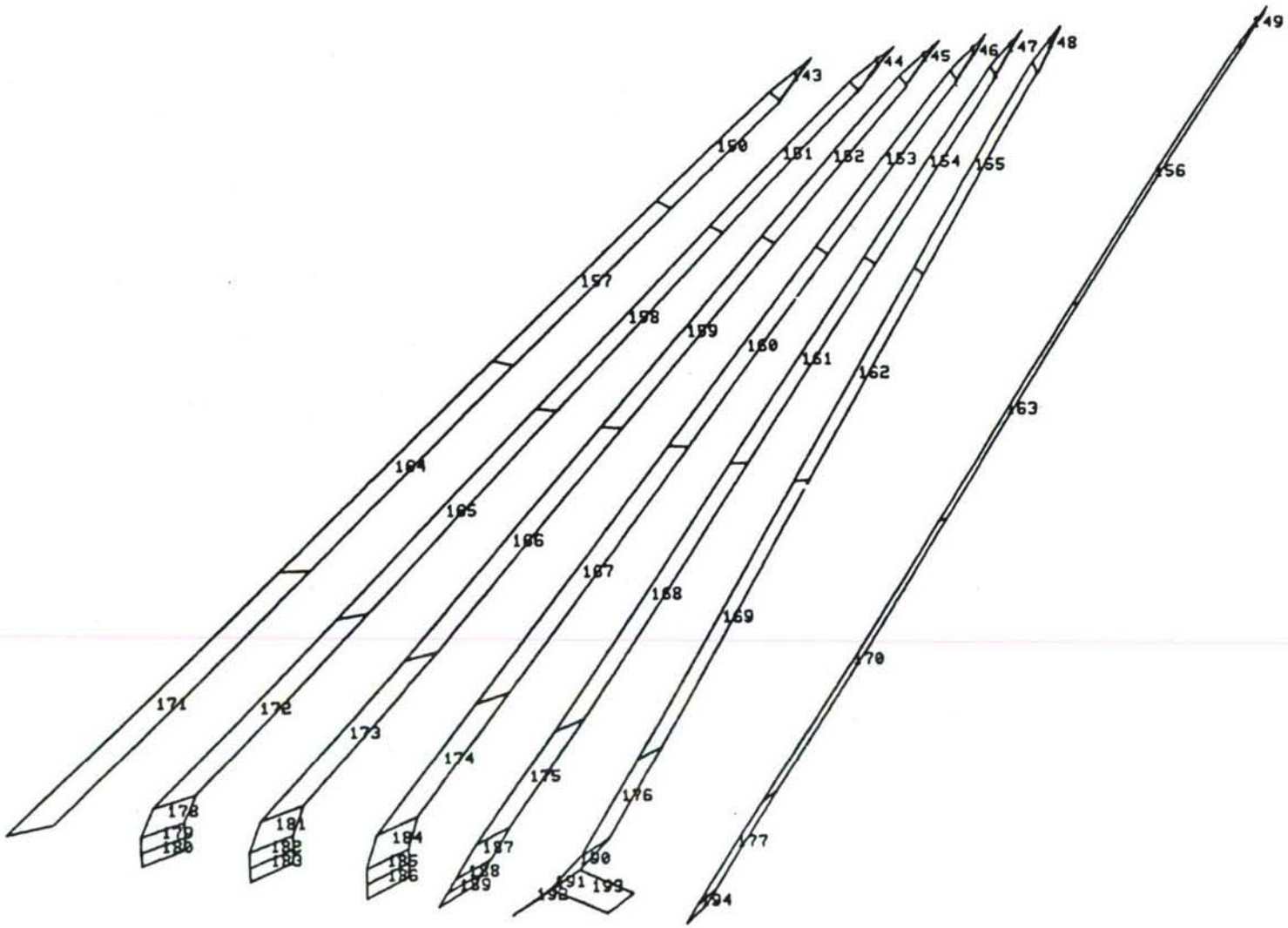

Figure 6.10. A-7 Outer Wing Panel Spar Panel Elements.

$\sigma_{CY1} = 45.6$ ksi

$\sigma_{CY2} = 45.6$ ksi

$\tau_{CR} = 30.5$ ksi

where the 1 and 2 subscripts denote properties in the longitudinal and transverse directions, respectively.

It was found that significant factors in the optimal design were the selection of the allowable skin stress level and the maneuver load factors after damage. The allowable stresses in tension for the skin after damage were computed in terms of the allowable, σ_{TU}, of the undamaged structure from the expression

$$\sigma^*_{TU} = \delta_d (N_z/N_z^*) \sigma_{TU} \tag{6.1}$$

where δ_d is a damage reduction factor based on impact fracture or residual strength considerations.[37] In developing the specific criteria, References 38 and 39 were used extensively.

For the metal design, the σ^*_{TU} for the cover elements was computed by equation (6.1) using $\delta_d = .16$, $N_z = 7$, and $N_z^* = 3$. Two sets of allowables were used for the composite designs. The nominal set was

$\sigma^*_{TU1} = 21.4$ ksi

$\sigma^*_{TU2} = 3.2$ ksi

$\sigma^*_{CY1} = 45.6$ ksi

$\sigma^*_{CY2} = 45.6$ ksi

$\tau^*_{CR} = 30.5$ ksi

A second set or "reduced" set consisted of

$\sigma^*_{TU1} = 11.3$ ksi

$\sigma^*_{TU2} = 4.3$ ksi

$\sigma^*_{CY1} = 45.6$ ksi

$\sigma^*_{CY2} = 45.6$ ksi

$\tau^*_{CR} = 27.0$ ksi

Details of the selection of these values and their relationship to ballistic damage are given in Reference 37.

Table 6.3 lists the damage cases studied. Cases 1, 2, 3, and 8 are for the metal wing. In Case 1 the wing was sized for stress constraints considering two applied loads, and no ballistic damage. Case 2 included damage to the two cover areas indicated in Figure 6.6. In Case 3 the ribs and spars were also damaged. The last metal design, Case 8, allowed for damage to all cover elements from the root to the tip between the third and fifth spar.

Cases 4 through 7 represent studies for the composite panel design. Case 4 included no damage, Case 5 included the cover damage of Case 2, Case 6 was the same as Case 5 but used the above "reduced" allowables, and Case 7 included the same damage as Case 3.

6.3 DESIGN RESULTS

The ADDRESS computer program was used to resize the metal and composite A7D panels. Table 6.4 summarizes the weights for the eight cases discussed in the previous section. Three cycles of energy resizing were used and the weights computed after each cycle. It is noted in Table 4 that the initial weights are not the same in all cases. This is due to the fact that the designs were uniformly scaled to reach the stress allowables for the various cases.

Figures 6.11, 6.12, and 6.13 give an indication for the Case 2 metal design how the material was redistributed among the covers, spars, and ribs. The various levels of shading correspond to the indicated range of the member sizes.

Figure 6.14 summarizes the Case 5 composite design of the covers. Ribs and spar element sizes were very similar to the metal design.

Using criteria for local failure set forth in Reference 37, the Case 2 and Case 5 optimal designs were further modified. The values of the member sizes so obtained are given in Table 6.5.

The weights shown in Table 6.6 summarize the "idealized" (ADDRESS) and "design" (Reference 37) weights. The first set of idealized

TABLE 6.3

A7D OPTIMIZATION CASE DESCRIPTIONS

Case	Description
1	Metal, no damage
2	Metal, 2 damages (covers only)
3	Metal, 2 damages (all elements)
4	Composite, no damage
5	Composite, 2 damages (covers only)
6	Case 5 with reduced allowables
7	Case 6, 2 damages (all elements)
8	Metal, 1 damage in second and third bay from root to tip (covers only)

TABLE 6.4

A-7D CASE WEIGHTS FOR ENERGY RESIZINGS

Case	Elements	Initial Weight	Cycle 1 Weight	Cycle 2 Weight	Cycle 3 Weight
1	C	325.1	88.3	73.4	69.7
	SP	181.5	36.7	28.0	25.9
	B	92.9	19.3	15.4	14.6
	Total	599.5	144.3	116.8	110.2
2	C	350.1	114.9	94.1	82.7
	SP	195.5	46.5	33.6	28.9
	B	100.1	25.5	20.5	19.1
	Total	645.7	186.9	148.2	130.7
3	C	361.1	125.2	107.3	99.2
	SP	201.6	50.8	38.0	33.9
	B	103.2	27.2	21.6	20.0
	Total	665.9	203.2	166.9	153.1
4	C	254.6	60.6	53.6	52.7
	SP	248.4	31.8	24.9	23.7
	B	127.2	17.2	13.4	11.8
	Total	630.2	109.6	91.9	88.2
5	C	277.4	84.3	75.1	70.9
	SP	270.7	43.2	31.2	27.8
	B	138.6	24.3	18.6	16.0
	Total	686.7	151.8	124.9	114.7
6	C	529.2	152.3	138.7	131.7
	SP	516.4	74.2	52.3	46.9
	B	264.4	40.0	29.9	25.3
	Total	1310.0	266.5	220.9	203.9
7	C	546.7	165.6	155.6	151.8
	SP	533.5	81.4	59.2	54.3
	B	273.2	42.6	30.9	25.2
	Total	1353.4	289.6	245.7	231.3
8	C	350.4	111.4	92.5	82.4
	SP	195.6	44.5	32.7	28.4
	B	100.2	24.6	20.4	19.1
	Total	646.2	180.5	145.6	129.9

C = Covers
SP = Shear Panels
B = Bars

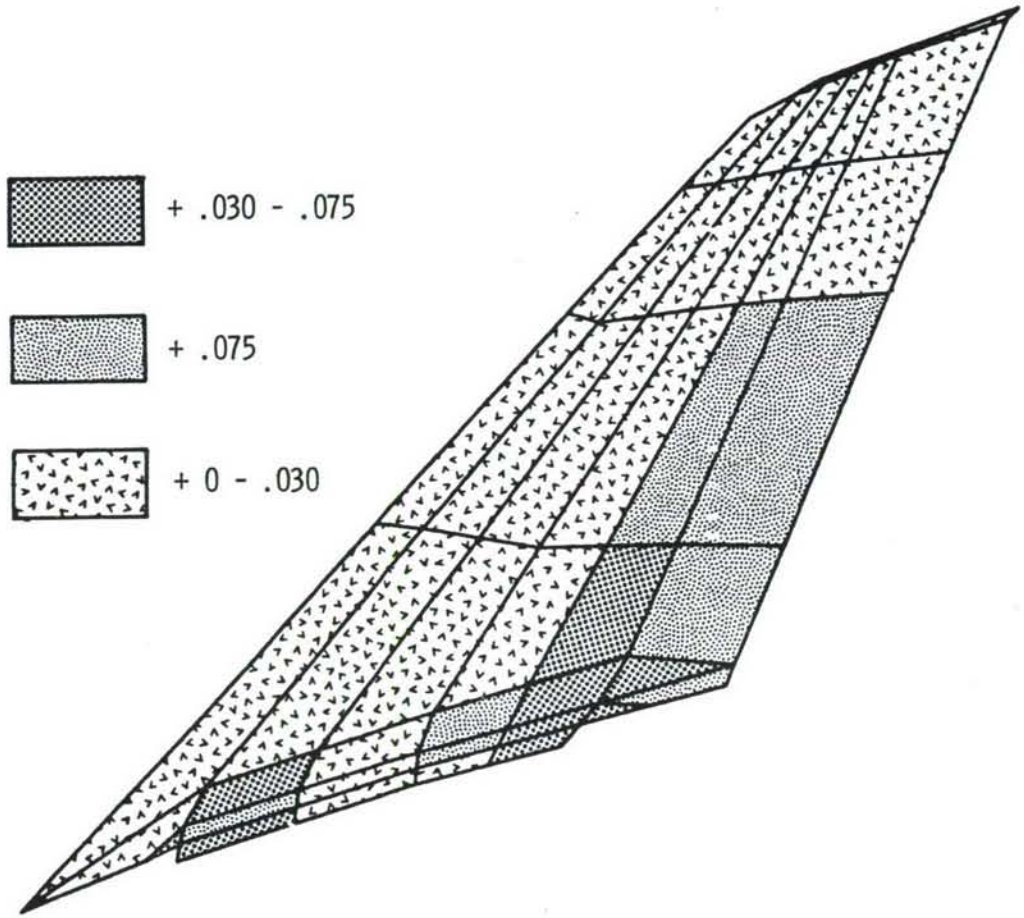

Figure 6.11. A-7D Covers Resized for Damage (Metal).

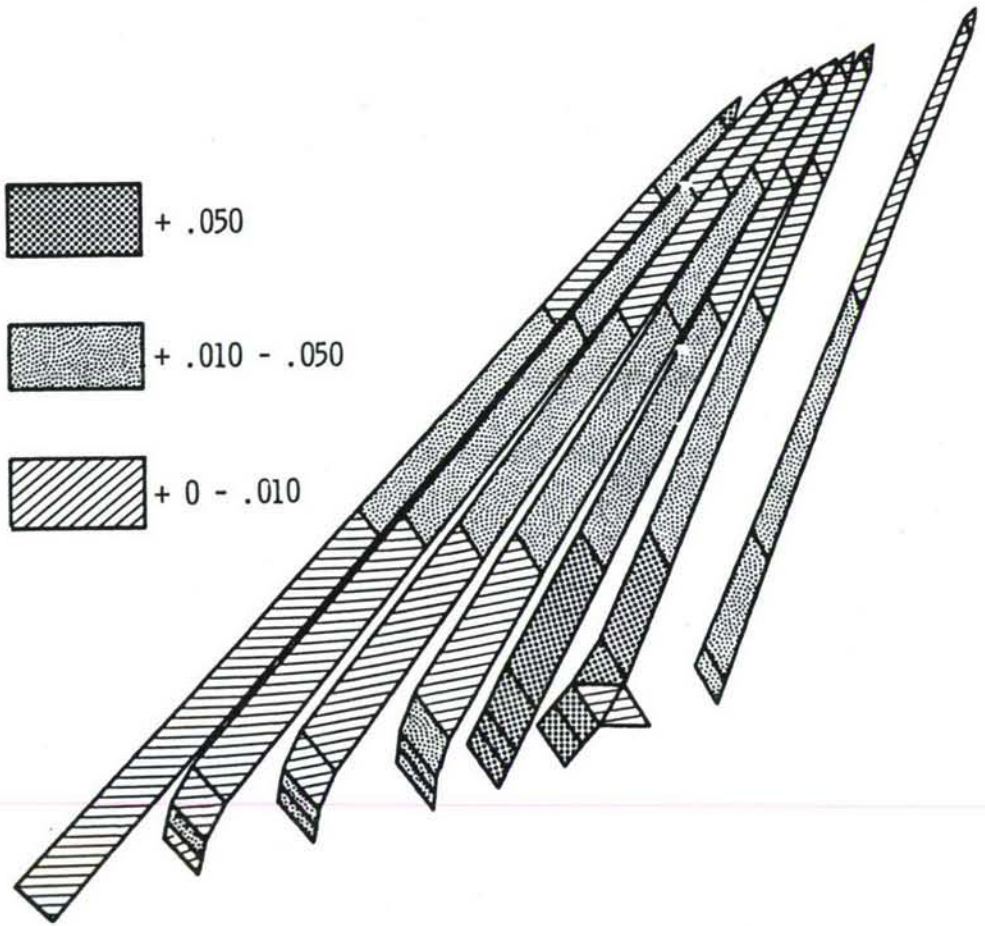

Figure 6.12. A-7D Spars Resized for Damage (Metal).

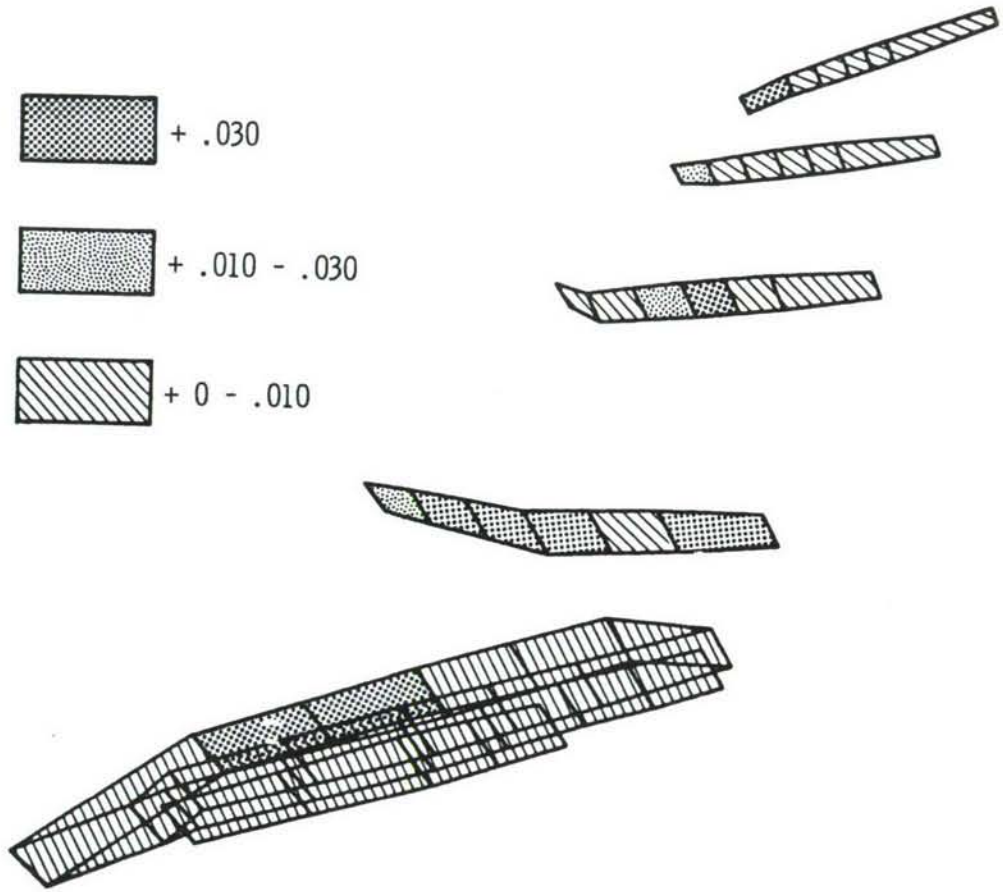

Figure 6.13. A-7D Rib Resized for Damage (Metal).

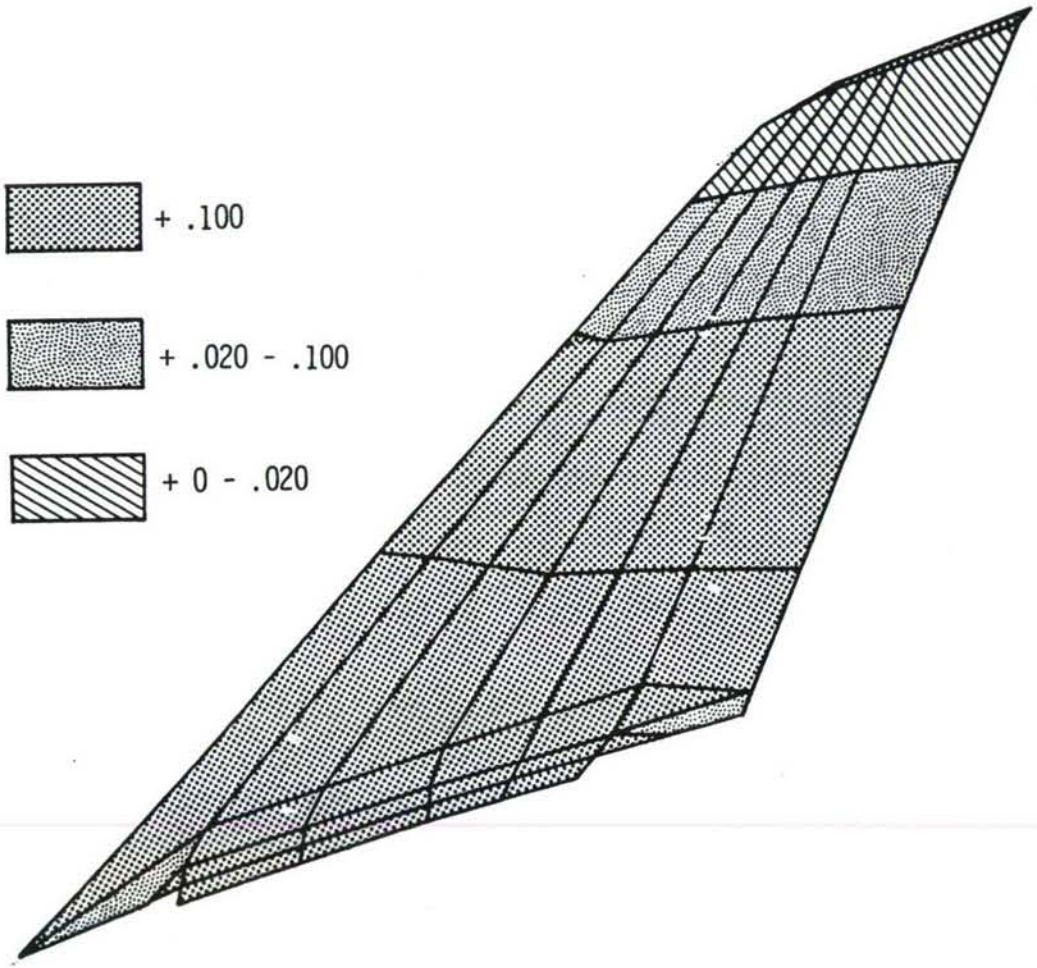

Figure 6.14. A-7D Covers Resized for Damage (Composite).

TABLE 6.5

FINAL DESIGNS FOR METAL AND COMPOSITE A-7D
OUTER WING PANEL

Element No.	Type	Metal Design	Composite Design	Element No.	Type	Metal Design	Composite Design
1	4	.432	.530	47	4	.069	.110
2		.343	.435	48		.080	.125
3		.052	.065	49		.040	.060
4		.051	.060	50		.054	.085
5		.052	.065	51		.247	.263
6		.051	.060	52		.304	.259
7		.052	.065	53		.253	.280
8		.051	.060	54		.301	.268
9		.052	.065	55		.269	.299
10		.051	.060	56		.319	.279
11		.121	.170	57		.272	.315
12		.121	.170	58		.346	.284
13		.036	.040	59		.124	.180
14		.036	.040	60		.141	.205
15		.059	.068	61		.039	.055
16		.055	.060	62		.036	.050
17		.059	.068	63		.096	.170
18		.055	.060	64		.096	.170
19		.059	.068	65		.138	.220
20		.054	.060	66		.127	.200
21		.059	.068	67		.284	.420
22		.054	.060	68		.273	.400
23		.036	.040	69		.340	.510
24		.036	.040	70		.365	.545
25		.045	.070	71		.309	.455
26		.036	.060	72		.327	.475
27		.076	.103	73		.167	.205
28		.059	.080	74		.073	.130
29		.080	.098	75		.090	.170
30		.059	.080	76		.099	.180
31		.078	.098	77		.157	.250
32		.059	.080	78		.145	.225
33		.078	.098	79		.274	.390
34		.059	.080	80		.286	.420
35		.036	.040	81		.554	.825
36		.036	.050	82		.531	.785
37		.072	.105	83		.504	.745
38		.082	.125	84		.563	.830
39		.134	.049	85		.036	.050
40		.097	.143	86		.036	.050
41		.134	.157	87		.134	.225
42		.097	.145	88		.117	.215
43		.132	.157	89		.173	.270
44		.096	.145	90		.163	.255
45		.130	.159	91		.227	.335
46		.094	.147	92		.220	.325

TABLE 6.5 (Continued)

Element No.	Type	Metal Design	Composite Design	Element No.	Type	Metal Design	Composite Design
93	4	.886	1.335	141	5	.036	.035
94	↓	.912	1.375	142	↓	.036	.035
95	5	.098	.082	143		.801	.722
96	↓	.040	.040	144		.063	.063
97		.040	.040	145		.063	.063
98		.040	.040	146		.063	.063
99		.040	.040	147		.063	.063
100		.036	.035	148		.063	.063
101		.042	.039	149		.043	.041
102		.050	.050	150		.049	.047
103		.050	.050	151		.063	.063
104		.050	.050	152		.063	.063
105		.050	.050	153		.063	.063
106		.036	.035	154		.063	.063
107		.036	.035	155		.063	.063
108		.063	.063	156		.036	.035
109		.063	.063	157		.036	.035
110		.063	.063	158		.063	.063
111		.063	.063	159		.063	.063
112		.036	.035	160		.063	.063
113		.074	.074	161		.063	.063
114		.090	.090	162		.063	.063
115		.090	.090	163		.036	.035
116		.090	.090	164		.072	.061
117		.090	.090	165		.080	.080
118		.112	.112	166		.080	.080
119		.036	.035	167		.080	.080
120		.100	.100	168		.080	.080
121		.100	.100	169		.080	.080
122		.100	.100	170		.075	.063
123		.100	.100	171		.037	.035
124		.036	.035	172		.125	.125
125		.036	.035	173		.125	.125
126		.036	.035	174		.125	.125
127		.036	.035	175		.125	.125
128		.036	.035	176		.125	.125
129		.036	.035	177		.060	.054
130		.036	.035	178		.041	.035
131		.036	.035	179		.055	.035
132		.036	.035	180		.077	.062
133		.036	.035	181		.137	.054
134		.036	.035	182		.055	.077
135		.036	.035	183		.092	.123
136		.036	.035	184		.134	.127
137		.036	.035	185		.169	.162
138		.055	.048	186		.174	.167
139		.039	.035	187		.227	.210
140	↓	.036	.035	188	↓	.312	.292

TABLE 6.5 (Continued)

Element No.	Type	Metal Design	Composite Design	Element No.	Type	Metal Design	Composite Design
189	5	.338	.314	305	2	.036	.035
190	↓	.223	.228	306	↓	.036	.035
191	↓	.338	.346	307	↓	.060	.060
192	↓	.347	.352	308	↓	.060	.059
193	↓	.036	.035	309	↓	.036	.035
194	↓	.063	.055	310	↓	.036	.035
195	2	.036	.035	311	↓	.036	.035
196	↓	.036	.035	312	↓	.036	.035
197	↓	.036	.035	313	↓	.036	.035
198	↓	.036	.035	314	↓	.036	.035
199	↓	.036	.035	315	↓	.036	.035
200	↓	.036	.035	316	↓	.036	.035
201	↓	.036	.035	317	↓	.036	.035
202	↓	.046	.040	318	↓	.036	.035
203	↓	.036	.035	319	↓	.036	.035
↓	↓	↓	↓	320	↓	.036	.035
↓	↓	↓	↓	321	↓	.036	.035
↓	↓	↓	↓	322	↓	.036	.035
274	↓	.036	.035	323	↓	.036	.035
275	↓	.060	.067	324	↓	.036	.035
276	↓	.036	.035	325	↓	.036	.035
277	↓	.036	.035	326	↓	.043	.035
278	↓	.026	.035	327	↓	.041	.035
279	↓	.036	.035	328	↓	.036	.035
280	↓	.036	.035	329	↓	.039	.035
281	↓	.036	.035	330	↓	.036	.035
282	↓	.036	.035	331	↓	.037	.035
283	↓	.036	.035	332	↓	.036	.035
284	↓	.036	.035	333	↓	.036	.035
285	↓	.036	.035	334	↓	.036	.035
286	↓	.036	.035	335	↓	.036	.035
287	↓	.036	.035	336	↓	.036	.035
288	↓	.036	.035	337	↓	.036	.035
289	↓	.036	.035	338	↓	.036	.035
290	↓	.036	.035	339	↓	.036	.035
291	↓	.036	.035	340	↓	.107	.073
292	↓	.036	.035	341	↓	.096	.068
293	↓	.036	.035	342	↓	.063	.044
294	↓	.036	.035	343	↓	.099	.068
295	↓	.036	.035	344	↓	.083	.057
296	↓	.036	.035	345	↓	.115	.080
297	↓	.734	.659	346	↓	.109	.076
298	↓	.422	.386	347	↓	.102	.073
299	↓	.036	.035	348	↓	.103	.074
300	↓	.036	.035	349	↓	.096	.072
301	↓	.036	.035	350	↓	.104	.077
302	↓	.036	.035	351	↓	.045	.035
303	↓	.036	.035	352	↓	.059	.040
304	↓	.036	.035	353	↓	.036	.035

TABLE 6.5 (Continued)

Element No.	Type	Metal Design	Composite Design	Element No.	Type	Metal Design	Composite Design
354	2	.036	.035	405	2	.036	.035
355		.066	.047	406		.036	.035
356		.045	.035	407		.036	.035
357		.189	.145	408		.036	.035
358		.167	.129	409		.036	.035
359		.686	.555	410		.036	.035
360		.654	.529	411		.036	.035
361		.460	.338	412		.036	.035
362		.470	.344	413		.036	.035
363		.195	.133	414		.036	.035
364		.212	.144	415		.036	.035
365		.036	.035	416		.036	.035
366		.036	.035	417		.036	.035
367		.054	.050	418		.036	.035
368		.073	.066	419		.036	.035
369		.042	.047	420		.036	.035
370		.057	.059	421		.036	.035
371		.050	.053	422		.036	.035
372		.094	.098	423		.036	.035
373		.124	.106	424		.036	.035
374		.118	.097	425		.036	.035
375		.121	.106	426		.036	.035
376		.084	.075	427		.036	.035
377		.068	.063	428		.036	.035
378		.052	.048	429		.036	.035
379		.176	.127	430		.045	.040
380		.159	.114	431		.036	.035
381		.148	.118	432		.036	.035
382		.154	.126	433		.036	.035
383		.237	.190	434		.036	.035
384		.217	.172	435		.036	.035
385		.397	.284	437		.036	.035
386		.358	.251	438		.036	.035
387		.281	.194	439		.036	.035
388		.378	.277	440		.127	.130
389		.149	.099	441		.205	.212
390		.125	.077	442		.036	.035
391		.298	.199	443		.036	.035
392		.313	.207	444		.036	.035
393		.473	.337	445		.142	.145
394		.527	.375	446		.248	.253
395		1.206	.969	447		.036	.035
396		1.279	1.016	448		.036	.035
397		.036	.035	449		.036	.035
398		.036	.035	450		.036	.035
399		.036	.035	451		.036	.035
400		.036	.035	452		.036	.035
401		.036	.035	453		.036	.035
402		.036	.035				
403		.036	.035				
404		.036	.035				

TABLE 6.6

A7D WEIGHT SUMMARY

Case	Metal Wingbox	Composite Wingbox
Idealized Weight (static criteria but with no ballistic damage)	116.9 lbs	88.2 lbs
Idealized Weight (UDRI results)	130.7 lbs	114.7 lbs
Final Design Weight (Vought results)	160.6 lbs	123.3 lbs

weights represents the undamaged structure which is sized according to static stress requirements. The second set of idealized weights represents the structure sized according to ballistic damage criteria (only covers damaged). The idealized weights are based solely upon the ADDRESS program output for the undamaged and damaged wingboxes. The design weights reflect a mix of UDRI output and Vought baseline wingbox data as reflected on the design drawings.

The design weights for the metal and the composite wingboxes increased due to the method by which the structure was sized. The method used made an element-by-element comparison of Vought input data with ADDRESS output. The larger of the two values was then used in the design. This method assured that the wingboxes would meet all static, fatigue and fracture requirements as well as the ballistic damage requirements. The design weight for the metal wingbox increased more than the composite design for the following reason. In sizing the metal wingbox, a comparison was made to the baseline A-7D outer wing. The skins of the baseline wingbox were thicker in some regions than the ADDRESS output and the Vought input (from a NASTRAN model). The metal skins were sized according to this information to assure that the wingbox met all static, fatigue and fracture requirements. A comparison of the computer runs for the metal wingbox shows that the majority of the increase from 130.7 lbs. to 160.55 lbs. was due to the increase in skin weights.

SECTION 7
COMMENTS AND CONCLUSIONS

An analytical procedure has been developed and demonstrated which provides optimal design information for lifting surfaces subjected to strength, stiffness, and damage requirements. The optimality criterion approach provides a framework in which efficient reanalysis techniques can be used to handle the multiple requirements. An examination of the optimal design which includes the effect of damage shows that the ADDRESS program provides alternate load paths around damaged structural members.

Execution times have been reduced by 33% to 50% compared to similar computer runs using ØPSTATCØMP or DANALYZ. The ADDRESS program because of its modularity provides a framework within which new program features can be easily added.

Computer output has been used by an airframe company (Vought Corporation) to establish viable designs for given damage conditions. Even with a fairly coarse finite element model, useful information can be obtained which assists the designer in arriving at lower weight, damage tolerant designs.

One disadvantage of the method appears to be that resulting designs obtained from ADDRESS have locally increased member sizes near the damage zone. Some type of redistribution technique is needed to compensate for this problem. One approach is to run the ADDRESS program for a wide variety of damage conditions and then take as the candidate design the envelope of the maximum member sizes so obtained. Another approach would be to impose a low level damage to every member and then optimize for this single uniform damage condition.

In general a more organized approach is needed for the selection of the most critical damage conditions. The capability is available within ADDRESS to treat this problem in a limited manner. It is possible to damage any individual element and determine by reanalysis the response of the structure. The most critical elements or groupings of elements could thus be identified and appropriate optimization runs then performed. The ADDRESS program

is currently limited in the number of damage cases it can handle and would need some modifications to be used in the above manner.

The problem also exists that it is difficult to convert a given ballistic damage condition into a single mass or stiffness reduction factor for the ADDRESS program. The bar, shear panel, and membrane structural model has limitations in representing complicated ballistic damage effects. On the other hand it is probable that far from the local damage, the member sizing is independent of the details of the damage. Further studies on a component level would be needed to establish a sound basis for the selection of reduction factors to be applied to the bar, shear panel, and membrane model. Mathematical programming techniques applied at the component level in a separate analysis and optimization program could provide useful input the the less sophisticated overall model which is resized by optimality criteria.

Further work is also needed to quantify the effects of ballistic damage on the applied loads. From an aerodynamic point of view, this load redefinition could be quite complex due to non-uniform airflow through or near the ballistic damage.

Other constraints need to be considered in the damage optimization problem. A constraint on the ratio of bending to torsional frequencies for a high aspect ratio wing could be quite important from an aeroelastic stability standpoint. Constraints on divergence and flutter speeds need to be considered together with the strength requirements.

REFERENCES

1. Venkayya, V. B., Survey of Optimization Techniques in Structural Design, International Journal for Numerical Methods in Engineering, Vol. 13, No. 2, 1978, pp. 203-228.

2. Arora, J. S., Haskell, D. J., and Gavill, A. K., "Optimal Design of Large Structures for Damage Tolerance," AIAA Journal, Vol. 18, No. 5, May 1980, pp. 563-570.

3. Venkayya, V. B., Khot, N. S., and Eastep, F. E., "Vulnerability Analysis of Optimized Structures," AIAA Journal, Vol. 16, No. 11, November 1978, pp. 1189-1195.

4. Argyris, J. H., "The Matrix Analysis of Structures with Cutouts and Modifications," Proceedings of the Ninth International Congress of Applied Mechanics, 1956, pp. 131-142.

5. Sack, R. L., Carpenter, W. C., and Hatch, G. L., "Modifications of Elements in the Displacement Methods," AIAA Journal, Vol. 5, No. 9, September 1967, pp. 1708-1710.

6. Melosh, R. J. and Luik, R., "Multiple Configuration Analysis of Structures," Journal of the Structural Division, ASCE, Vol. 94, November 1968, pp. 2581-2595.

7. Kavlie, D. and Powell, G. H., "Efficient Reanalysis of Modified Structures," Journal of the Structural Division, ASCE, Vol. 97, January 1971, pp. 377-391.

8. Kirsch, U. and Rubenstein, M. F., "Structural Reanalysis by Iteration," Computers and Structures, Vol. 2, 1972, pp. 497-510.

9. Phansalkar, S. R., "Matrix Iterative Methods for Structural Reanalysis," Computers and Structures, Vol. 4, 1974, pp. 779-800.

10. Switzky, H., "Rapid Analysis of Damaged Structure," AIAA Journal, Vol. 14, No. 8, August 1976, pp. 1139-1141.

11. Venkayya, V. B., "A Perturbation Method for the Analysis of Damaged Structures," paper presented at the Symposium on Applications of Computer Methods in Engineering, University of Southern California, Los Angeles, August 23,26, 1977.

12. Fox, R. L., "Constraint Surface Normals for Structural Synthesis Techniques," AIAA Journal, Vol. 3, No. 8, August 1968, pp. 1517-1518.

13. Stooraasli, O. O. and Sobiesyzanski, J., "On the Accuracy of the Taylor Approximation for Structural Resizing," AIAA Journal, Vol. 12, No. 2, February 1974, pp. 231-233.

14. Noor, A. K. and Lowder, H. E., "Approximate Techniques of Structural Reanalysis," Computers and Structures, Vol. 4, 1974, pp. 801-812.

15. Arora, J. S. and Haug, E. J., "Methods of Design Sensitivity Analysis for Structural Optimization," AIAA Journal, Vol. 17, No. 9, September 1979, pp. 970-974.

16. Fox, R. L. and Miura, H., "An Approximate Analysis Technique for Design Calculations," AIAA Journal, Vol. 9, No. 1, January 1971, pp. 177-179.

17. Noor, A. K. and Lowder, H. E., "Approximate Reanalysis Techniques with Substructuring," Journal of the Structural Division, ASCE, Vol. 101, August 1975, pp. 1687-1698.

18. Noor, A. K. and Lowder, H. E., "Structural Reanalysis via a Mixed Method," Computers and Structures, Vol. 5, 1975, pp. 9-12.

19. Fox, R. L. and Kapoor, M. P., "Rates of Change of Eigenvalues and Eigenvectors," AIAA Journal, Vol. 6, No. 12, 1968, pp. 2426-2429.

20. Rogers, L. C., "Derivatives of Engenvalues and Eigenvectors," AIAA Journal, Vol. 8, No. 5, May 1970, pp. 943-944.

21. Nelson, R. B., "Simplified Calculation of Eigenvector Derivatives," AIAA Journal, Vol. 14, No. 9, September 1976, pp. 1201-1205.

22. Rudisill, C. S. and Chu, Y.-Y., "Numerical Methods for Evaluating the Derivatives of Eigenvalues and Eigenvectors," AIAA Journal, Vol. 13, No. 6, June 1975, pp. 834-837.

23. Andrew, A. L., "Convergence of an Iterative Method for Derivatives of Eigensystems," Journal of Computational Physics, Vol. 26, No. 1, January 1978, pp. 107-112.

24. Hemming, F. G., Venkayya, V. B. and Eastep, F. E., "Flutter Speed Degradation of Damaged, Optimized Flight Vehicles," Proceedings of the 20th AIAA/ASME/ASCE/AHS Structures, Structural Dynamics and Materials Conference, St. Louis, Mo., April 4-6, 1979.

25. Venkayya, V. B. and Tischler, V. A., OPTSTAT - A Computer Program for the Optimal Design of Structures Subjected to Static Loads, AFFDL-TM-FBR-79-67, June 1979.

26. Popov, E. P., Mechanics of Materials. Prentice-Hall, 2nd ed., 1976, pp. 186-190.

27. Dahlquist, G. and Bjorck, A., Numerical Methods. Prentice-Hall, Englewood Cliffs, N. J., 1970, pp. 74-75.

28. Conte, S. D. and deBoor, C., Elementary Numerical Analysis: An Algorithmic Approach. McGraw-Hill, New York, 1972, pp. 44-55.

29. Corr, R. B. and Jennings, A., "A Simultaneous Iteration Algorithm for Symmetric Eigenvalue Problems," International Journal for Numerical Methods in Engineering, Vol. 10, 1976, pp. 647-663.

30. Venkayya, V. B., Khot, N. S., and Berke, L., "Application of Optimality Criteria Approaches to Automated Design of Large Practical Structures," AGARD Conference Proceedings No. 123, April 1973.

31. Venkayya, V. B., Khot, N. S., Tischler, V. A., and Taylor, R. F., "Design of Optimum Structures for Dynamic Loads," paper at the Third Air Force Conference on Matrix Methods in Structural Mechanics, October 1971.

32. McMahon, T. A., Applib User's Manual: Numerical Analysis Software for Engineering Applications on a Microcomputer, UDR-TM-82-24, August 1982.

33. Kuisalaas, J., Minimum Weight Design of Structures Via Optimality Criteria, NASA TN D7115, December 1972.

34. Turner, M. J., "Design of Minimum Mass Structures with Specified Natural Frequencies," AIAA Journal, Vol. 5, No. 3, March 1967, pp. 406-412.

35. Ketter, R. L. and Prawel, S. P., Modern Methods of Engineering Computation. McGraw-Hill, New York, 1969, pp. 460-462.

36. Ortega, J., "The Givens-Householder Method for Symmetric Matrices," Chapter 4 of Mathematical Methods for Digital Computers, Vol. II, ed. A. Ralston and H. Wilf, New York, 1967.

37. Cazzell, B. D. and Zikos, N. J., "Optimization and Damage Assessment of Aerospace Structures," Final Report to the University of Dayton Research Institute, Vought Corporation, July 1982.

38. Avery, J. G. and Porter, T. R., Survivable Combat Aircraft Structures--Design Guidelines and Criteria, AFFDL-TR-74-49 and 50, April 1974.

39. Avery, J. G., Bradley, S. J. and Bristow, R. J., Survivable Composite Structure for Combat Aircraft, AFFDL-TR-79-3132, November 1979.

* U.S. GOVERNMENT PRINTING OFFICE: 1983 - 659-062/765